



RESULTS
&
DISCUSSION
&
DISCUSSION

Results and Discussion

In this chapter the various results obtained from different experiments carried out are compiled and conclusions drawn from the results are discussed and reported.

4.1. *Leonotis nepetaefolia*

The detailed systematic pharmacognostical and phytochemical evaluation of plant and plant material provides means of standardization of an herb that can be used as drug or as raw material. The major problem faced in herbal formulation industry is the identification of authenticated raw material and in the absence of data one can use adulterant in the drug formulation [236]. Here we are reporting preliminary data for identification of leaves and roots of *L. nepetaefolia* and its extract for use of this plant as drug.

4.1.1. Macroscopic Features

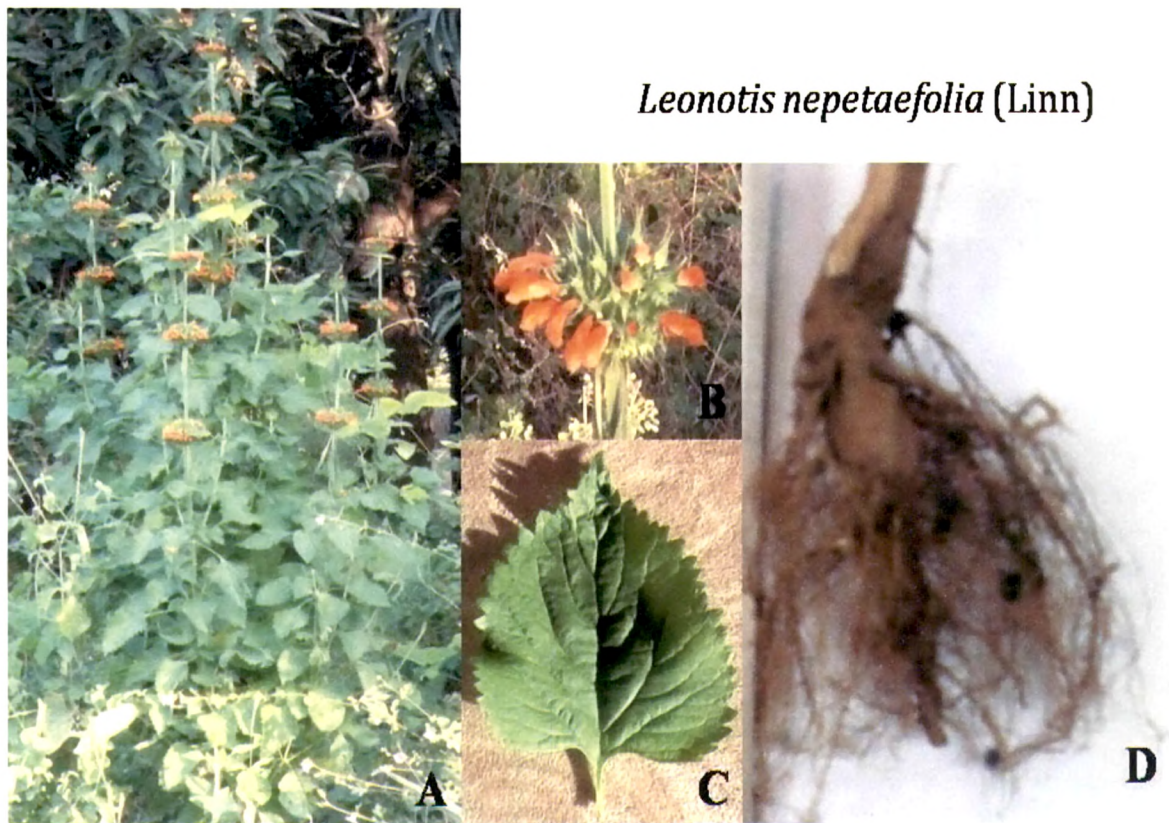


Figure 4.1: *Leonotis nepetaefolia* plant: A; whole plant, B; inflorescence, C; leaf, D; root

Results and Discussion

Herb is deciduous, stout, erect, woody and 2-3 meters in length. Leaves are cauline, ramal, opposite, charactaceous and membranous. Leaves are 3-8 cm long with dentate margin, trichomes on lamina and acute apex. Because of its leaf shape the plant is known as *Lion's ear*. Inflorescence is globuse, axillary whorls with numerous orange-scarlet, complete, zygomorphic flowers. Stem is quadrangular and woody. Root system is well developed with numerous thin, hairy lateral roots arise from main primary root (0.5-1 cm in diameter). Roots are grayish yellow in colour with few longitudinal furrows that are in accordance to earlier reports [237].

4.1.2. Microscopic Features

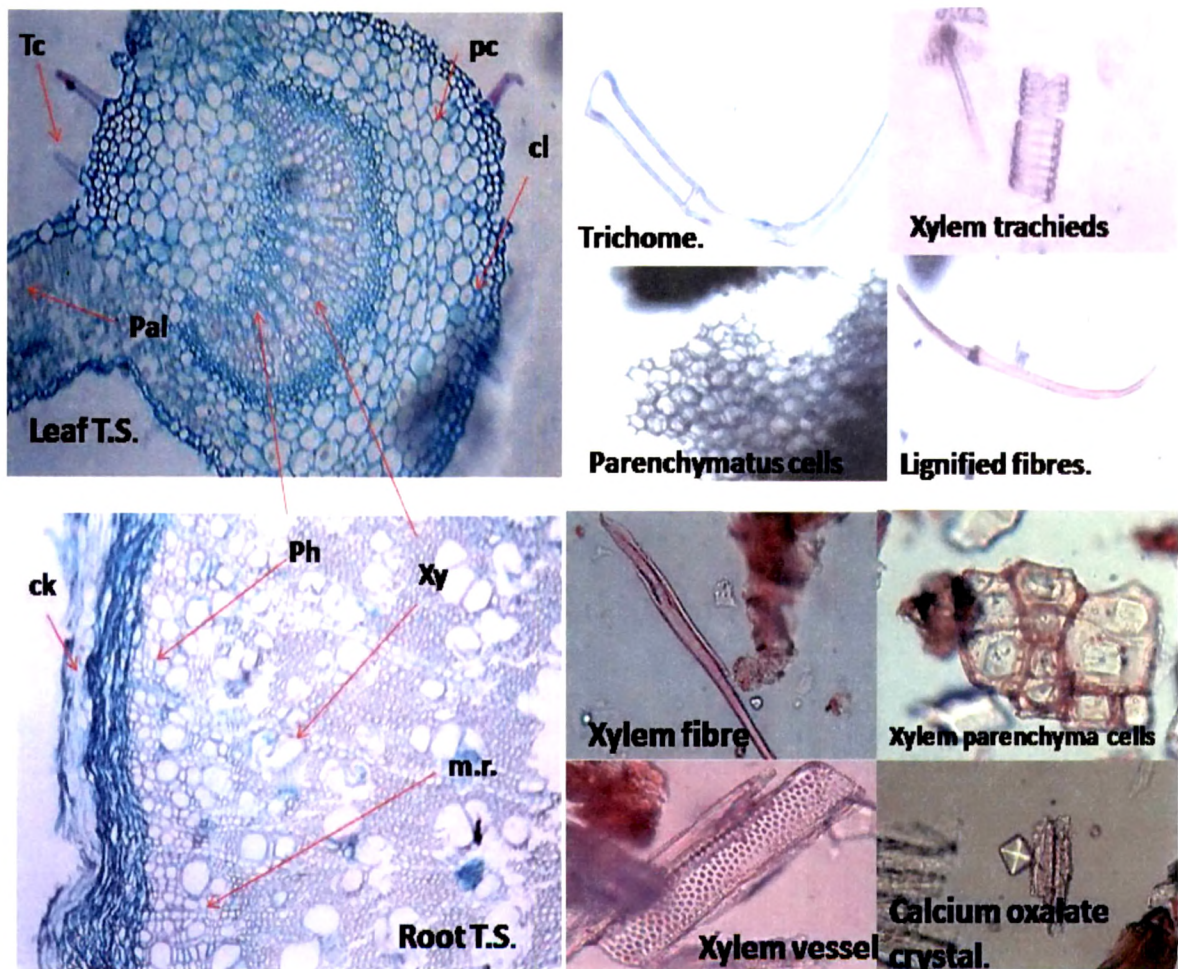


Figure 4.2: Transverse sections (TS) and powder microscopy of leaf and root of *L.nepetaefolia*. Tc-trichomes; Pc-mesophyll parenchyma; Pal-palisade cells; cl-collenchyma; Ph-phloem; Xy-xylem; ck-cork cells; m.r.-medullary rays

Results and Discussion

4.1.2.1. Leaf: A thin section of leaf showed the presence of non- lignified, multicellular, trichomes on both the surfaces. Single layer of rectangular epidermal cells covered with thin cuticle is observed. Mesophyll is not differentiated into palisade and spongy parenchyma, but, mostly consists of spongy parenchyma which is thin walled and loosely arranged. In the midrib region there are conjoint, colleteral, lignified vascular bundles. Tightly packed 2-3 layers of collenchymatous cells are seen below epidermis on both the sides in the mid rib region. Starch grains are absent. These findings were in accordance to powder microscopy study of leaf.

4.1.2.2. Root: Mature root shows a thin bark and a very wide xylem, cork exfoliating, generally detached. Sometime cork is also seen and consists of a few layers of tangentially elongated compressed cells possessing brown matter. Cortex forms a narrow zone and composed of 3-6 or more layers of rounded, irregular or tangentially elongated, thin- walled, parenchymatous cells having brown matter. Secondary phloem consists of thin-walled cells of sieve elements. Phloem fibres are generally not observed. Secondary xylem forms major part of root consisting of vessels, xylem fibres and xylem parenchyma. Vessels are distributed throughout secondary xylem and it contains bordered pits and of various shapes and sizes, a few having elongated projection at one or both ends. Xylem fibres elongated, lignified with pointed ends with moderately wide lumen. Xylem parenchyma is rectangular or square in shape and pitted. Medullary rays are uni to triseriate, uni and biseriate rays.

4.1.3. Proximate analysis

In quantitative microscopy, the stomatal index for upper and lower surfaces was found to be 7.8 to 9.0 to 10.6 and 9.7 to 10.3 to 11.8 respectively. Vein islet number and vein- let termination number are 9 to 12 (Average 10. 5) and 11 to 16 (Average 13) respectively.

Proximate analysis and estimation of secondary metabolites in extracts serves as means of physicochemical evaluation of plant and plant material. The total moisture is found to be 7.8% and 5.1 % w/w for leaf and root respectively. The total ash for leaf and root is found to be 5.88% w/w and 4.08% w/w respectively, of which, 1.01 % w/w and 0.71% w/w is the acid insoluble ash. Alcohol and water extractive values were found to be 29. 2 %w/w and 27.92 %w/w for leaf, and 21.83% w/w and 28.39% w/w for root respectively.

Results and Discussion

Table 4.1: Proximate analysis of *L. nepetaefolia*

<i>Parameters</i>	<i>Leaf Values</i>	<i>Root Values</i>
Moisture content (%w/w)	7.8±0.2309	5.1±0.1732
Foreign matter (%w/w)	0.85	1.85
Total Ash Value (%w/w)	5.88±0.1922	4.083±0.4512
Acid Insoluble ash value (%w/w)	1.003±0.12	0.7067±0.0425
Water soluble ash value (%w/w)	4.1±0.1155	3.15±0.1386
Alcohol soluble extractive value (%w/w)	29.2±0.5432	21.83±0.1622
Water soluble extractive value (%w/w)	27.97±1.133	28.39±0.5476
Total Phenolic content (%w/w)	19.44±0.5562	13.53±0.4015
Total Flavanoid content (%w/w)	25.54±0.6214	17.48±0.5269
Foaming Index	Less than 100	Less than 100
Swelling Index	Less than 1 cm	Less than 1 cm
Haemolytic Index	107.4±1.652	82.47±0.6688
Elements		
• Sodium	0.85 ppm	1.05 ppm
• Potassium	7.99 ppm	19.038 ppm
• Magnesium	504.58 ppm	576.05 ppm
• Manganese	34.72 ppm	96.55 ppm
• Copper	12.98 ppm	8.20 ppm
• Zinc	53.33 ppm	60 ppm
• Mercury	Nil	Nil
• Lead	0.23 ppm	0.43 ppm
• Cadmium	Nil	Nil
• Arsenic	Nil	Nil

4.1.4. Phytochemical screening

Powdered LNL and LNR were subjected to successive extraction, quantities obtained are given in the table with consistency. Qualitative phytochemical screening showed the presence of various types of phytoconstituents like alkaloids, volatile oils, phytosterols, fats and oils, flavonoids, amino acids, carbohydrates etc in LNL and phytosterols, terpenes, fats and oils, carbohydrates in LNR (Table 4.3 and 4.4).

Results and Discussion

Table 4.2: Successive extract profile of *L. nepetaefolia*

Solvent	Extractive value (% w/w)		Colour & consistency	
	Leaf	Root	Leaf	Root
Pet. Ether (60-80 °C)	4.48	0.05	Dark green & sticky mass	Yellow and dry powder
Benzene	4.17	0.48	Dark green & dry powder	Dark green and dry powder
Chloroform	1.63	2.43	Green & dry powder	Green & dry powder
Ethyl Acetate	1.47	0.16	Green and oily	Brown and dry
Methanol	21.4	22.53	Greenish brown and sticky	Brown and dry
Water	15.04	18.25	Brown and dry	Brown and dry

Table 4.3: Phytochemical screening of successive extracts of LN leaves

	Pet. Ether	Benzene	Chloroform	Et. Ac.	Methanol	Water
Carbohydrate	-	-	-	-	++	++
Protein/	-	-	-	-	-	+
Amino Acid						
Phenolics & Tannins	-	-	-	+	++	++
Flavonoids	-	-	-	++	++	++
Saponins	-	+	-	-	+	+
Alkaloids	-	-	-	-	-	+
Sterols and steroids	+	+	+	+	++	-

Results and Discussion

Table 4.4: Phytochemical screening of successive extracts of LN roots

	Pet. Ether	Benzene	Chloroform	Et. Ac.	Methanol	Water
Carbohydrate	-	-	-	-	++	++
Protein/ Amino Acid	-	-	-	-	-	+
Phenolics & Tannins	-	-	-	+	++	++
Flavonoids	-	-	-	+	++	++
Saponins	-	+	-	-	+	+
Alkaloids	-	-	-	-	-	-
Sterols and steroids	-	+	++	-	++	-

4.1.5. TLC and HPTLC Studies of methanol extracts

Phytoconstituents present in the successive extracts were confirmed by thin layer chromatography (TLC) studies. R_f values were noted in Table 4.5 and 4.6. Total methanol extract of LNL and LNR were separated in three different solvent systems to separate non-polar, medium polar and polar components on HPTLC. This provides the rapid quality control method to standardize crude plant material as well as extracts.

Table 4.5: TLC Profile of successive extracts of *Leonotis nepetaefolia* leaves

	Solvent system	Detection	Pet. Ether	Benzene	Chloroform	Et. Ac.	Methanol	Water
Carbohydrate	Butanol: GAA: H ₂ O (4:1:5)	10% H ₂ SO ₄	-	-	-	-	0.45, 0.64, 0.86	0.42, 0.68, 0.84
Phenolics	Tol: Et Ac: FA: Water (20:100:10:10)	5% FeCl ₃	-	-	-	0.24, 0.44, 0.48, 0.55, 0.64, 0.72	0.28, 0.44, 0.48, 0.55, 0.72, 0.92	0.24, 0.41, 0.48, 0.58, 0.72, 0.96
Flavonoids	Et Ac: GAA: FA: H ₂ O (100:11:11:26)	Alk. KOH & NPPEG	-	-	-	0.58, 0.7, 0.92, 0.97	0.5, 0.58, 0.92, 0.97	0.58, 0.65, 0.92, 0.97
Alkaloids	Et Ac: MeOH: CHCl ₃ : NH ₃	Dragendroff's reagent	-	-	-	-	-	0.70
Sterols and steroids	Pet Eth: Et Ac (4:1)	Libermann burchad's reagent	0.35, 0.38, 0.56, 0.78, 0.95	0.23, 0.52, 0.59, 0.84, 0.95	0.36, 0.56, 0.62, 0.78	-	0.23, 0.28, 0.32, 0.54, 0.62, 0.68, 0.98	-
Terpenoids	Benzene: Ether (2:3)	20 % SbCl ₃ in CHCl ₃	-	0.35, 0.45, 0.58, 0.65, 0.84	0.35, 0.48, 0.53, 0.62, 0.88	0.45, 0.56, 0.68, 0.86	-	-

Results and Discussion

Table 4.6: TLC Profile of successive extracts of *Leonotis nepetaefolia* root

	Solvent system	Detection	Pet. Ether	Benzene	Chloroform	Et. Ac.	Methanol	Water
Carbohydrate	Butanol: GAA: H ₂ O (4:1:5)	10% H ₂ SO ₄	-	-	-	-	0.42, 0.58, 0.74	0.42, 0.57, 0.75
Phenolics	Tol: Et Ac: FA: Water (20:100:10:10)	5% FeCl ₃	-	-	-	0.28, 0.45, 0.48, 0.57, 0.68, 0.79	0.32, 0.45, 0.52, 0.59, 0.74, 0.93	0.43, 0.48, 0.58, 0.76, 0.94
Flavonoids	Et Ac: GAA: FA: H ₂ O (100:11:11:26)	Alk. KOH & NPPEG	-	-	-	0.34, 0.58, 0.7, 0.92, 0.97	0.42, 0.63, 0.92, 0.97	0.58, 0.65, 0.94, 0.96
Alkaloids	Dioxane: NH ₃	Dragendroff reagent	-	-	-	-	-	-
Sterols and steroids	Pet Ether: Et Ac (4:1)	Libermann burchad's reagent	-	0.35, 0.38, 0.52, 0.76	0.34, 0.55, 0.62, 0.79	-	0.24, 0.28, 0.54, 0.66, 0.98	-
Terpenoids	Benzene: Ether (2:3)	20 % SbCl ₃ in CHCl ₃	0.35, 0.56	0.38, 0.45, 0.68	0.34, 0.57, 0.72, 0.84	0.40, 0.54, 0.68, 0.88	-	-

4.1.6. Estimation of secondary metabolites

Successive extraction process separated polar and non polar constituents. It was evaluated by TLC method and major secondary metabolite like phenolic and flavonoids were estimated by reported methods. Higher amounts of flavonoids (31.23% w/w of total aqueous extract) were observed in total aqueous extract in LNL (Table 4.7 and 4.8).

Table 4.7: Secondary metabolites *Leonotis nepetaefolia* leaves

Plant extract	Successive ethyl acetate extract	Successive methanol extract	Successive water extract	Total methanol extract	Total water extract
Total phenolics (% w/w)	13.52	16.71	24.23	18.43	25.62
Total Flavonoids (%w/w)	18.56	24.62	28.23	25.81	31.23

Results and Discussion

Table 4.8: Secondary metabolites *Leonotis nepetaefolia* roots

Plant extract	Successive ethyl acetate extract	Successive methanol extract	Successive water extract	Total methanol extract	Total water extract
Total phenolics (% w/w)	10.16	13.15	15.23	16.24	18.56
Total Flavonoids (% w/w)	15.24	13.32	14.43	14.68	16.34

4.1.7. Fractionation and HPTLC studies of fractions

Dried leaf and root powder (2 kg, separately) was extracted in methanol using soxhlet extraction method, while aqueous extract was prepared by decoction, resulting in Total Methanol extract of leaf (TMLNL- 615 g), root (TMLNR-511 g) and total Aqueous extract of leaf (TWLNL-728 g) and root (TWLNR- 489 g). Total methanol extract was then diluted with hot distilled water and successively fractionated to diethyl ether (ET of TMLNL-82.5 g and ET of TMLNR- 76.4 g), ethyl acetate (EA of TMLNL-78.5 g and EA of TMLNR- 65 g) and n-butanol (n BuOH of TMLNL- 102 g and nBuOH of TMLNR-45 g) fractions and the residual methanol extract (RMLNL-84.4 g and RMLNR- 63.3 g) was collected. All the extracts, were then dried in vacuum and subjected to TLC for detection of phytoconstituents [196].

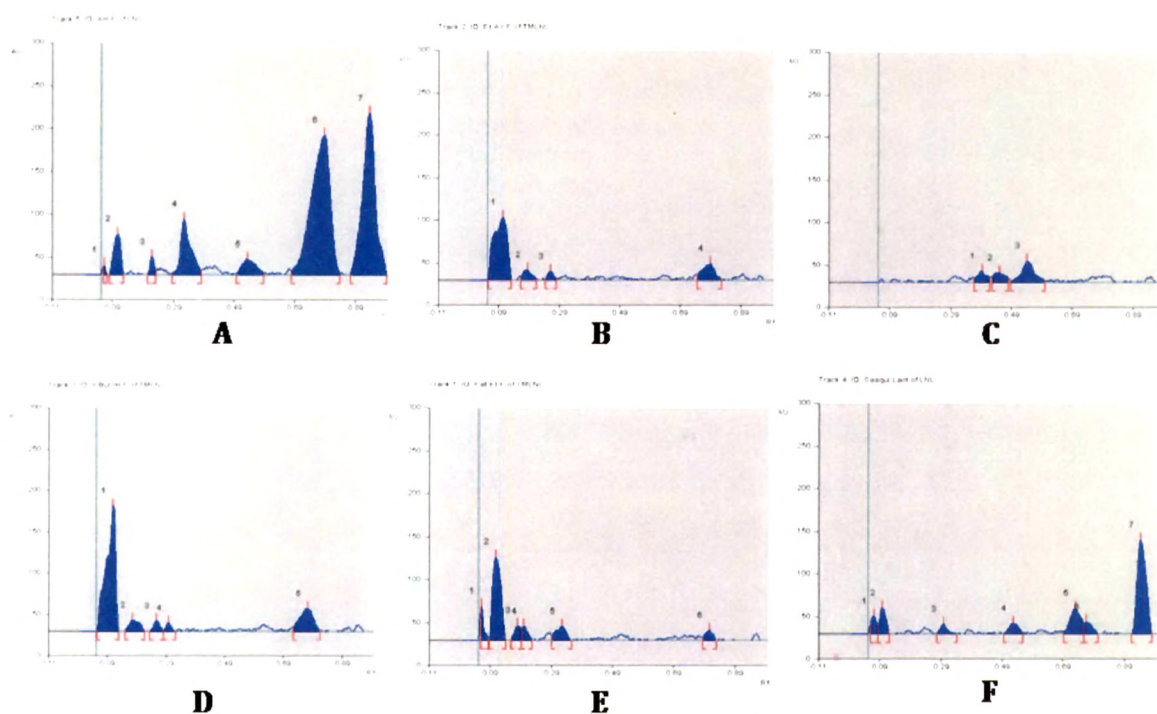
Terpene rich unsaponifiable fraction of LNL (yield 1.15% w/w) and LNR (yield 1.38% w/w) was prepared. Flavonoids were found in LNL and it is used as antioxidant, therefore, flavonoids rich fraction of LNL (yield 3.62 %w/w) was prepared. Alkaloid fraction of LNL (yield 0.86 %w/w) was prepared and one alkaloid LNLAL-01 was isolated. Total methanol extract was fractionated as chart shown below for bioactivity guided isolation of active compound as antiinflammatory. All the fractions were monitored by TLC and finger print was obtained in two mobile phases. Non-polar and polar compounds were separated on HPTLC and developed chromatograms were scanned and peaks of separated compounds are shown in figures 4.3-4.14. HPTLC fingerprints of the fractions were developed using suitable solvent systems which were optimized to resolve the major phytoconstituents present in particular fraction.

All the fractions were subjected to HPTLC fingerprint analysis. Different proportions of hexane, toluene, chloroform, ethyl acetate, methanol and water were tried, among these Petroleum ether:

Results and Discussion

ethyl acetate (3:1 v/v), Ethyl acetate: formic acid: methanol (4:0.25:0.5 v/v), Toluene: ethyl acetate: methanol: ammonia (1:1.5:2:0.25 v/v) mobile phases were found most suitable for separation of non polar, medium polar and polar compounds of methanolic extract of leaf of *L. nepetaefolia*. Hexane: ethyl acetate (3:1 v/v), Benzene: diethyl ether (2:3 v/v) and ethyl acetate: methanol: formic acid: water (2:1:0.25:0.5 v/v) were found to be most suitable solvent system for separation of phytoconstituents of *L. nepetaefolia* root extract.

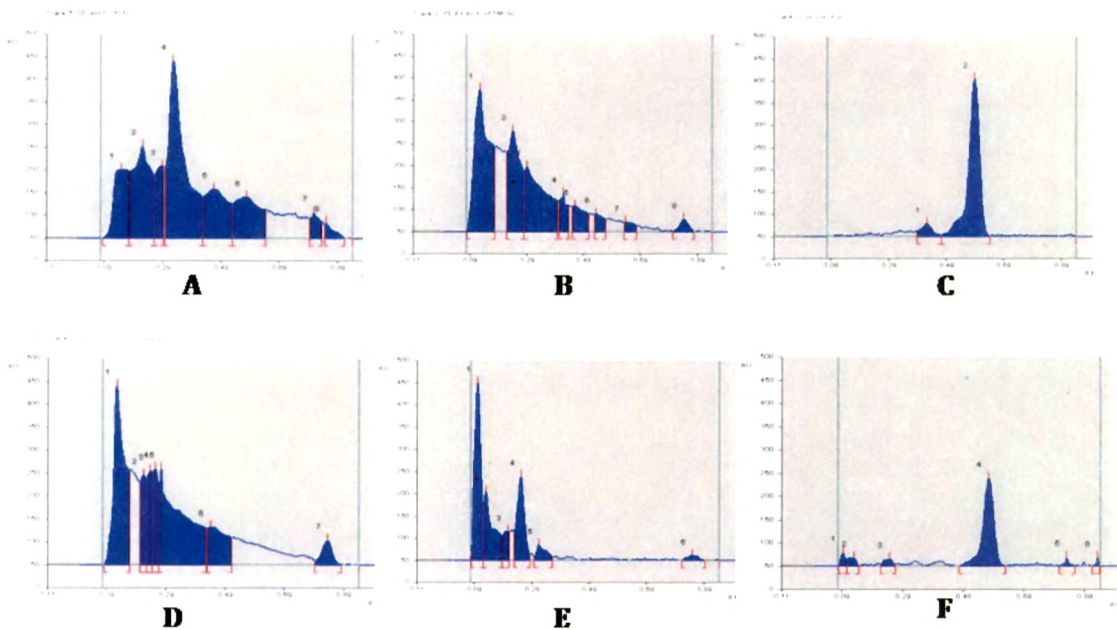
Detection was carried out by scanning at 254 and 366 nm. Plates were derivatized by anisaldehyde-sulphuric acid reagent and heated in an oven at 110°C for 10 min. Plates were scanned at 540 nm.



Fingerprinting of non-polar compounds at 254 nm from fractions of LN leaves extract

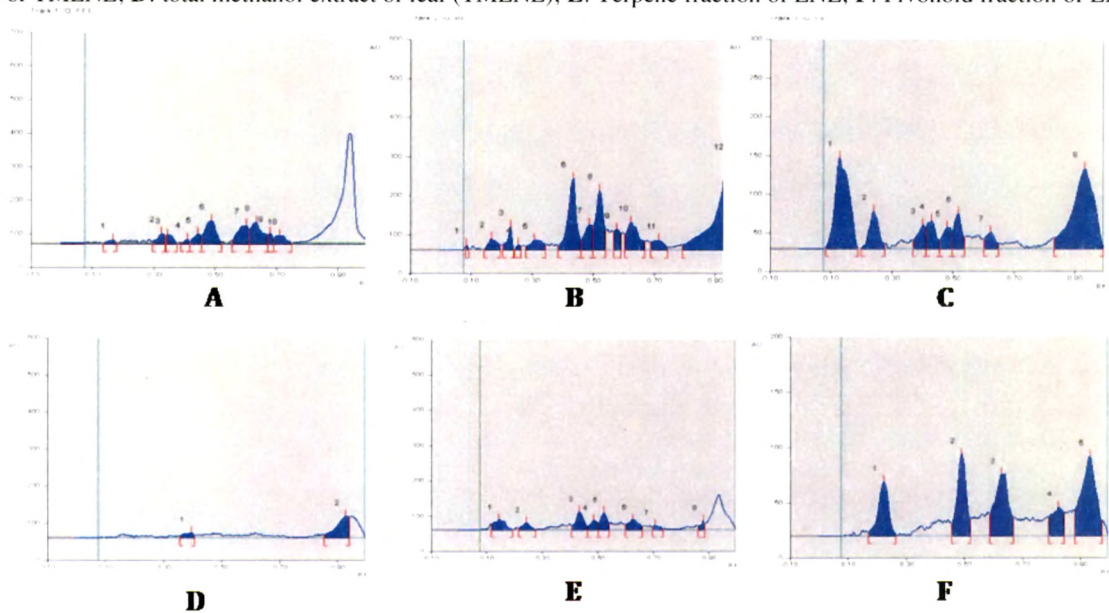
Figure 4.3: HPTLC fingerprint of LNL; **A:** Ether fraction of TMLNL; **B:** Ethyl acetate fraction of TMLNL; **C:** n-butanol fraction of TMLNL; **D:** total methanol extract of leaf (TMLNL); **E:** Terpene fraction of LNL; **F:** Flavonoid fraction of LNL

Results and Discussion



Fingerprinting of non-polar compounds at 366 nm from fractions of LN leaves extract

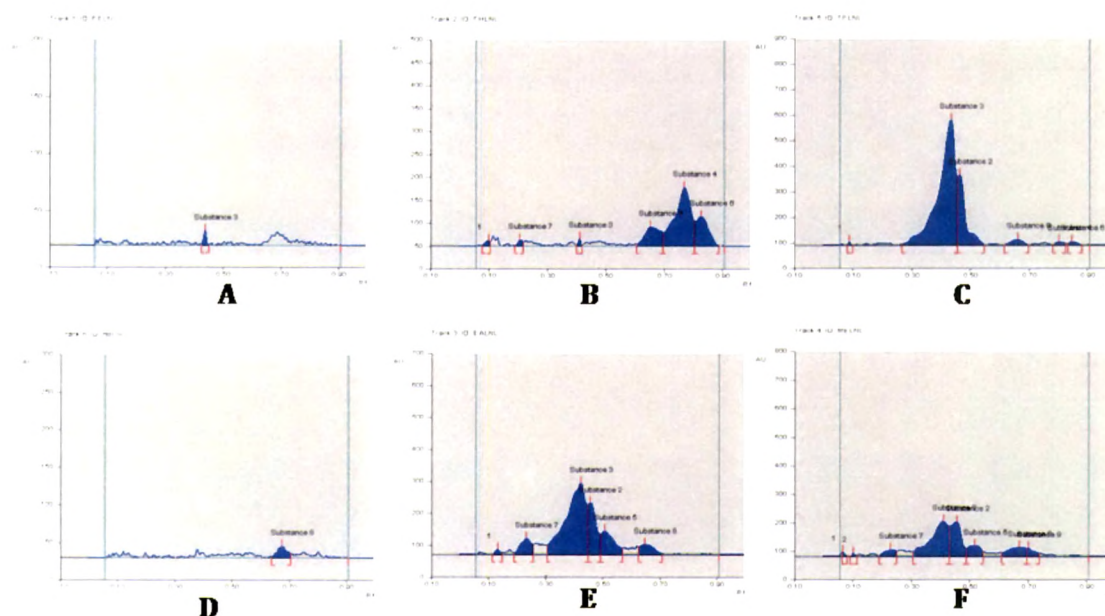
Figure 4.4: HPTLC fingerprint of LNL; **A:** Ether fraction of TMLNL; **B:** Ethyl acetate fraction of TMLNL; **C:** n-butanol fraction of TMLNL; **D:** total methanol extract of leaf (TMLNL); **E:** Terpene fraction of LNL; **F:** Flvonoid fraction of LNL



Fingerprinting of non-polar compounds at 540 nm from fractions of LN leaves extract

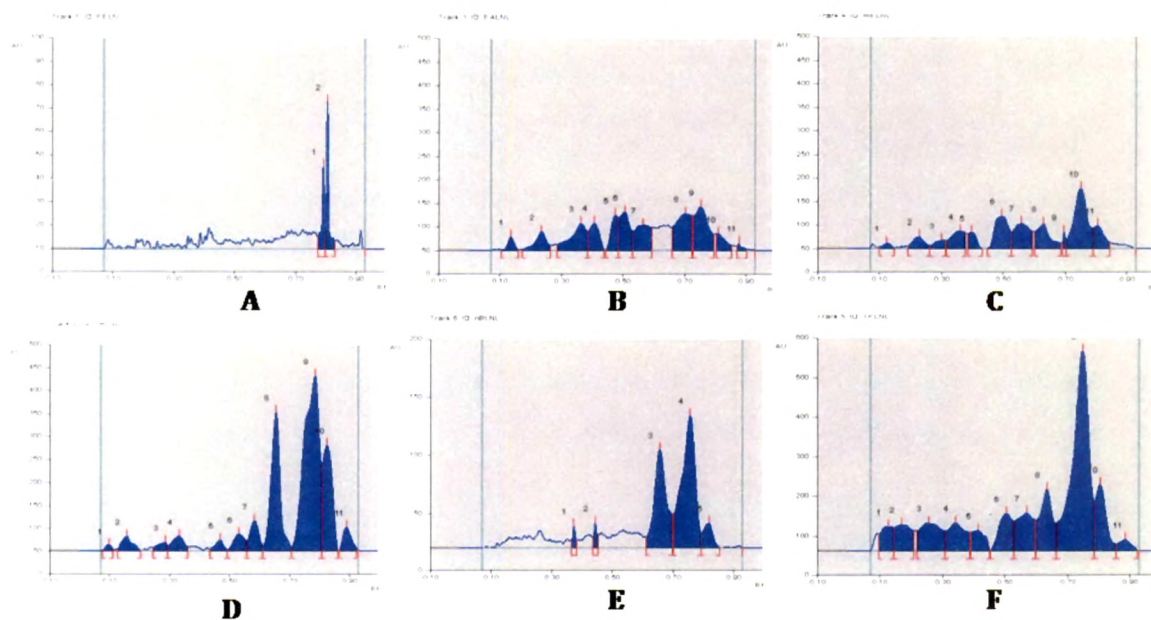
Figure 4.5: HPTLC fingerprint of LNL; **A:** Ether fraction of TMLNL; **B:** Ethyl acetate fraction of TMLNL; **C:** n-butanol fraction of TMLNL; **D:** total methanol extract of leaf (TMLNL); **E:** Terpene fraction of LNL; **F:** Flvonoid fraction of LNL

Results and Discussion



Fingerprinting of polar compounds at 254 nm from fractions of LN leaves extract

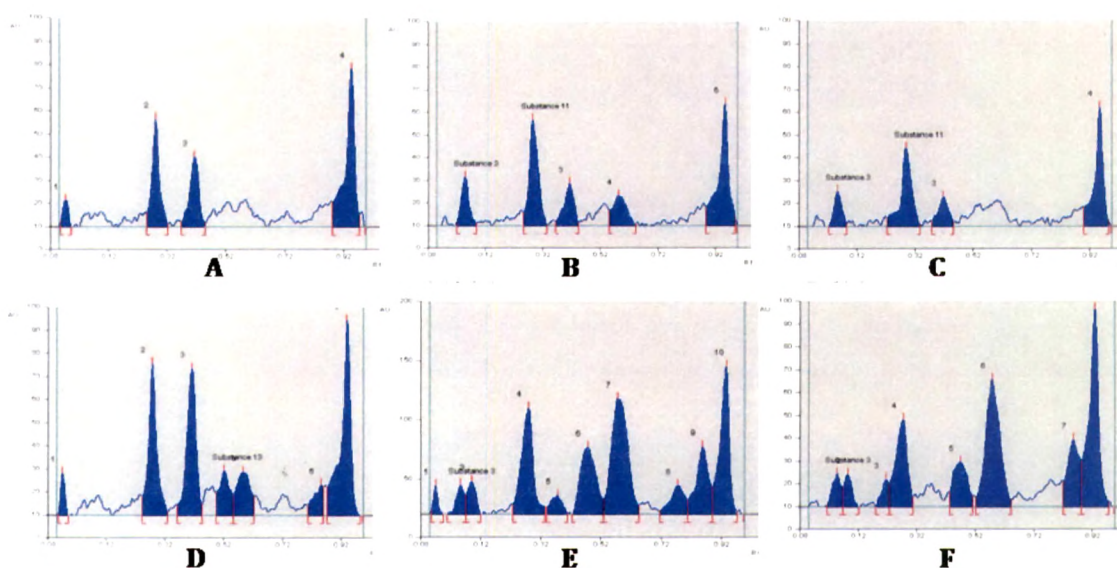
Figure 4.6: HPTLC fingerprint of LNL; **A:** Ether fraction of TMLNL; **B:** Ethyl acetate fraction of TMLNL; **C:** n-butanol fraction of TMLNL; **D:** total methanol extract of leaf (TMLNL); **E:** Terpene fraction of LNL; **F:** Flavonoid fraction of LNL



Fingerprinting of polar compounds at 366 nm from fractions of LN leaves extract

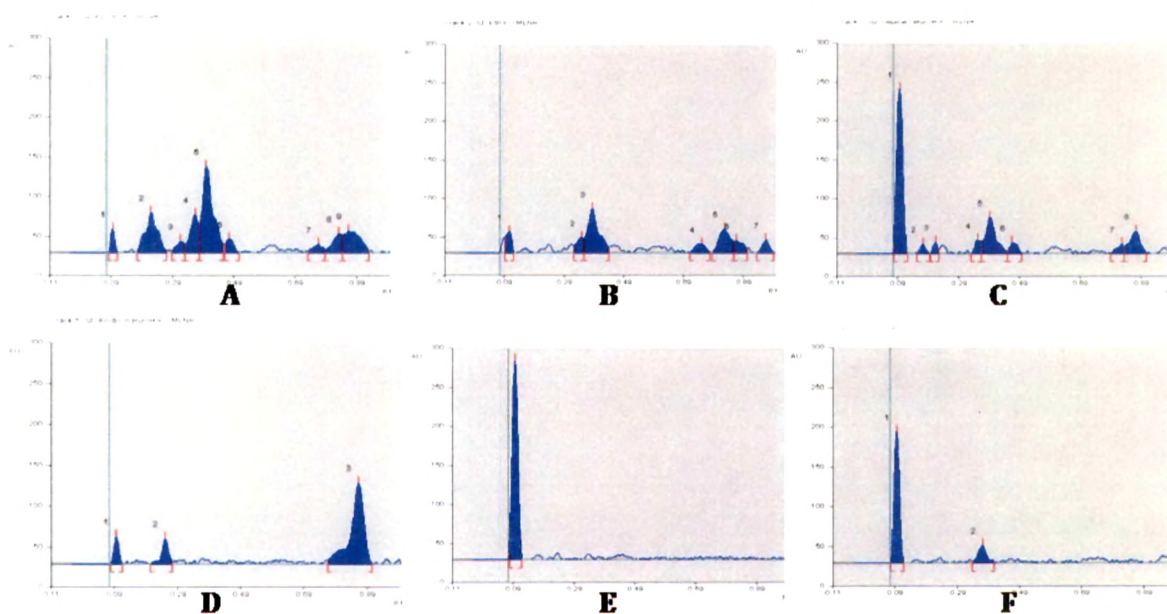
Figure 4.7: HPTLC fingerprint of LNL; **A:** Ether fraction of TMLNL; **B:** Ethyl acetate fraction of TMLNL; **C:** n-butanol fraction of TMLNL; **D:** total methanol extract of leaf (TMLNL); **E:** Terpene fraction of LNL; **F:** Flavonoid fraction of LNL

Results and Discussion



Fingerprinting of polar compounds at 540 nm from fractions of LN leaves extract

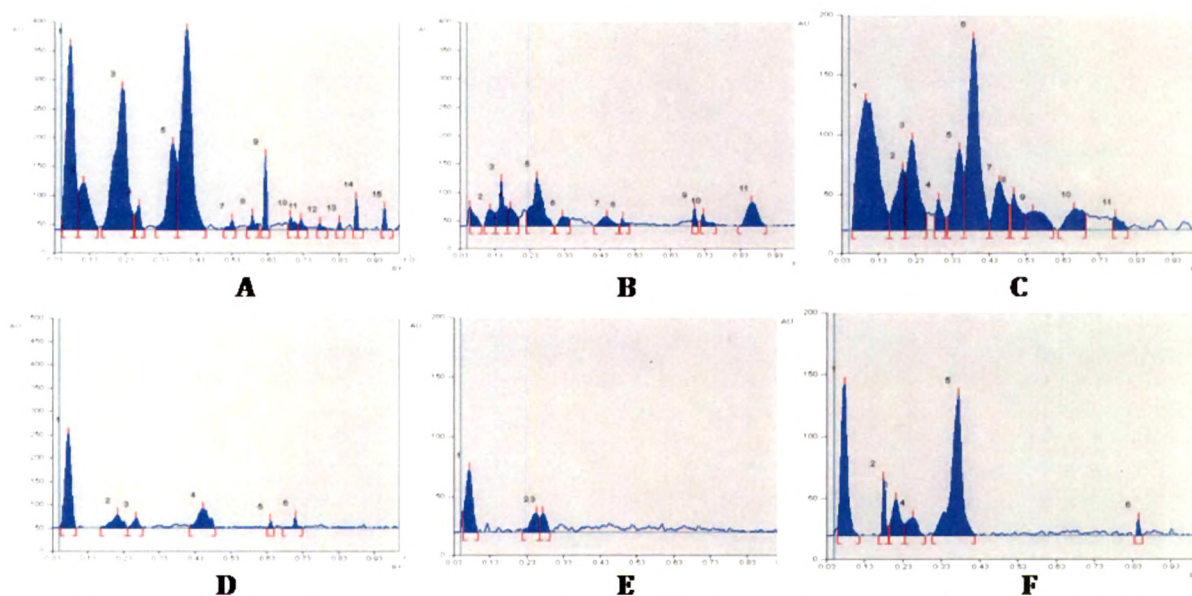
Figure 4.8: HPTLC fingerprint of LNL; A: Ether fraction of TMLNL; B: Ethyl acetate fraction of TMLNL; C: n-butanol fraction of TMLNL; D: total methanol extract of leaf (TMLNL); E: Terpene fraction of LNL; F: Flavonoid fraction of LNL



Fingerprinting of non-polar compounds at 254 nm from fractions of LN root extract

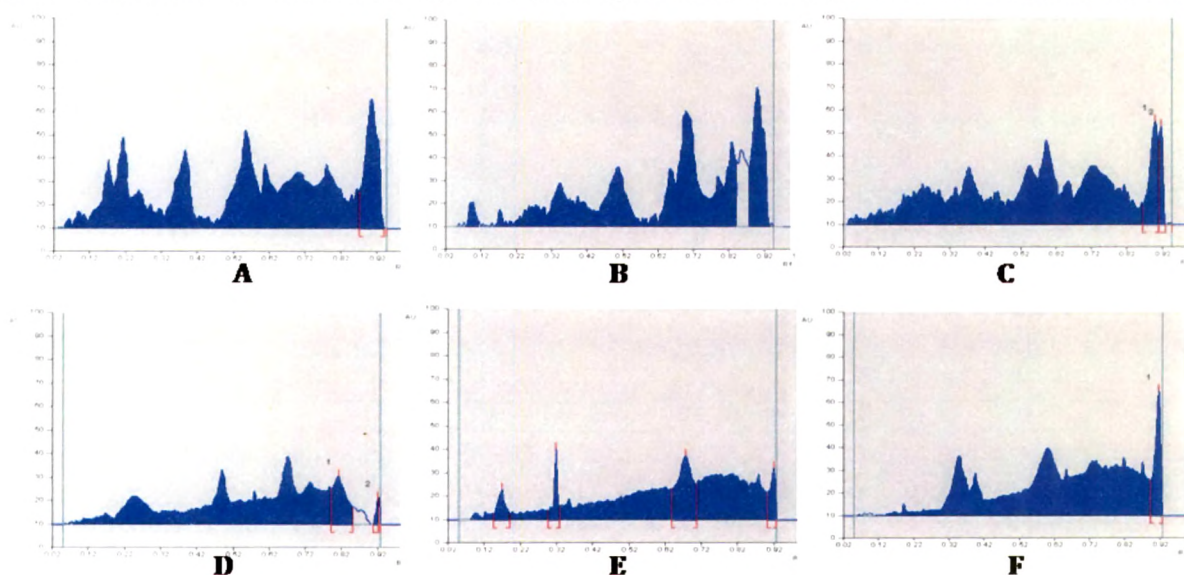
Figure 4.9: HPTLC fingerprint of LNR; A: Ether fraction of TMLNR; B: Ethyl acetate fraction of TMLNR; C: n-butanol fraction of TMLNR; D: total methanol extract (TMLNR); E: Terpene fraction of LNR; F: Residual methanol fraction of LNR

Results and Discussion



Fingerprinting of non-polar compounds at 366 nm from fractions of LN root extract

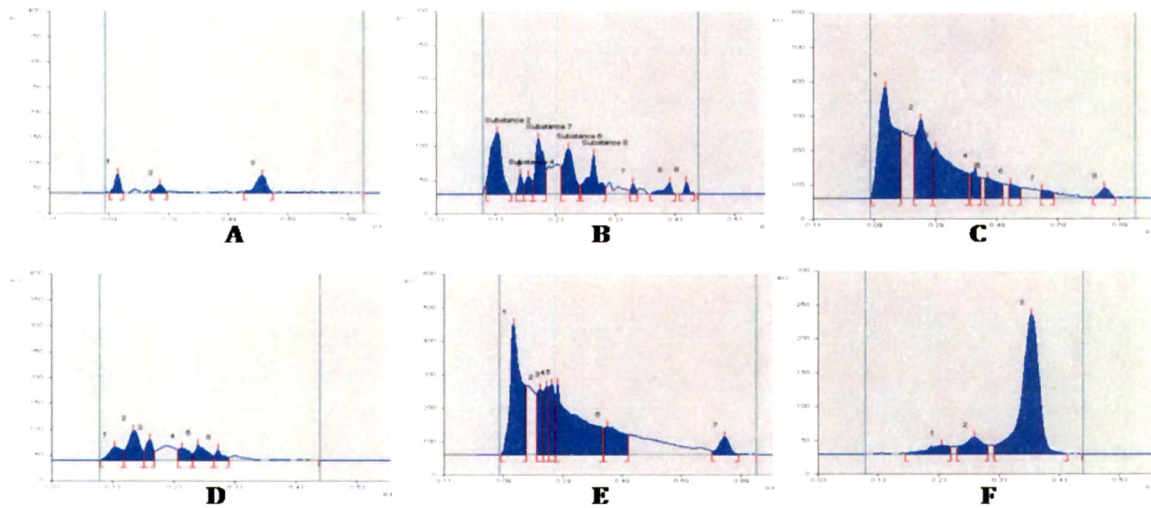
Figure 4.10: HPTLC fingerprint of LNR; **A:** Ether fraction of TMLNR; **B:** Ethyl acetate fraction of TMLNR; **C:** n-butanol fraction of TMLNR; **D:** total methanol extract (TMLNR); **E:** Terpene fraction of LNR; **F:** Residual methanol fraction of LNR



Fingerprinting of non-polar compounds at 540 nm from fractions of LN root extract

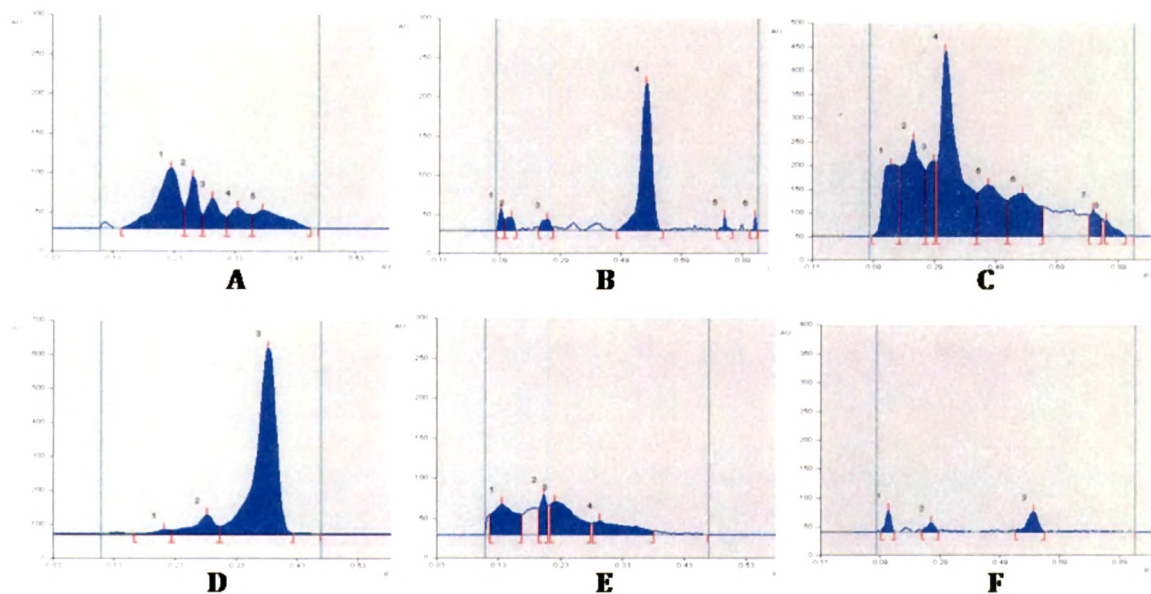
Figure 4.11: HPTLC fingerprint of LNR; **A:** Ether fraction of TMLNR; **B:** Ethyl acetate fraction of TMLNR; **C:** n-butanol fraction of TMLNR; **D:** total methanol extract (TMLNR); **E:** Terpene fraction of LNR; **F:** Residual methanol fraction of LNR

Results and Discussion



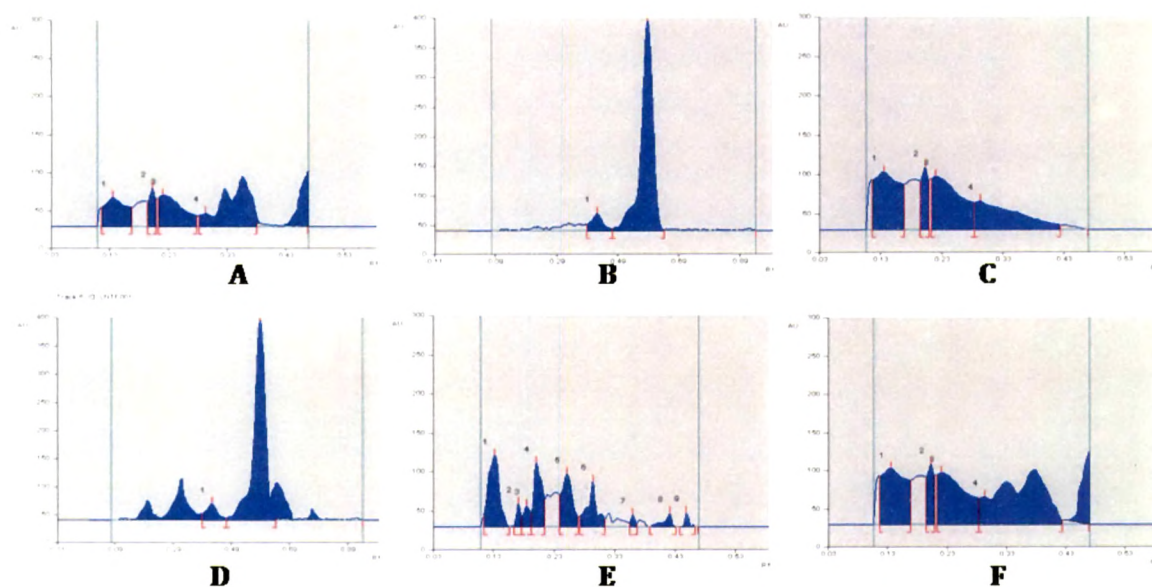
Fingerprinting of polar compounds at 254 nm from fractions of LN root extract

Figure 4.12: HPTLC fingerprint of LNR; **A:** Ether fraction of TMLNR; **B:** Ethyl acetate fraction of TMLNR; **C:** n-butanol fraction of TMLNR; **D:** total methanol extract (TMLNR); **E:** Terpene fraction of LNR; **F:** Residual methanol fraction of LNR



Fingerprinting of polar compounds at 366 nm from fractions of LN root extract

Figure 4.13: HPTLC fingerprint of LNR; **A:** Ether fraction of TMLNR; **B:** Ethyl acetate fraction of TMLNR; **C:** n-butanol fraction of TMLNR; **D:** total methanol extract (TMLNR); **E:** Terpene fraction of LNR; **F:** Residual methanol fraction of LNR



Fingerprinting of polar compounds at 540 nm from fractions of LN root extract

Figure 4.14: HPTLC fingerprint of LNR; **A:** Ether fraction of TMLNR; **B:** Ethyl acetate fraction of TMLNR; **C:** n-butanol fraction of TMLNR; **D:** total methanol extract (TMLNR); **E:** Terpene fraction of LNR; **F:** Residual methanol fraction of LNR

4.1.8. Quantitative estimation of alkaloid LNLAL-01 in *L. nepetaefolia* leaves

Different compositions of the mobile phase were tested and the desired resolution of LNLAL-01 with symmetrical and reproducible peaks was achieved by using mobile phase of chloroform: ethyl acetate: methanol (3.5:1.0:0.5 v/v) with 20 min of chamber saturation with the mobile phase. A peak corresponding to LNLAL-01 was seen at R_f 0.52 (Figure 4.15). Alkaloid fraction of LNL, when subjected to TLC, showed the presence of LNLAL-01 peaks. A comparison of the spectral characteristics of the peaks for isolated LNLAL-01 and that of the fraction revealed the identity of alkaloid present in the leaves. Peak purity test of LNLAL-01 was done by comparing its UV-visible spectra in standard and sample track.

Results and Discussion

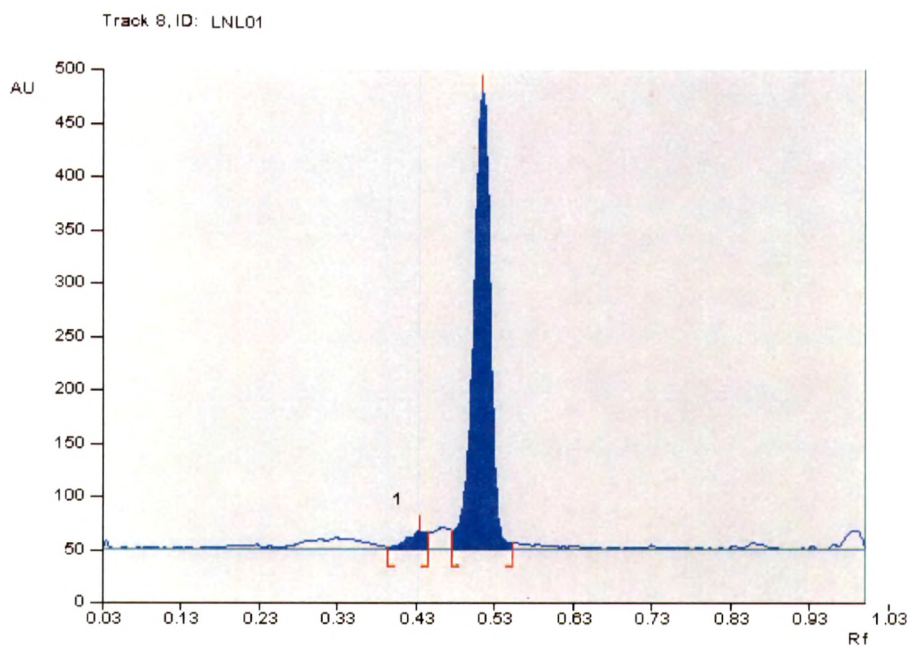


Figure 4.15: HPTLC estimation of LNLAL-01; A: isolated LNLAL-01 track

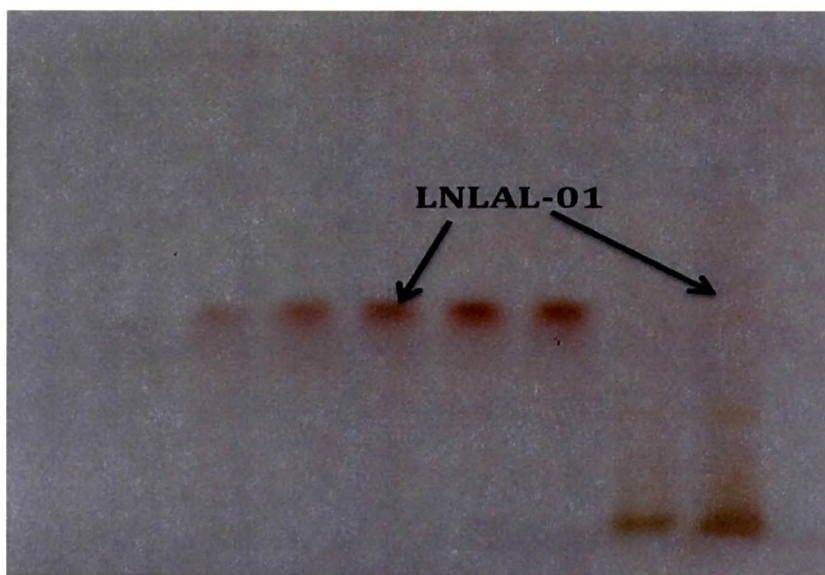


Figure 4.15: HPTLC estimation of LNLAL-01; B TLC plate showing isolated LNLAL-01 with alkaloid fraction of LNL, sprayed with Dragendorff's reagent.

Results and Discussion

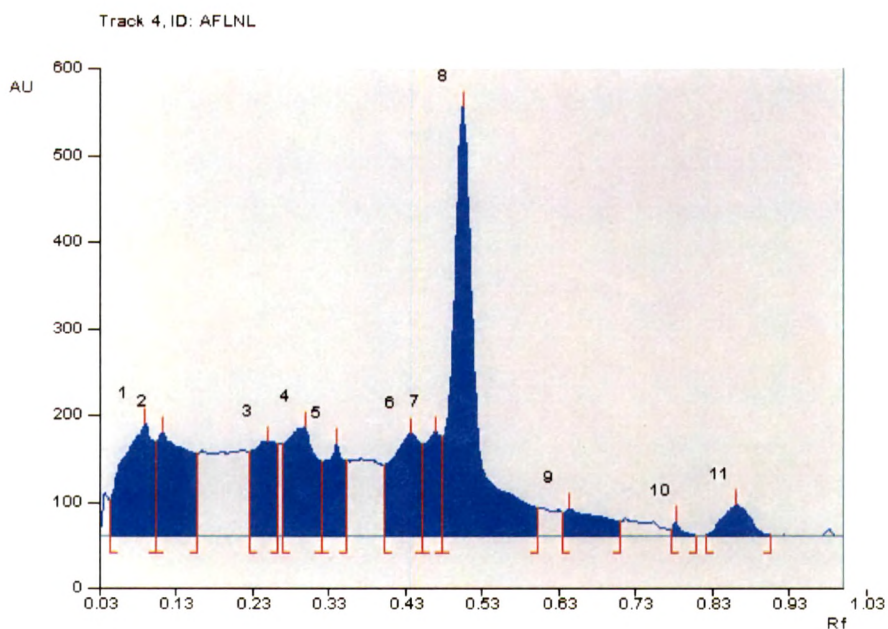


Figure 4.15: HPTLC estimation of LNLAL-01; C: track of alkaloidal fraction of LNL

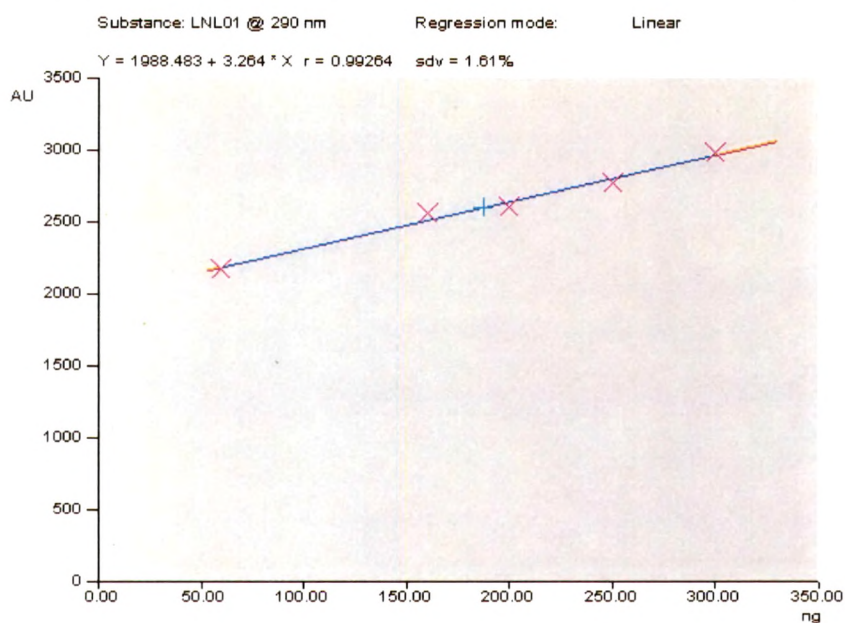


Figure 4.15: HPTLC estimation of LNLAL-01; D: Calibration curve of LNLAL-01

Results and Discussion

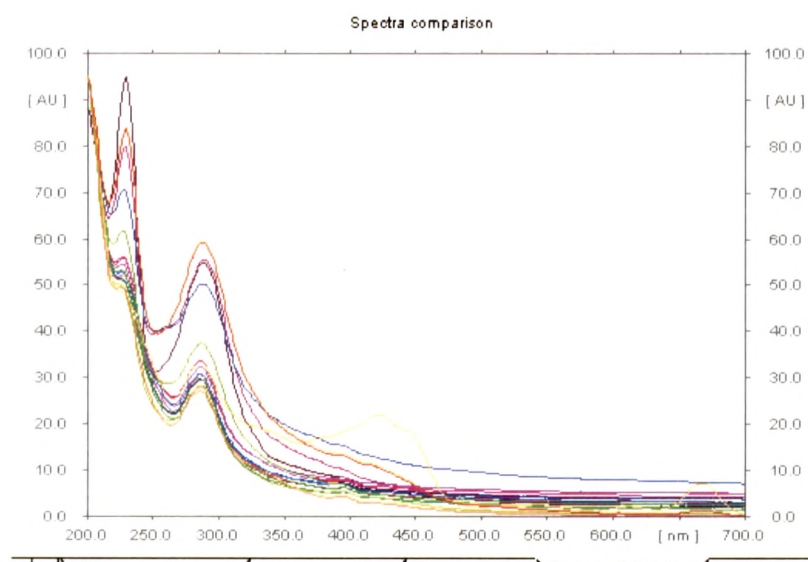


Figure 4.15: HPTLC estimation of LNLAL-01; E: overlaid spectra of LNLAL-01 in all the tracks

4.1.8.1. Method validation

Linearity was checked by applying standard solutions of LNLAL-01 at six different concentration levels. The calibration curve was drawn in the concentration range of 50–400 ng/spot. Results of regression analysis on calibration curve and detection limits are presented in table 4.9. Instrumental precision was checked by repeated scanning of the same spots (200 and 500 ng/spot) of standard LNLAL-01 three times and the RSD values were 1.46 and 2.13 for 200 and 500 ng/spot, respectively. To determine the precision of the developed assay method 200 and 500 ng/spot of alkaloid standard was analyzed three times within the same day to determine the intra-day variability. The RSD values were 1.18 and 0.85 for 200 and 500 ng/spot, respectively. Similarly, the inter-day precision was tested on the same concentration levels on two days and the RSD values were 0.92 and 1.60, respectively.

For the examination of recovery rates, 80, 100 and 120% of pure LNLAL-01 were spiked to preanalyzed sample and quantitative analysis was performed. The content of LNLAL-01 in the *L. nepetaefolia* leaves by HPTLC method was found to be 0.082% w/w.

Results and Discussion

Table 4.9: Validation parameters for quantification of LNLAL-01 by HPTLC

Parameters	Values
Detection wavelength	290 nm
Range	50-400 ng/spot
Limit of Detection (LOD)	20 ng
Limit of Quantification (LOQ)	73.26 ng
Regression equation	$Y = 2006.48 + 3.228 * X$
Correlation coefficient (linearity)	0.9927
Recovery study	
80% level	96.48 ± 0.743
100% level	103.43 ± 1.232
120% level	98.34 ± 0.983
Precision study (%RSD)	
Intra-day	0.92
Inter-day	1.60

4.1.9. Quantification of β -sitosterol in *L. nepetaefolia*

Different compositions of the mobile phase were tested and the desired resolution of β -sitosterol with symmetrical and reproducible peaks was achieved by using mobile phase of toluene: chloroform: methanol (4:4:1 v/v) with 20 min of chamber saturation with the mobile phase. The post chromatographic derivatization was carried out in anisaldehyde-sulphuric acid followed by heating at 110 °C for 5 min. A peak corresponding to β -sitosterol was seen at R_f 0.42 (Figure 4.16). Unsaponifiable fraction of LNL and LNR, when subjected to TLC, showed the presence of β -sitosterol peaks. A comparison of the spectral characteristics of the peaks for standard β -sitosterol and that of the fraction revealed the identity of β -sitosterol present in the plant. Peak purity test of β -sitosterol was done by comparing its UV-visible spectra in standard and sample track.

Results and Discussion

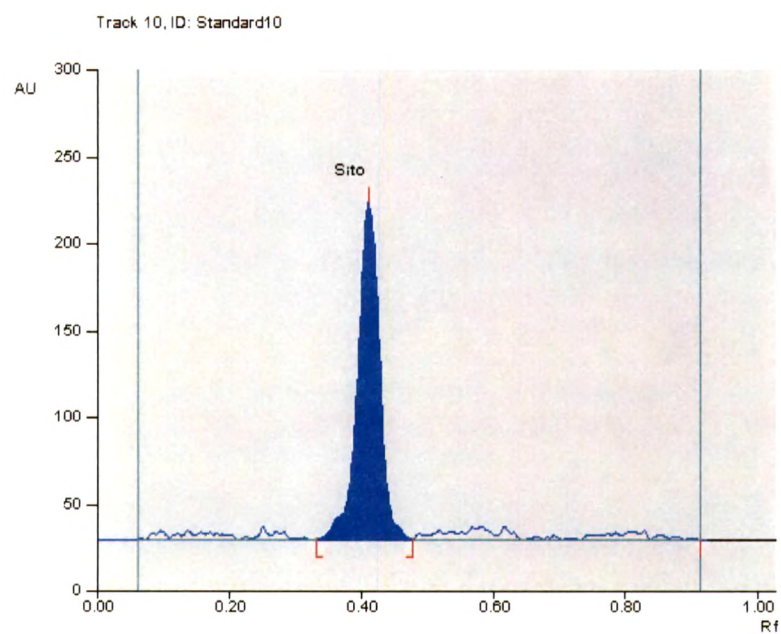


Figure 4.16: HPTLC estimation of LN-02 in LN; **A:** Standard β -sitosterol track after spraying with anisaldehyde-sulphuric acid reagent.

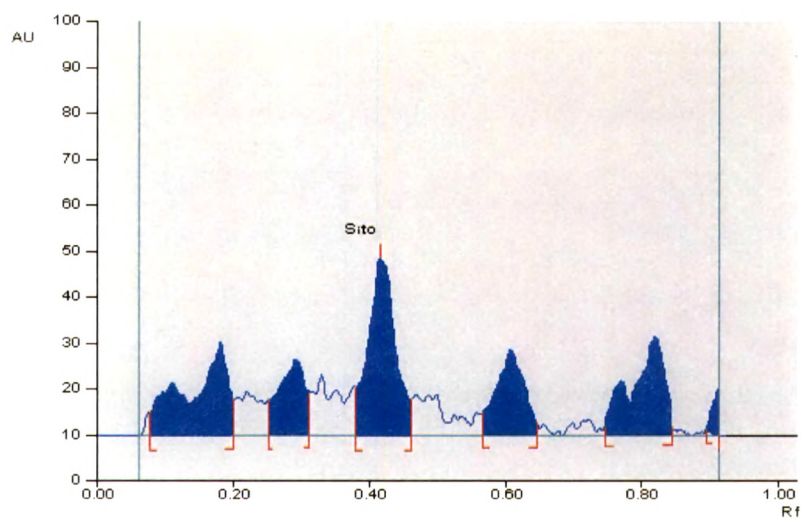


Figure 4.16: HPTLC estimation of LN-02 in LN; **B:** Unsaponifiable fraction of LNL

Results and Discussion

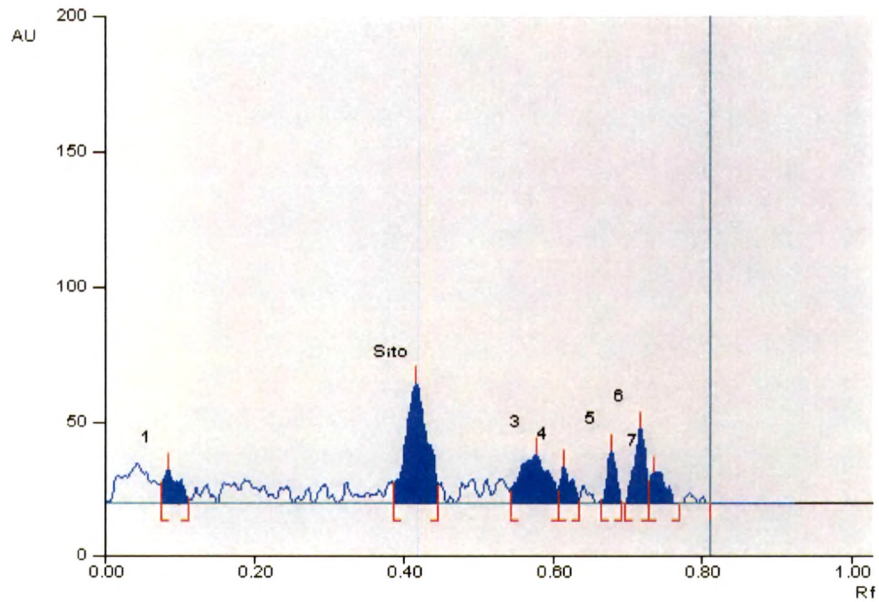


Figure 4.16: HPTLC estimation of LN-02 in LN; **C:** Unsaponifiable fraction of LNR

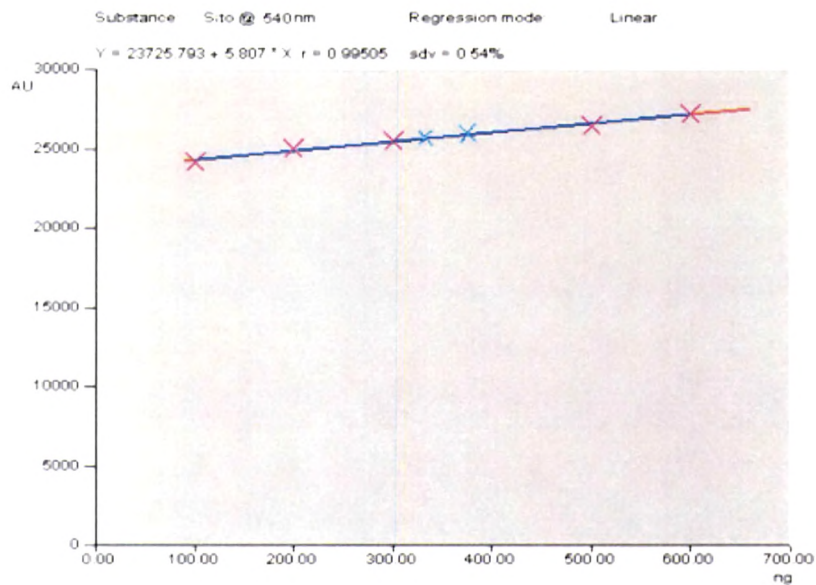


Figure 4.16: HPTLC estimation of LN-02 in LN; **D:** calibration curve of standard β -sitosterol

Results and Discussion

4.1.9.1. Method validation

Linearity was checked by applying standard solutions of β -sitosterol at six different concentration levels. The calibration curve was drawn in the concentration range of 100–600 ng/spot. Results of regression analysis on calibration curve and detection limits are presented in table 4.10. To determine the precision of the developed method 200 and 500 ng/spot of β -sitosterol standard was analyzed three times within the same day to determine the intra-day variability. The RSD values were 1.48 and 1.28 for 200 and 500 ng/spot, respectively. Similarly, the inter-day precision was tested on the same concentration levels on two days and the RSD values were 0.89 and 1.37, respectively.

Table 4.10: Validation parameters for quantification of β -sitosterol by HPTLC

Parameters	Values
Detection wavelength	540 nm
Range	100-600 ng/spot
Limit of Detection (LOD)	30 ng
Limit of Quantification (LOQ)	99.39 ng
Regression equation	$Y = 23725.79 + 5.807 * X$
Correlation coefficient (linearity)	0.99505
Recovery study	
80% level	96.48 \pm 0.743
100% level	103.43 \pm 1.232
120% level	98.34 \pm 0.983
Precision study (%RSD)	
Intra-day	0.89
Inter-day	1.37

The content of β -sitosterol in the LNL and LNR by HPTLC method was found to be 0.083% w/w and 0.0646 % w/w respectively. For the examination of recovery, 80, 100 and 120% of pure β -sitosterol were spiked to preanalyzed sample and quantitative analysis was performed.

Results and Discussion

4.1.10. Quantitative estimation of LNLAL-01 in *L. nepetaefolia* leaves by HPLC

LNLAL-01 was estimated by HPLC in alkaloid fraction of LNL at 290 nm wavelength with flow rate of 0.8 mL/min. The retention time (R_t) of isolated alkaloid was found to be 3.447 min in mobile phase consisting acetonitrile-water (3.5:6.5, v/v) with 1% diethylamine (Figure 4.17). LNLAL-01 was quantified in alkaloid fraction by using regression equation $y = 1.918x + 2.639$ with correlation coefficient $R^2 = 0.994$.

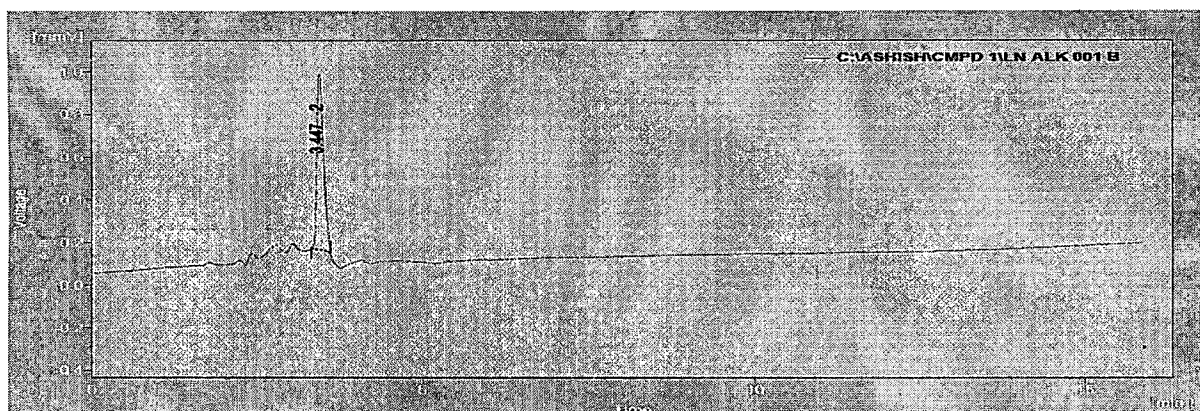


Figure 4.17: HPLC Chromatogram of isolated LNLAL-01

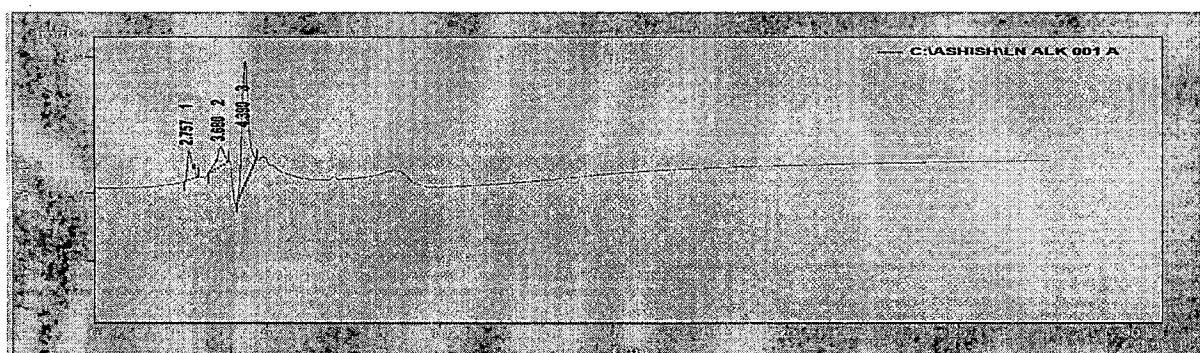


Figure 4.18: HPLC Chromatogram of alkaloid fraction of *L. nepetaefolia* leaves

4.1.10.1. Method validation

The calibration curve was drawn in the concentration range of 20-150 $\mu\text{g/mL}$. Results of regression analysis on calibration curve and detection limits are presented in table 4.11.

Results and Discussion

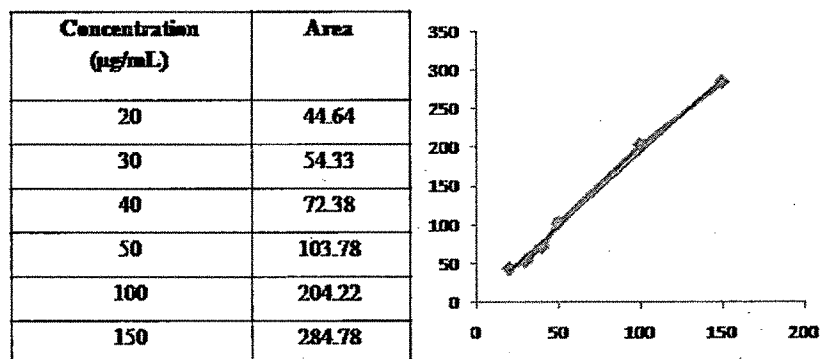


Figure 4.19: Calibration curve of LNLAL-01 for quantification in alkaloid fraction by HPLC

Linearity was checked by applying standard solutions of LNLAL-01 at six different concentration levels. Instrumental precision was checked by repeated injection of the sample (50 $\mu\text{g/mL}$) of standard LNLAL-01 five times and the mean % RSD value was 0.48 ± 0.07842 .

Table 4.11: Validation parameters for quantification of LNLAL-01 by HPLC

Parameters	Values
Detection wavelength	290 nm
Flow rate	0.8 mL/min
Range	20-150 $\mu\text{g/mL}$
Limit-of Detection (LOD)	5 $\mu\text{g/mL}$
Limit of Quantification (LOQ)	16.65 $\mu\text{g/mL}$
Regression equation	$y = 1.918 * X + 2.639$
Correlation coefficient (linearity)	0.994
Recovery study	
80% level	94.72 ± 0.0433
100% level	98.33 ± 1.73
120% level	96.34 ± 0.563
Precision study (%RSD)	
Intra-day	0.84
Inter-day	0.88

Results and Discussion

To determine the precision of the developed assay method 50 and 100 µg/injection of alkaloid standard was analyzed three times within the same day to determine the intra-day variability. The RSD values were found to be 0.52, 1.15 for 50 and 100 µg/mL, respectively. Similarly, the inter-day precision was tested on the same concentration levels on two days and the RSD values were 0.71 and 1.05, respectively.

For the examination of recovery, 80, 100 and 120% of isolated alkaloid were spiked to preanalyzed sample and quantitative analysis was performed. The content of LNLAL-01 in the *L. nepetaefolia* leaves by HPLC method was found to be 0.076% w/w.

4.1.11. Biological studies

4.1.11.1. Acute toxicity studies

Acute toxicity studies were performed following OECD guidelines (2001) (OECD 423, Acute Toxic Class Method) (Roll et al., 1986) [208]. Oral dose of 2000 mg/kg and 3000 mg/kg of the test extracts and 500 mg/kg and 1000 mg/kg of fractions were given orally to different groups of female rats. The animals were observed for first 4 hours of treatment to next 14 days. There were no signs of any toxicity in animals after the administration of the test doses. All the animals showed similar food intake, body weight gain and clinical signs as that of the control group. No morbidity or mortality was observed in the treated animals. The necropsy studies did not detect any abnormality.

4.1.11.2. In-vitro antioxidant activity

All fractions were studied for their antioxidant potential at concentration of 10, 20, 40, 80, 100 µg/mL. Three methods were selected viz. DPPH radical scavenging assay, FeCl₂ reducing power and phosphomolybdenum method. Ascorbic acid and Butylated Hydroxy Toluene (BHT) were selected as standard.

4.1.11.2.1. DPPH radical scavenging

L. nepetaefolia constituents show antioxidant property in DPPH radical scavenging assay. The antioxidant activity of extracts was evaluated by their ability to scavenge free radicals by using DPPH assay. The extract concentration that caused scavenging of 50% of DPPH, (IC₅₀) was detected. As shown in (Table 4.12), IC₅₀ of extracts varied from 25.34 to 60.45 µg/mL giving significantly lower potencies than ascorbic acid (IC₅₀ -10.44). IC₅₀ of terpene rich fractions of LNL (TER LNL-32.42 µg/mL, UNS of LNL- 43.29 µg/mL), flavonoids rich fraction of LNL,

Results and Discussion

nBuOH of TMLNL-35.78 µg/mL, and total methanol extract of LNR (TMLNR- 25.34 µg/mL) was comparable to standards.

Table 4.12: % inhibition by various fractions of LN by DPPH method and IC₅₀ values

Samples	10	20	40	80	100	Linearity	IC ₅₀
TMLNL	24.32	38.53	45.66	67.32	78.31	y = 0.558x + 22.91	46.07
TWLNL	18.43	28.45	53.22	68.34	81.32	y = 0.665x + 16.67	50.12
TER LNL	32.53	46.42	59.53	71.34	87.43	y = 0.537x + 32.59	32.42
ET of TMLNL	22.32	35.23	49.42	61.22	74.22	y = 0.517x + 22.61	52.97
EA of TMLNL	12.34	29.55	41.24	62.24	72.42	y = 0.616x + 12.76	60.45
nBuOH of TMLNL	31.24	44.32	58.72	68.35	84.22	y = 0.515x + 31.57	35.78
UNS of LNL	23.11	39.79	52.32	72.11	83.59	y = 0.616x + 23.33	43.29
RTMLNL	18.34	27.53	39.53	59.34	82.15	y = 0.655x + 12.60	57.01
FFLNL	27.35	41.32	58.37	74.98	84.25	y = 0.590x + 27.71	37.78
TMLNR	31.32	51.22	68.42	77.42	82.53	y = 0.495x + 37.38	25.34
TWLNR	24.42	37.97	53.77	63.98	75.88	y = 0.51x + 25.70	47.64
TER LNR	15.35	28.93	47.52	68.89	79.78	y = 0.683x + 13.93	52.81
ET of TMLNR	14.34	32.57	44.54	57.78	78.9	y = 0.613x + 14.94	57.19
EA of TMLNR	11.21	24.58	36.75	72.42	82.42	y = 0.790x + 5.973	55.73
nBuOH of TMLNR	24.42	39.68	52.42	71.43	87.83	y = 0.640x + 23.13	41.98
UNS of LNR	16.54	28.89	46.26	68.32	79.12	y = 0.669x + 14.37	53.25
RTMLNR	23.23	31.08	48.88	61.32	73.56	y = 0.527x + 21.22	54.61
Ascorbic acid	38.45	47.51	68.32	78.42	94.32	y = 0.618x + 33.04	10.44
BHT	39.53	51.25	62.26	74.78	84.64	y = 0.482x + 37.57	23.78

TMLNL: Total methanol extract of *L. nepetaefolia* leaf, TWLNL: Total water extract of *L. nepetaefolia* leaf, TERLNL: Terpene fraction of *L. nepetaefolia* leaf, ET of TMLNL: ether fraction of TMLNL, EA of TMLNL: ethyl acetate fraction of TMLNL, nBuOH of TMLNL: n-butanol fraction of TMLNL, UNS of LNL: unsaponifiable fraction of LNL, RTMLNL: residual of TMLNL, FFLNL: flavonoid fraction of LNL, TMLNR: Total methanol extract of *L. nepetaefolia* root, TWLNR: Total water extract of *L. nepetaefolia* root, TERLNR: Terpene fraction of *L. nepetaefolia* root, ET of TMLNR: ether fraction of TMLNR, EA of TMLNR: ethyl acetate fraction of TMLNR, nBuOH of TMLNR: n-butanol fraction of TMLNR, UNS of LNR: unsaponifiable fraction of LNR, RTMLNR: residual of TMLNR, BHT: butylated hydroxytoluene.

4.1.11.2.2. FeCl₃ reducing power assay

The reducing power of a compound is related to its electron transferability and may serve as a significant indicator of its potential antioxidant activity. In this assay, the color of test solution changes to green and blue depending on the reducing power of test samples. The results (Table 4.13) show following fractions; TMLNL- 35.89 µg/mL, TWLNL- 37.82 µg/mL, EA of TMLNL- 34.29 µg/mL, nBuOH of TMLNL- 35.79 µg/mL, FFLNL- 34.74 µg/mL, TER LNR- 38.22 µg/mL and UNS of LNR- 46.27 µg/mL, have IC₅₀ comparable to standard ascorbic acid- 10.44 µg/mL and BHT 23.78 µg/mL.

Results and Discussion

Table 4.13: % inhibition by various fractions of LN by FeCl₃ method and IC₅₀ values

Samples	10	20	40	80	100	Linearity	IC ₅₀
TMLNL	24.52	42.32	61.22	74.28	97.52	$y = 0.707x + 24.62$	35.89
TWLNL	28.88	41.72	58.39	68.32	87.92	$y = 0.575x + 28.25$	37.82
TER LNL	19.52	27.89	48.92	61.22	82.31	$y = 0.640x + 15.92$	53.25
ET of TMLNL	21.29	36.72	52.81	72.22	92.42	$y = 0.717x + 19.20$	42.95
EA of TMLNL	24.62	46.02	61.51	76.31	94.28	$y = 0.670x + 27.02$	34.29
nBuOH of TMLNL	32.91	41.78	52.11	72.98	96.87	$y = 0.657x + 26.48$	35.79
UNS of LNL	23.49	31.92	42.89	58.78	80.02	$y = 0.573x + 18.76$	54.52
RTMLNL	11.45	27.52	35.55	52.31	71.53	$y = 0.584x + 10.45$	72.18
FFLNL	30.01	42.42	54.53	78.91	98.78	$y = 0.714x + 25.19$	34.74
TMLNR	27.61	37.81	47.21	62.31	90.07	$y = 0.610x + 22.48$	45.11
TWLNR	22.11	31.41	44.41	52.41	89.51	$y = 0.629x + 16.49$	53.27
TER LNR	31.32	40.05	52.18	72.12	91.32	$y = 0.625x + 26.11$	38.22
ET of TMLNR	27.71	31.23	45.21	61.22	84.21	$y = 0.591x + 20.33$	50.20
EA of TMLNR	24.81	33.42	41.31	58.32	81.03	$y = 0.565x + 19.50$	53.98
nBuOH of TMLNR	18.92	27.62	34.21	49.21	78.76	$y = 0.581x + 12.68$	64.23
UNS of LNR	22.31	31.51	47.14	74.87	87.72	$y = 0.720x + 16.68$	46.27
RTMLNR	16.32	27.23	42.31	62.48	81.43	$y = 0.675x + 12.17$	56.04
Ascorbic acid	39.44	52.11	64.31	78.51	94.55	$y = 0.549x + 38.29$	11.33
BHT	38.21	44.81	64.7	82.32	98.32	$y = 0.644x + 33.45$	25.69

TMLNL: Total methanol extract of *L. nepetaefolia* leaf, TWLNL: Total water extract of *L. nepetaefolia* leaf, TERLNL: Terpene fraction of *L. nepetaefolia* leaf, ET of TMLNL: ether fraction of TMLNL, EA of TMLNL: ethyl acetate fraction of TMLNL, nBuOH of TMLNL: n-butanol fraction of TMLNL, UNS of LNL: unsaponifiable fraction of LNL, RTMLNL: residual of TMLNL, FFLNL: flavonoid fraction of LNL, TMLNR: Total methanol extract of *L. nepetaefolia* root, TWLNR: Total water extract of *L. nepetaefolia* root, TERLNR: Terpene fraction of *L. nepetaefolia* root, ET of TMLNR: ether fraction of TMLNR, EA of TMLNR: ethyl acetate fraction of TMLNR, nBuOH of TMLNR: n-butanol fraction of TMLNR, UNS of LNR: unsaponifiable fraction of LNR, RTMLNR: residual of TMLNR, BHT: butylated hydroxyl toluene.

4.1.11.2.3. Total antioxidant capacity by Phosphomolybdenum method

The formation of a green-colored complex of phosphate and Mo (V) was presented by Fiske and Subbarow [238] as the basis of a spectrophotometric method to determine inorganic phosphate. This method was later revised and modified by Chen *et al.* [239]. The required reducing species should be supplied with reagent mixture to produce Mo (V) from the Mo (VI). Plant extracts contain variety of antioxidant compounds and *L. nepetaefolia* has been evaluated for its antioxidant activity. Terpene and flavonoids present in fractions of *L. nepetaefolia* found to reducing molybdenum, IC₅₀ of fractions, TER LNL-23.50 µg/mL, nBuOH of TMLNL- 14.01 µg/mL, FFLNL- 22.51 µg/mL, TMLNR-22.48 µg/mL and EA of TMLNR-13.86 µg/mL, are comparable with standards.

Results and Discussion

Table 4.14: % inhibition by various fractions of LN by phosphomolybdenum method and IC values

Samples	10	20	40	80	100	Linearity	IC ₅₀
TMLNL	14.01	52.82	65.67	85.41	89.08	$y = 0.702x + 26.27$	33.80
TWLNL	24.42	48.33	63.44	78.41	88.42	$y = 0.618x + 29.66$	32.91
TER LNL	34.5	47.72	71.33	82.7	88.94	$y = 0.567x + 36.67$	23.50
ET of TMLNL	9.8	56.6	71.33	82.7	87.43	$y = 0.674x + 27.82$	32.90
EA of TMLNL	10.43	38.42	49.42	62.53	73.53	$y = 0.581x + 17.79$	55.43
nBuOH of TMLNL	22.68	70.91	78.4	85.18	90.14	$y = 0.540x + 42.43$	14.01
UNS of LNL	12.53	32.53	51.32	68.59	72.55	$y = 0.615x + 16.71$	54.13
RTMLNL	27.45	38.54	48.32	72.43	87.42	$y = 0.634x + 23.11$	42.41
FFLNL	34.56	52.45	68.52	78.53	92.42	$y = 0.556x + 37.49$	22.51
TMLNR	26.4	57.99	71.6	85.69	89.91	$y = 0.592x + 36.69$	22.48
TWLNR	8.91	57.79	73.41	82.44	85.18	$y = 0.651x + 28.97$	32.30
TER LNR	20.68	45.88	66.66	83.15	87.23	$y = 0.664x + 27.50$	33.88
ET of TMLNR	29.53	48.53	59.33	72.55	81.22	$y = 0.501x + 33.17$	33.59
EA of TMLNR	34.32	57.88	78.35	88.14	91.43	$y = 0.553x + 42.33$	13.86
nBuOH of TMLNR	8.9	27.52	38.45	66.35	73.24	$y = 0.681x + 8.838$	60.44
UNS of LNR	13.53	38.53	53.53	69.35	82.51	$y = 0.662x + 18.37$	47.77
RTMLNR	23.55	34.32	51.35	73.53	81.35	$y = 0.631x + 21.25$	45.57
Ascorbic acid	47.12	56.6	73.33	85.48	87.79	$y = 0.439x + 48.08$	4.37
BHT	35.21	67.37	74.3	83.02	88.69	$y = 0.458x + 46.78$	7.03

TMLNL: Total methanol extract of *L. nepetaefolia* leaf, TWLNL: Total water extract of *L. nepetaefolia* leaf, TERLNL: Terpene fraction of *L. nepetaefolia* leaf, ET of TMLNL: ether fraction of TMLNL, EA of TMLNL: ethyl acetate fraction of TMLNL, nBuOH of TMLNL: n-butanol fraction of TMLNL, UNS of LNL: unsaponifiable fraction of LNL, RTMLNL: residual of TMLNL, FFLNL: flavonoid fraction of LNL, TMLNR: Total methanol extract of *L. nepetaefolia* root, TWLNR: Total water extract of *L. nepetaefolia* root, TERLNR: Terpene fraction of *L. nepetaefolia* root, ET of TMLNR: ether fraction of TMLNR, EA of TMLNR: ethyl acetate fraction of TMLNR, nBuOH of TMLNR: n-butanol fraction of TMLNR, UNS of LNR: unsaponifiable fraction of LNR, RTMLNR: residual of TMLNR, BHT: butylated hydroxyl toluene.

4.1.11.2.4. Rapid screening of antioxidant constituent by HPTLC

Various extracts (10 μ L) viz. TER LNL, nBuOH of TMLNL, FFLNL, TMLNR, EA of TMLNR, TMLNL, TWLNL, UNS of LNR were applied on TLC plate and plate was developed in a solvent system consisting of ethyl acetate: chloroform: methanol: water (3:0.5:0.5:0.25). The plate was scanned at 254 and 366 nm and then dipped in 0.2% w/v solution of DPPH in methanol, and scanned at 445 nm. The appearance of white and yellow coloured spots on violet colour background was the indirect measure of radical scavenging components from extracts and fractions (Figure 4.20).

Results and Discussion

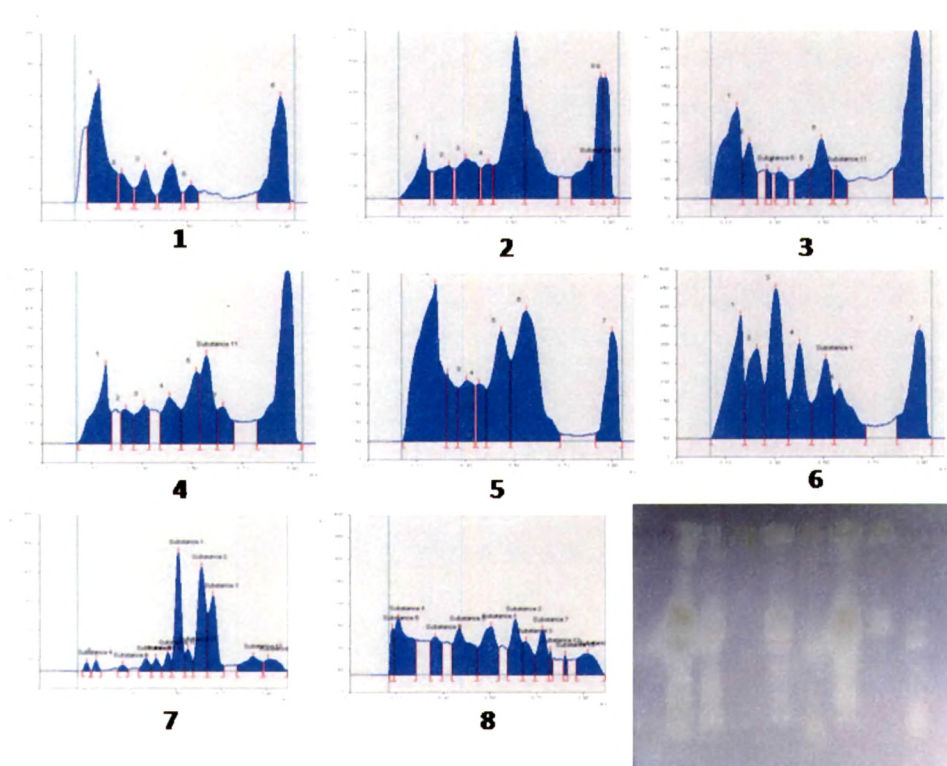


Figure 4.20: Rapid screening of antioxidant constituents of LN by HPTLC. 1: TERLNL: Terpene fraction of *L. nepetaefolia* leaf, 2: nBuOH of TMLNL: n-butanol fraction of TMLNL, 3: FFLNL: flavonoid fraction of LNL, 4: TMLNR: Total methanol extract of *L. nepetaefolia* root, 5: EA of TMLNR: ethyl acetate fraction of TMLNR, 6: TWLNL: Total water extract of *L. nepetaefolia* leaf, 7: UNS of LNR: unsaponifiable fraction of LNR, 8: TWLNR: Total water extract of *L. nepetaefolia* root.

4.1.11.3. Anti-proliferative assay (MTT assay)

Lung cancer is the most frequent cause of cancer-related death and accounts for more than a million deaths yearly worldwide with non-small cell lung cancer (NSCLC) accounting for 75-85% of lung cancer [240]. Herbs have been considered valuable sources for anticancer drug discovery [241]. Herbal medicine, recorded in many countries, e.g., Ayurveda, Chinese pharmacopoeia, has been prescribed for many diseases over centuries and began to be matched by increasing scientific attention [242]. For example, the lead compound, Taxol, a natural product isolated initially from the Pacific Yew (*Taxus brevifolia*) in the late 1980s destroys the

Results and Discussion

spindle, leading to a loss of chromosome segregation with consequent inhibition of cell division and cell death [243].

Apoptosis or programmed cell death has an essential role in controlling cell numbers in many developmental and physiological settings and in chemotherapy-induced tumor cell killing. It is a genetically regulated biological process guided by the ratio of proapoptotic and antiapoptotic proteins [244]. Apoptosis is impaired in many human tumors suggesting that disruption of apoptotic function contributes substantially to the transformation of a normal cell to a tumor cell. These pathways lead to caspase activation and cleavage of specific cellular substrates. The receptor-triggered apoptosis pathway includes ligands and their receptors such as FAS, TNF, and TRAIL as well as downstream molecules such as caspases and Bcl-2 family members [245].

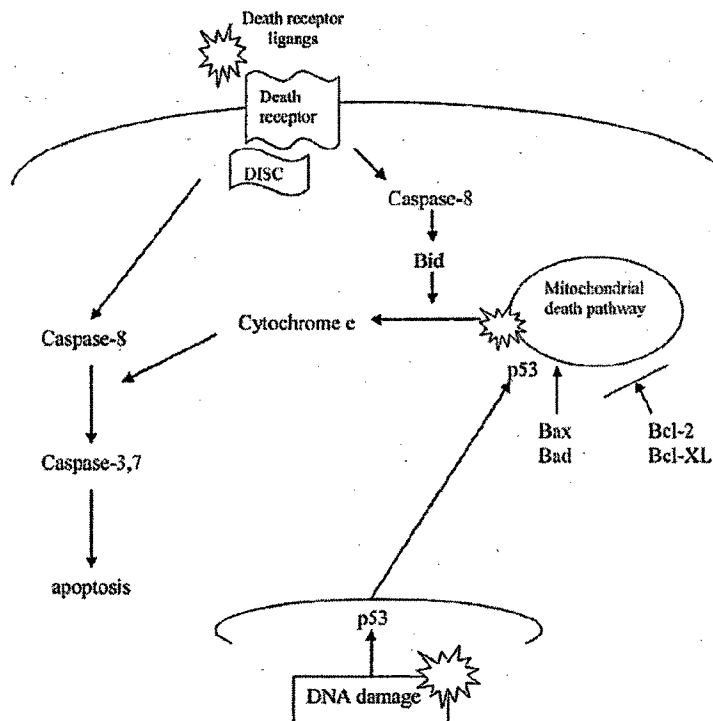


Figure 4.21: Multiple pathways of apoptosis: Binding of ligands to death receptor such as Fas causes activation of the death inducing signaling complex (DISC) and direct activation of caspases, resulting in apoptosis. Another initial event is by directly damaging DNA or by producing oxidative injury to mitochondria. In response, p53 is activated and induces pro-apoptotic proteins including Bax which can occur through proteolysis, dephosphorylation and several other mechanisms. Cross-talk between the death receptor and mitochondrial pathway is provided by Bid, which causes release of cytochrome c from mitochondria. Alternatively, p53 directly targets mitochondria, initiating cytochrome c release [246]

Results and Discussion

4.1.11.3.1. Effect of plant extracts/sub-fractions on cell growth

The herbal medications of Labiatae family, including the genus *Mentha*, are famous for their cytotoxic effects [247]. *Mentha* family decoction or infusions have been used for the treatment of various cancers [248].

David *et al.* reported methanol extract of aerial parts of the plant has in-vitro antioxidant activity and significant activity observed in Brine shrimp lethality test [249]. The effects of *L. nepetaefolia* extracts/fractions and isolates (Cmpd1: LNLAL-01, Cmpd-02: LN-02, Cmpd-03: LNR-01 and Cmpd-04: LNR-03) on the proliferation of non-small cell lung cancer A549 were determined using the MTT assay.

Table 4.15: IC₅₀ of active fractions from LN

Test sample	IC ₅₀ (µg/mL)
Ether TMLNL	229.75±5.483
TMLNL	850±10.337
TW LNL	889.06±6.3824
Unsaponifiable franc LNL	478.94±7.4932
Ether TMLNR	486.48±8.2849
Flav fraction LNL	220.87±6.4832
Pet ether LNR	922.58±8.290

Methanol extract of leaf and non polar fraction show significant cell growth inhibition on A549 cell lines. Fractions that significantly inhibited cell growth were unsaponifiable fraction of LNL 22.17%, TMLNL 25.67%, ether fraction of TMLNL 36.91%, flavonoid fraction of TMLNL 38.75%, petroleum ether LNR 23.12%, terpene LNR 33.26% and ether TMLNR 23.57%.

Results and Discussion

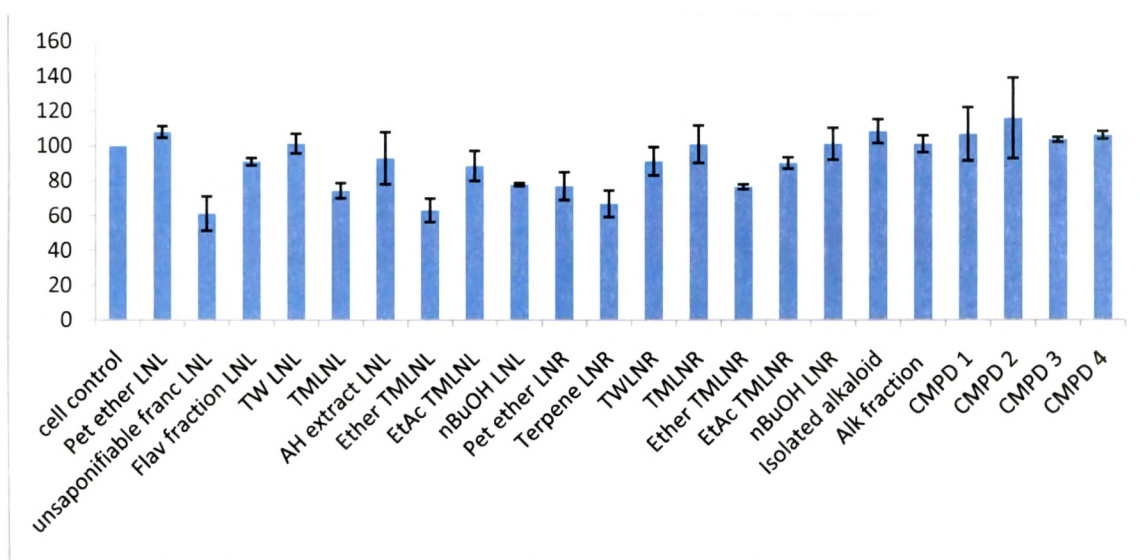


Figure 4.22: % viability of cells with SEM of various fraction/isolates from LN

A549 cell lines were growth inhibited in a dose-dependent manner after exposure to the plant extracts (Figure 4.23) those found active in the screening. The IC_{50} values for ranged from 220.87 ± 6.4832 to 922.58 ± 8.290 $\mu\text{g}/\text{mL}$ (Table 4.15).

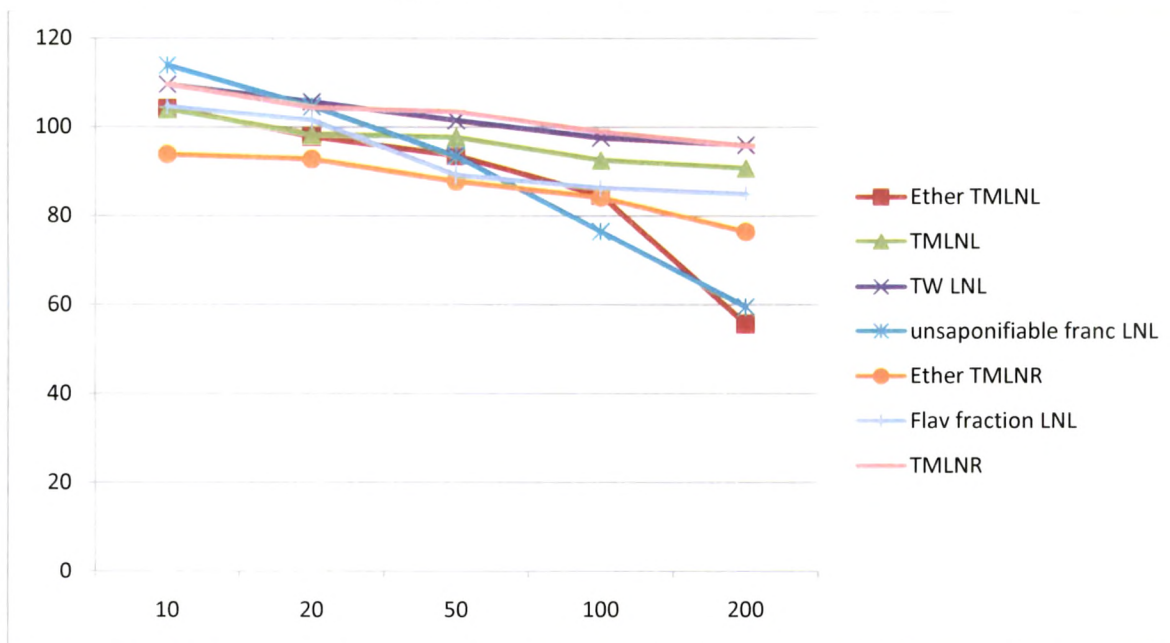
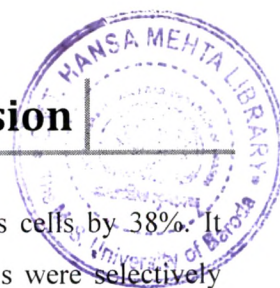


Figure 4.23: Dose dependent anti-proliferation of active fractions from LN on A549 cells

Results and Discussion



Terpene rich fraction of TMLNL was found to inhibit growth of cancerous cells by 38%. It appears that the plant extracts/fractions could induce apoptosis and fractions were selectively toxic against the cancer cell lines tested, motivating further work to determine the underlying mechanism(s), signal transduction pathways, leading to growth inhibition induced by phytoconstituents.

4.1.11.4. Lipoxygenase inhibitory assay

Lipoxygenases (LOX) constitute a family of non-haem iron containing dioxygenases that are widely distributed in animals and plants. It has been found that these LOX products play a role in a variety of disorders such as bronchial asthma, inflammation [250] and tumor angiogenesis [251]. In mammals, the 5-lipoxygenase pathway has been the major focus of study due to the pronounced pro-inflammatory role of the leukotrienes. The leukotrienes were well known to medicine as the slow reacting substance of anaphylaxis (SRS-A) long before their chemical structure was elucidated [252, 253]. The recent approvals of 5-lipoxygenase inhibitors for the clinical treatment of asthma are clear evidence for the importance of lipoxygenase metabolites in human biology. LOXs are, therefore, potential target for the rational drug design and discovery of mechanism-based inhibitors for the treatment of bronchial asthma, inflammation, cancer and autoimmune diseases. Many constituents of *L. nepetaefolia* show significant activity against lipoxygenase (Table 4.16).

Lipoxygenases catalyze the stereospecific insertion of molecular oxygen into polyunsaturated fatty acids containing an unconjugated (Z,Z)-1,4-pentadiene moiety. The products formed are optically active (S) - or (R)-hydroperoxides. Lipoxygenases (LOX's) are sensitive to antioxidants and the most of their action may consist in inhibition of lipid hydroperoxide formation due to scavenging of lipidoxy or lipidperoxy-radicals formed in course of enzymic peroxidation. This can limit the availability of lipid hydroperoxide substrate necessary for the catalytic cycle of LOX. The results obtained from the studies *L. nepetaefolia* has shown potential anti-inflammatory and antioxidant activity. This was carried out according to Shinde *et al.* [254] using activity of soyabean lipoxidase as enzyme and linoleic acid as substrate.

Results and Discussion

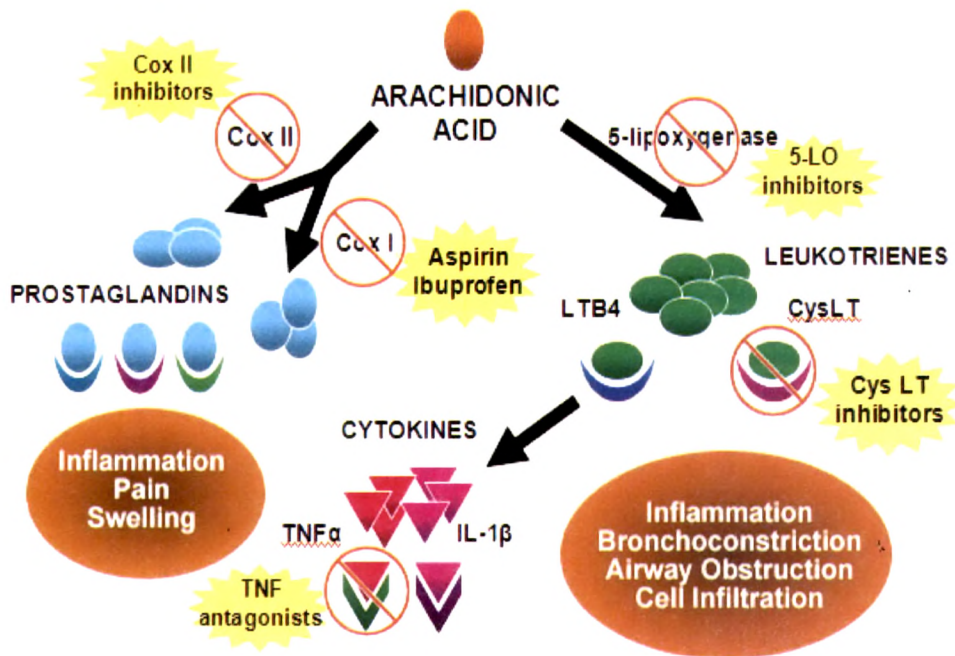


Figure 4.24: Role of 5-lipoxygenase in inflammation and bronchoconstriction [255]

The results of the enzyme inhibition study are presented as % inhibition in Table 4.16 and as IC_{50} in Figure 4.25. Compound LNLAL-01 an alkaloid, was found to be most active against the enzyme.

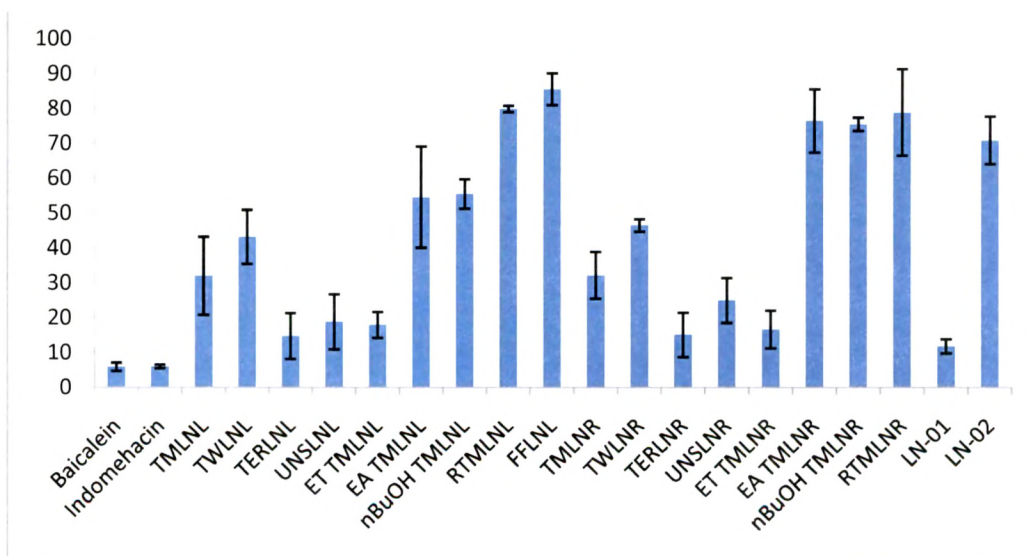


Figure 4.25: IC_{50} of different fractions and isolates in LOX inhibition assay

Results and Discussion

Table 4.16: % inhibition of different fractions in LOX inhibition assay

Sample	A (25 µg)	B (50 µg)	C (100 µg)	D (200 µg)
Indomethacin	34.59	75.83	85.38	90.8
Baicalein	34.32	75.13	77.83	83.96
TMLNL	39.29	66.37	75.23	95.17
TWLNL	35.43	69.6	72.32	91.23
TERLNL	25.71	73.61	85.68	89.64
UNSLNL	44.18	66.32	78.22	90.93
ET TMLNL	26.06	73.99	88.99	92.58
EA TMLNL	38.82	62.32	78.8	91.66
nBuOH TMLNL	24.42	65.34	77.98	86.34
RTMLNL	22.43	42.22	69.27	88.13
FFLNL	18.23	43.32	68.21	72.72
TMLNR	26.93	73.72	77.64	84.26
TWLNR	28.31	58.34	77.41	90.23
TERLNR	28.13	70.12	86.37	89.45
UNSLNR	32.52	62.13	78.85	82.51
ET TMLNR	44.21	65.32	82.99	91.35
EA TMLNR	25.42	44.32	74.2	88.22
nBuOH TMLNR	19.79	42.34	78.34	87.23
RTMLNR	14.31	35.41	66.42	72.42
LNLAL-01	33.75	74.62	84.21	89.77
LNR-01	28.32	44.42	74.32	78.42

TMLNL: Total methanol extract of *L. nepetaefolia* leaf, TWLNL: Total water extract of *L. nepetaefolia* leaf, TERLNL: Terpene fraction of *L. nepetaefolia* leaf, ET of TMLNL: ether fraction of TMLNL, EA of TMLNL: ethyl acetate fraction of TMLNL, nBuOH of TMLNL: n-butanol fraction of TMLNL, UNS of LNL: unsaponifiable fraction of LNL, RTMLNL: residual of TMLNL, FFLNL: flavonoid fraction of LNL, TMLNR: Total methanol extract of *L. nepetaefolia* root, TWLNR: Total water extract of *L. nepetaefolia* root, TERLNR: Terpene fraction of *L. nepetaefolia* root, ET of TMLNR: ether fraction of TMLNR, EA of TMLNR: ethyl acetate fraction of TMLNR, nBuOH of TMLNR: n-butanol fraction of TMLNR, UNS of LNR: unsaponifiable fraction of LNR, RTMLNR: residual of TMLNR

There are relatively very few reports on the anti-inflammatory activity of *L. nepetaefolia*. Baicalein and Indomethacin were used as standards. Fractions and sub-fractions viz. TMLNL, TWLNL, UNSLNL, ETTMLNL, EATMLNL, TWLNR and ETTMLNR achieved more than 90% inhibition in the assay. IC₅₀ values ranged from LNLAL-01-11.91±2.052 to FFLNL-85.64±4.532 µg/mL. IC₅₀ of Baicalein and Indomethacin was found to be 5.927±1.215 and 6.01±0.5273 µg/mL, respectively. It was observed that both root and leaf parts are active against the enzyme and non-polar fractions shows significantly better activity in LOX assay.

Results and Discussion

4.1.11.5. ROS inhibitory activity

Most studies using blood leukocytes obtained from asthmatic patients indicate that these cells generate more ROS compared to cells isolated from control subjects. For instance, eosinophils isolated from the blood of symptomatic asthmatics generate more lucigenin-enhanced chemiluminescence upon activation with platelet-activating factor or phorbol myristate acetate in vitro as compared to eosinophils isolated from allergic asymptomatic subjects [256].

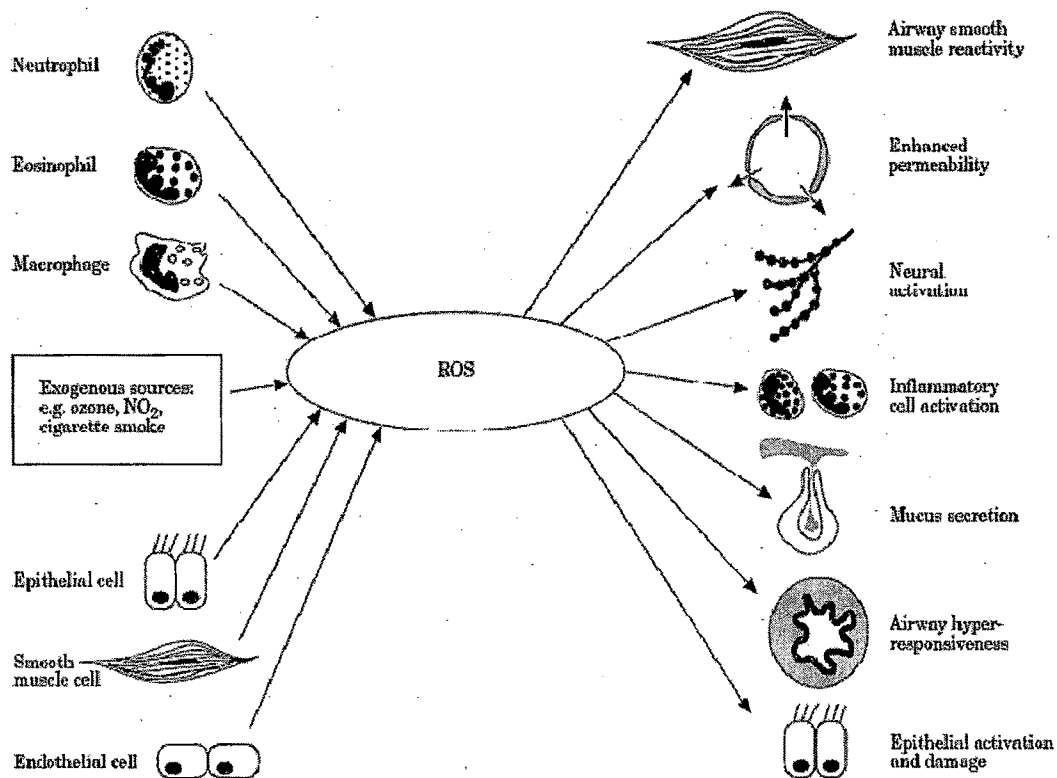


Figure 4.26: General overview of sources of ROS and types of cells affected by ROS [257]

Also, neutrophils and monocytes purified from blood of asthmatic patients have been shown to be activated and to possess an enhanced capacity to release ROS than cells obtained from healthy controls [256, 257].

Evidence for increased oxidative stress in asthma is further provided by the finding of a decreased antioxidant capacity in plasma and BAL fluid of asthmatic patients [258, 259]. Bronchial epithelial cells isolated from asthmatics not receiving inhaled corticosteroids possess less Cu, Zn-superoxide dismutase activity than epithelial cells obtained from control subjects [260].

Results and Discussion

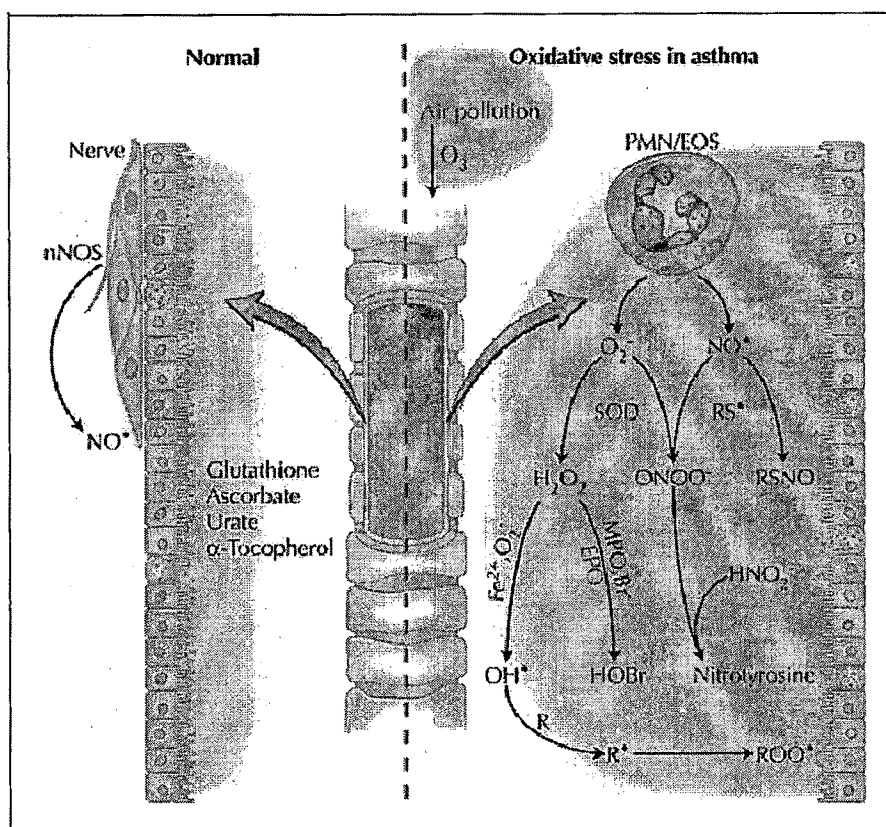


Figure 4.27: Oxidative and nitrosative stress in asthma. There are many sources of ROS/RNS in asthmatic patients (see text). HNO_2 —nitrous acid; H_2O_2 —hydrogen peroxide; NO —nitric oxide; O_2^- —superoxide; O_3 —ozone; OH^\bullet —hydroxyl radical; ONOO^- —peroxynitrite; R^\bullet —lipid radical; ROO^\bullet —lipid peroxide; RSNO —nitrosothiol; SOD—superoxide dismutase [261]

Several studies suggest that the source of increased ROS/RNS in asthmatics might be airway inflammatory cells. The main cells involved in the inflammatory response are monocytes/macrophages, polymorphonuclear leucocytes (PMNs), and endothelial cells. When these cells become activated, they aggregate and infiltrate tissue where they undergo a respiratory burst, increasing their oxygen use and production of cytokines, ROS, and other mediators of inflammation. ROS can initiate and also perpetuate inflammatory cascades and cause subsequent tissue damage (Figure 4.27) [262].

The primary defense against ROS is endogenous antioxidants; enzymatic and non-enzymatic. The enzymatic antioxidants include the families of SOD, catalase, glutathione peroxidase, glutathione S-transferase, and thioredoxin. The nonenzymatic category of antioxidant defenses includes low molecular weight compounds such as glutathione, ascorbate, urate, and α -tocopherol.

Results and Discussion

The increase in ROS during an asthma exacerbation might encourage endogenous antioxidant defenses such as glutathione, ascorbic acid (vitamin C), urate, and α -tocopherol (vitamin E). Augmentation of dietary antioxidants and herbal antioxidants might also be beneficial [263, 264]

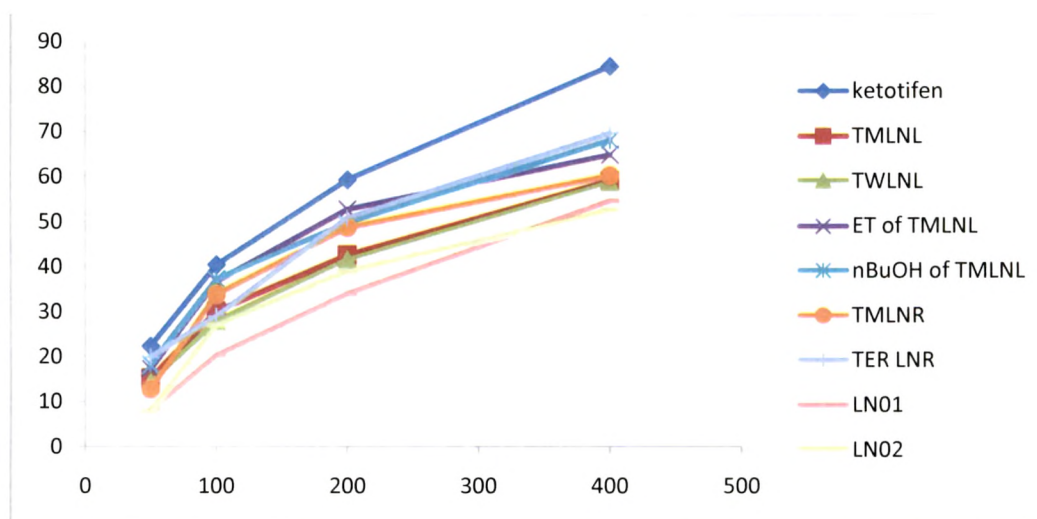


Figure 4.28: Dose dependent inhibition of oxidative stress by ketotifen and constituents of *L. nepetaefolia*

The anti-inflammatory effects of the test samples, that were found active in lipoxygenase activity, were assessed *in vitro* using the modified cell based assay of Tan and Berridge (2000) [218] based on reduction of the highly water-soluble tetrazolium salt WST-1 in the presence of activated neutrophils. The obtained data are expressed in figure 4.28 as % inhibition and calculated IC_{50} values in Table 4.17.

The analysis revealed that the effect of the terpene fraction exceeded that of the more polar n-butanol, methanol and water extracts. TER LNR, ET of TMLNL and TMLNR showed the highest inhibitory effects at 400 $\mu\text{g/mL}$ viz. 69.54%, 64.89% and 60.28% with IC_{50} values $241.91 \pm 16.669 \mu\text{g/mL}$, $245.36 \pm 18.2046 \mu\text{g/mL}$ and $279.01 \pm 12.8694 \mu\text{g/mL}$, respectively. IC_{50} values ranged from ketotifen ($178.81 \pm 13.6163 \mu\text{g/mL}$) to LN-02-identified as β -sitosterol ($351.21 \pm 10.6823 \mu\text{g/mL}$).

Results and Discussion

Table 4.17: IC₅₀ of active fractions from *L. nepetaefolia*

Test samples	IC ₅₀ (µg/mL)
Ketotifen	178.81±13.6163
TMLNL	301.55±16.6265
TWLNL	309.32±11.3562
ET of TMLNL	245.36±18.2046
nBuOH of TMLNL	240.16±15.2938
TMLNR	279.01±12.8694
TER LNR	241.91±16.669
LN01	350.28±17.6707
LN02	351.21±10.6823

Furthermore, it is interesting to note that the significant antioxidant effect of non-polar sub-fractions is in correlation with the observed cytotoxic activity and antiinflammatory activity of this fraction.

4.1.11.6. Inhibition of mast cells degranulation induced by compound 48/80

Mast cell degranulation is important in the initiation of immediate responses following exposure to allergens [265]. Once binding of allergen to cell-bound IgE occurs, mediators such as histamine; eosinophil and neutrophil chemotactic factors; leukotrienes C₄, D₄ and E₄; prostaglandins; platelet-activating factor; and large and growing list of chemokines (including IL-4, IL-5, IL-12, IL-13, IL-15, IL-25 and IL-33) are released from mast cells which are responsible development of airway inflammation and bronchoconstriction (Figure 4.29). An attempt was made to find out whether extracts/fractions of *L. nepetaefolia* have any effect on the rate of disruption of mast cells following exposure to compound 48/80, an agent which causes degranulation and histamine release [266].

Results and Discussion

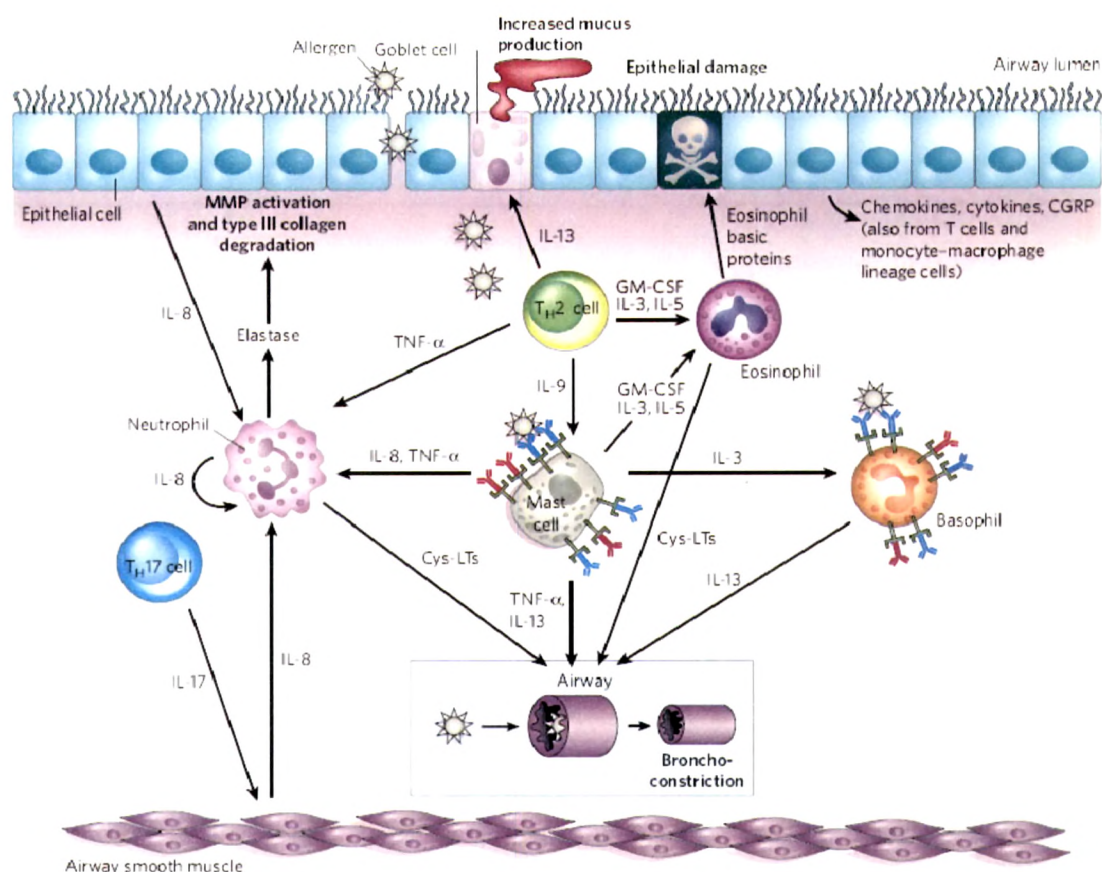


Figure 4.29: Involvement of mast cells in allergen-induced airway inflammation: Late-phase reactions typically occur hours after allergen challenge and are thought to reflect the actions of innate and adaptive immune cells that have been recruited from the circulation, as well as the secretion of inflammatory mediators by tissue-resident cells. The innate immune cells include neutrophils, monocytes (not shown), eosinophils and basophils. Other cells that secrete inflammatory mediators include mast cells that have been activated by IgE- and allergen-dependent Fc ϵ RI aggregation, and tissue-resident or recruited T cells that recognize allergen-derived peptides. Therefore, in a late-phase reaction, for example, elastase released by neutrophils promotes the activation of matrix metalloproteinases (MMPs) and the degradation of type III collagen. In addition, basic proteins released by eosinophils can injure epithelial cells, and several other mediators produced by recruited or tissue-resident cells can induce bronchoconstriction. CGRP, calcitonin-gene-related peptide; GM-CSF, granulocyte-macrophage colony-stimulating factor; Th17 cell, IL-17-producing Th cell [267].

Brightling et al. [268] have recently demonstrated that mast cells are the predominant inflammatory cells in the smooth muscle layer of bronchial biopsies and that their number is elevated in patients with asthma compared with those with eosinophilic bronchitis or healthy controls. In both patients with fatal asthma and those with asthma who died of other causes, mast cells are also found in airway smooth muscle; in fatal asthma these mast cells appeared degranulated [269]. Work by Brightling et al. [268] has demonstrated that human lung mast cells

Results and Discussion

express a number of chemokine receptors (CCR3, CXCR1, CXCR3, and CXCR4) and that their ligands cause mast cell chemotaxis in vitro.

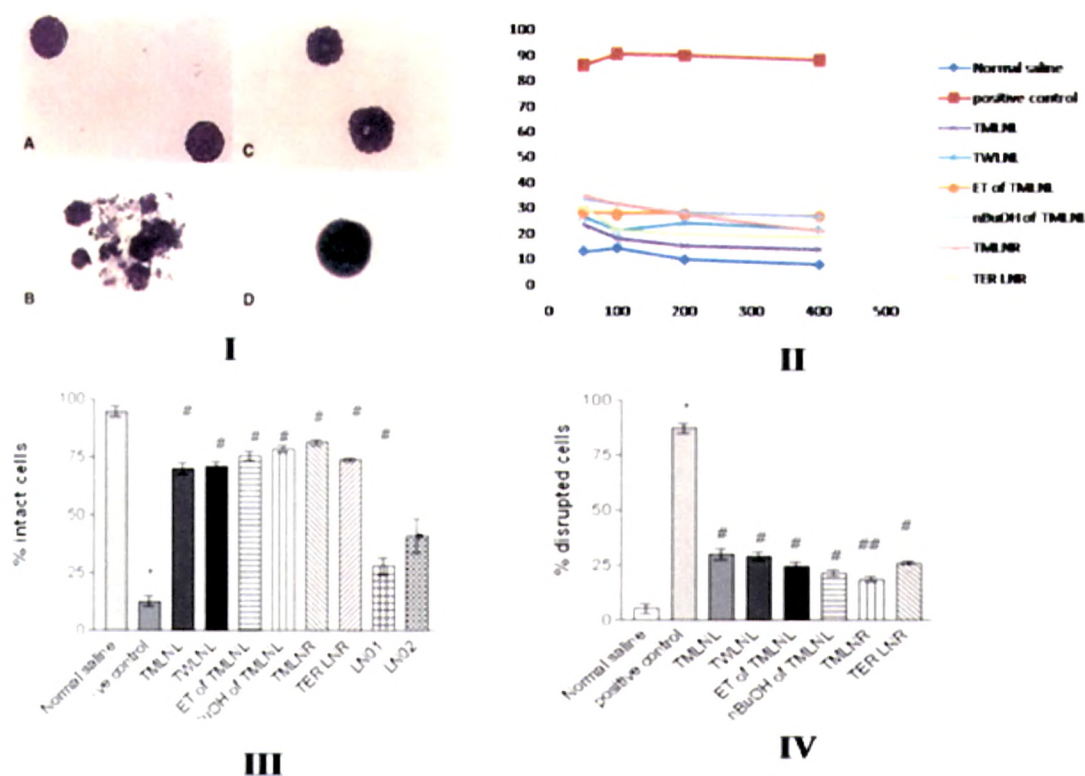


Figure 4.30: Results of mast cell degranulation; **I:** Mast cells light microscopy photograph (100X) **A)** mast cell of normal rat **B)** mast cell from only compound 48/80 group **C)** and **D)** mast cells of treated group. **II:** dose dependent % inhibition of mass degranulation by fractions of *L. nepetaefolia*, **III:** % of intact mast cells in various groups; TMLNL: Total methanol extract (200 mg/kg), TWLNL: Total water extract (200 mg/kg), ET of TMLNL: ether sub-fraction of TMLNL (50 mg/kg), nBuOH of TMLNL: n-butanol fraction of TMLNL (50 mg/kg), TMLNR: Total methanol extract of root (200 mg/kg), TERLNR: Terpene fraction of root (50 mg/kg), LN-01: isolated alkaloid (20 mg/kg), LN-02: isolated compound from LN (20 mg/kg). **IV:** % of degranulated mast cells in various groups; TMLNL: Total methanol extract (400 mg/kg), TWLNL: Total water extract (400 mg/kg), ET of TMLNL: ether sub-fraction of TMLNL (100 mg/kg), nBuOH of TMLNL: n-butanol fraction of TMLNL (100 mg/kg), TMLNR: Total methanol extract of root (400 mg/kg), TERLNR: Terpene fraction of root (100 mg/kg).

*-p<0.001 when compared to vehicle control group

#-p<0.001 when compared to positive control group.

In a mouse model of chronic asthma, mast cells can substantially influence features of chronic allergic inflammation and tissue remodelling (including expansion of the number of goblet cells), independently of mast-cell signaling through either IgE–FcεRI or antigen–IgG1–FcγRIII [270]. Thus mast cells have the potential to drive important features of allergic inflammation independently of IgE. Mast cells may be instrumental in orchestrating TReg-cell-mediated peripheral tolerance is unprecedented.

Results and Discussion

Almost all the extracts/fractions at higher dose had significant inhibitory effect on mast cell degranulation produced by compound 48/80 (Figure 4.30). Extracts at the dose of 200 mg/kg had non-significant results on inhibition of degranulation on mast cells. Degranulation was observed significantly in positive control group when compare to normal control. The percentage of intact cells in various groups were found to be TMLNL (400 mg/kg) 70.02 ± 2.711 , TWLNL (400 mg/kg) 70.97 ± 2.022 , ET TMLNL (100 mg/kg) 75.47 ± 2.006 , nBuOH TMLNL (100 mg/kg) 78.54 ± 1.362 , TMLNR (400 mg/kg) 81.44 ± 1.305 , TERLNR (100 mg/kg) 73.87 ± 0.7077 , LN-01(20 mg/kg) 27.83 ± 3.82 , LN-02 (20 mg/kg) 41.08 ± 7.483 and the percentage of disrupted cells were found to be in groups as TMLNL (400 mg/kg) 29.98 ± 2.711 , TWLNL (400 mg/kg) 29.03 ± 2.022 ET TMLNL (100 mg/kg) 24.53 ± 2.006 nBuOH TMLNL (100 mg/kg) 21.46 ± 1.362 , TMLNR (400 mg/kg) 18.56 ± 1.305 TERLNR (100 mg/kg) 26.13 ± 0.7077 LN-01(20 mg/kg) 72.17 ± 3.82 LN-02 (20 mg/kg) 58.92 ± 7.483 . It was observed that isolated compounds LN-01 and LN-02 had significantly less effect on mast cells degranulation in-vitro when compared to fractions.

4.1.11.7. Milk induced leukocytosis

Subcutaneous injection of milk at dose of 4 mL/kg produced a significant ($p < 0.001$) increase in the total leucocytes count after 24 h of its administration. Amongst mice pretreated with various extracts of *L. nepetaefolia* ether sub-fraction of total methanol extract of leaves and roots (100 mg/kg) showed significant reduction in leukocyte count induced by milk, whereas other extracts had non significant reduction in leukocyte count (Figure 4.31).

Physical and chemical stressors such as trauma, allergen, polluted air exposure, radiation etc. has been reported to concurrently produce immunodeficiency and oxidative stress. Suppression of immunity takes place due to exposure to allergen and leads to respiratory diseases. Reactive oxygen and nitrogen species (ROS/RNS) damages airways and play a role in pathophysiology of asthma. So, a drug having antistress activity induces a state of non-specific increased resistance (SNIR) against a variety of stress [271].

After parental administration of milk, there is increase in total leukocytes count, and this stressful condition can be made normalized by administration of an antistress or drugs having antioxidant ability. Furthermore, leukocytes during asthmatic inflammation release the inflammatory mediators like cytokines, histamine and major basic protein, which promote the ongoing inflammation [272].

Results and Discussion

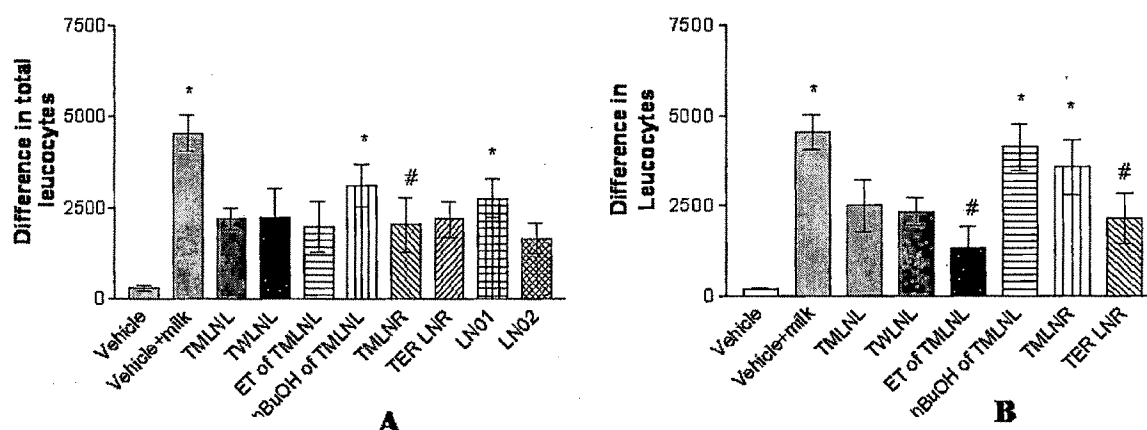


Figure 4.31: A) Difference in leucocytes count of control and treated rats. ; TMLNL: Total methanol extract (200 mg/kg), TWLNL: Total water extract (200 mg/kg), ET of TMLNL: ether sub-fraction of TMLNL (50 mg/kg), nBuOH of TMLNL: n-butanol fraction of TMLNL (50 mg/kg), TMLNR: Total methanol extract of root (200 mg/kg), TERLNR: Terpene fraction of root (50 mg/kg), LN-01: isolated alkaloid (20 mg/kg), LN-02: isolated compound from LN (20 mg/kg) **B)** TMLNL: Total methanol extract (400 mg/kg), TWLNL: Total water extract (400 mg/kg), ET of TMLNL: ether sub-fraction of TMLNL (100 mg/kg), nBuOH of TMLNL: n-butanol fraction of TMLNL (100 mg/kg), TMLNR: Total methanol extract of root (400 mg/kg), TERLNR: Terpene fraction of root (100 mg/kg).

*- $p < 0.001$ when compared to vehicle control group

#- $p < 0.05$ when compared to positive control (vehicle+milk) group.

Thus non polar sub-fraction of methanol extract of leaves and roots showed protective effect against milk-induced leucocytosis. Pretreated animals with isolated compounds tested had significantly higher leucocyte count than normal control group.

4.1.11.8. Effect of LN on milk-induced Eosinophilia

The type-I hypersensitivity reaction leads to the development of edema, vascular dilation and eosinophilic infiltration [273]. In late phase, especially in the development of allergic asthma, eosinophil plays a role as inflammatory cells as it secretes mediators which results in epithelial shedding, broncho-constriction and promotion of inflammation in respiratory tract [274]. Therefore, abnormal increase in peripheral eosinophil to more than 4% of total leukocyte count (eosinophilia) is associated with respiratory disorder, often allergic in nature together with pulmonary infiltrates [275].

Amongst mice pretreated with various extracts/isolates of *L. nepetaefolia*, ether sub-fraction of total methanol extract of leaves (100 mg/kg), terpene fraction (100 mg/kg) and methanol extract of roots (400 mg/kg) showed significant reduction ($p < 0.001$) in eosinophil count induced by milk, whereas other extracts did not reduced eosinophil count significantly (Figure 4.32).

Results and Discussion

Eosinophiles are thought to mediate inflammatory and cytotoxic events associated with allergic disorders, including bronchial asthma, rhinitis and urticaria [276, 277]. The eosinophilic response has been identified as a key alteration in the pathogenesis of asthma and other allergic diseases. A close correlation between disease severity and eosinophilia, and the eosinophil ability to provide toxic and proinflammatory agents are the major elements supporting the interpretation that there is indeed a causal relationship between these phenomena [278].

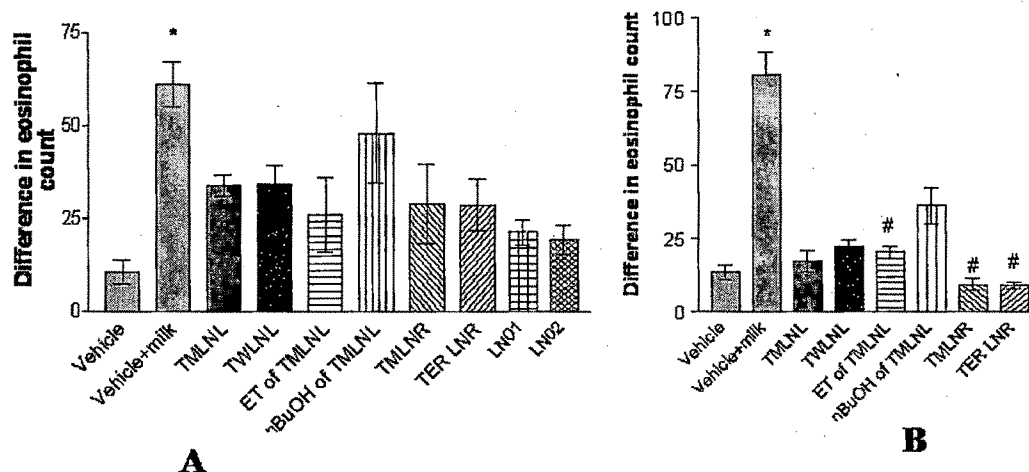


Figure 4.32: A) Difference in eosinophil count of control and treated rats TMLNL: Total methanol extract (200 mg/kg), TWLNL: Total water extract (200 mg/kg), ET of TMLNL: ether sub-fraction of TMLNL (50 mg/kg), nBuOH of TMLNL: n-butanol fraction of TMLNL (50 mg/kg), TMLNR: Total methanol extract of root (200 mg/kg), TERLNR: Terpene fraction of root (50 mg/kg), LN-01: isolated alkaloid (20 mg/kg), LN-02: isolated compound from LN (20 mg/kg). **B)** Difference in eosinophil count of control and treated rats. TMLNL: Total methanol extract (400 mg/kg), TWLNL: Total water extract (400 mg/kg), ET of TMLNL: ether sub-fraction of TMLNL (100 mg/kg), nBuOH of TMLNL: n-butanol fraction of TMLNL (100 mg/kg), TMLNR: Total methanol extract of root (400 mg/kg), TERLNR: Terpene fraction of root (100 mg/kg).

*- $p < 0.001$ when compared to vehicle control group

#- $p < 0.05$ when compared to positive control (vehicle+milk) group.

The eosinophil is well recognized as a central effector cell in the inflamed asthmatic airway. Eosinophils release toxic basic proteins and lipid mediators such as cysteinyl-leukotrienes that cause bronchial epithelial damage and airflow obstruction. Eosinophil-selective cytokines and chemokines including interleukin (IL)-5, eotaxin and may represent targets for novel asthma therapies [279].

Subcutaneous injection of milk at dose of 4 mL/kg produced a significant ($p < 0.001$) increase in the eosinophile count (about 5.6 %) after 24 h of its administration. As seen from the results higher dose of all the extracts/fractions showed significant reduction ($p < 0.001$) in the eosinophile

Results and Discussion

counts except in the animals pretreated with TWLNL and n-butanol sub-fraction of methanol extract of leaf.

4.1.11.9. Carrageenan-induced paw oedema

The carrageenan-induced paw oedema is commonly used as an experimental model of acute inflammation [280]. In the present study, an attempt has been made to evaluate the anti-inflammatory activity of *Leonotis nepetaefolia* by use of the carrageenan-induced paw oedema model.

The development of carrageenan-induced paw oedema is believed to be biphasic [281], of which the first phase is mediated by release of histamine and serotonin while the delayed phase is linked to the neutrophil infiltration, eicosanoid release, production of free radicals and also release of other neutrophil derived mediators [282, 283].

Table 4.18: Difference in paw volume (ΔV mL) of control and treated rats

Treatment groups	Increase in paw volume(ΔV mL)			
	1 h	2 h	3 h	4 h
Normal control	0.346±0.0324	0.352±0.0283	0.356±0.032	0.363±0.0143
Positive control	0.475±0.0243	0.55±0.0296 ^a	0.681±0.034 ^a	0.725±0.0365 ^a
TMLNL (200 mg/kg)	0.403±0.0199	0.471±0.022 ^a	0.491±0.020 ^a	0.465±0.0399 ^a
TWLNL (200 mg/kg)	0.371±0.0170	0.521±0.025 ^a	0.54±0.026 ^a	0.533±0.0251 ^a
ET of TMLNL (50 mg/kg)	0.406±0.0224	0.46±0.0109	0.476±0.009 ^{ab}	0.44±0.0106 [#]
nBuOH of TMLNL (50 mg/kg)	0.401±0.030	0.478±0.032 ^a	0.495±0.029 ^a	0.491±0.0285 ^a
TMLNR (200 mg/kg)	0.376±0.033	0.423±0.026 [#]	0.441±0.025	0.431±0.0310 [#]
TERLNR (50 mg/kg)	0.393±0.036	0.413±0.035 [#]	0.423±0.032 [#]	0.371±0.0273 [#]
LN01 (20 mg/kg)	0.35±0.0239	0.433±0.023	0.493±0.027 ^a	0.486±0.0255 ^a
LN02 (20 mg/kg)	0.388±0.0256	0.411±0.026	0.43±0.018	0.426±0.0506 [#]

TMLNL: Total methanol extract, TWLNL: Total water extract, ET of TMLNL: ether sub-fraction of TMLNL, nBuOH of TMLNL: n-butanol fraction of TMLNL, TMLNR: Total methanol extract of root, TERLNR: Terpene fraction of root, LN-01: isolated alkaloid, LN-02: isolated compound from LN.

a- p<0.05 when compared to vehicle control group

#-p<0.05 when compared to positive control group.

When the first 3-h segment of the curve is analyzed, a biphasic response has been seen. A rapid rise in foot volume occurs immediately after sub-plantar injection of carrageenan. Subsequently, a diminution of foot volume occurs at the end of 1 h, which has been designed as the first phase or early phase oedema. A second period of oedema formation begins to develop at a slow rate from the end of 1 h. Around 90 min, a strong acceleration of oedema formation occurs which tapers off after 3 h.

Results and Discussion

The oedema produced in between early and late phase is thought to be due to the release of kinin-like substances (e.g. bradykinin), which later induces the biosynthesis of prostaglandin and other autacoids, which are responsible for the formation of the inflammatory exudates [284]. It is well known that expression of COX-1 and COX-2 are maximal at the early phase and late phase of carrageenan-induced paw oedema respectively [285].

The results indicate ether sub-fraction of TMLNL (50 mg/kg) showed significant ($p < 0.05$) inhibition 16.37% at 1 h and 39.31% at 4 h. Total methanol extract of root (200 mg/kg) produced significant ($p < 0.05$) inhibition of 40.45% at 4 h. Maximum inhibition was observed with terpene rich fraction of root (50 mg/kg) 37.87% at 3 h and 59.78% at 4 h. Terpene rich fraction of root (400 mg/kg) produced significant ($p < 0.05$) 24.84% inhibition at 2 h and 45.28% inhibition of oedema at 4 h.

Table 4.19: Difference in paw volume (ΔV mL) of control and treated rats

Treatment groups	Increase in paw volume (ΔV mL)			
	1 h	2 h	3 h	4 h
Normal control	0.346±0.0324	0.352±0.0283	0.356±0.032	0.363±0.0143
Positive control	0.475±0.0243	0.55±0.0296 ^a	0.681±0.034 ^a	0.725±0.0365 ^a
TMLNL (400 mg/kg)	0.398±0.0231	0.431±0.016	0.48±0.017 [#]	0.488±0.0213 [#]
TWLNL (400 mg/kg)	0.395±0.0289	0.515±0.044 ^a	0.583±0.025 ^a	0.601±0.0273 ^a
ET of TMLNL (100 mg/kg)	0.38±0.0284	0.39±0.0226 [#]	0.423±0.024 [#]	0.408±0.0234 [#]
nBuOH of TMLNL (100 mg/kg)	0.446±0.0337 ^a	0.525±0.028 ^a	0.566±0.023 ^a	0.583±0.0259 ^a
TMLNR (400 mg/kg)	0.38±0.0340	0.426±0.0239	0.45±0.0235 ^a	0.465±0.0236 [#]
TERLNR (100 mg/kg)	0.391±0.0362	0.413±0.0352 [#]	0.426±0.031 [#]	0.396±0.0264 [#]

TMLNL: Total methanol extract, TWLNL: Total water extract, ET of TMLNL: ether sub-fraction of TMLNL, nBuOH of TMLNL: n-butanol fraction of TMLNL, TMLNR: Total methanol extract of root, TERLNR: Terpene fraction of root.

a- $p < 0.05$ when compared to vehicle control group

#- $p < 0.05$ when compared to positive control group.

In the carrageenan-induced paw oedema model, *L. nepetaefolia* inhibited the oedema (inflammation) partially or completely at early or late phase of an acute inflammation with maximum inhibitory effect in the late phase. This indicates non polar phytoconstituents of the plant have actions on early phase mainly by inhibiting histamine, which is abundantly present in the pro-inflammatory cells like neutrophils and mast cells.

Results and Discussion

4.1.11.10. Effect of *L. nepetaefolia* fractions on histamine induce bronchospasm in guinea pigs

Histamine is a potent bronchoconstrictor stimulant, which stimulates histamine H₁ receptors on airway smooth muscle, leading to direct bronchoconstriction, and also on sensory nerve endings, leading to vaguely mediated reflex bronchoconstriction [286]. Allergen-induced bronchial hyperreactivity is often associated with airway inflammation. Histamine causes expression of adhesion molecules on endothelial cells [287] and potently increases vascular permeability, therewith facilitating migration of inflammatory cells through the pulmonary vasculature upon activation. Prevention of these processes by LN fractions could result in reduction of cells infiltrations.

Table 4.20: Pre convulsion time of various groups

Treatment groups	Pre-convulsive time (sec)	Protection (%)
Vehicle control	125.8±4.324	-
Alkaloid fraction of LNL (50 mg/kg)	129.6±5.128	2.94
Alkaloid fraction of LNL (100 mg/kg)	142.2±10.425	11.54
Terpene fraction of LNR (50 mg/kg)	163.4±21.232	23.01
Terpene fraction of LNR (100 mg/kg)	198.4±25.783	36.59

*Values are expressed as time (s) ± sdv; n=6

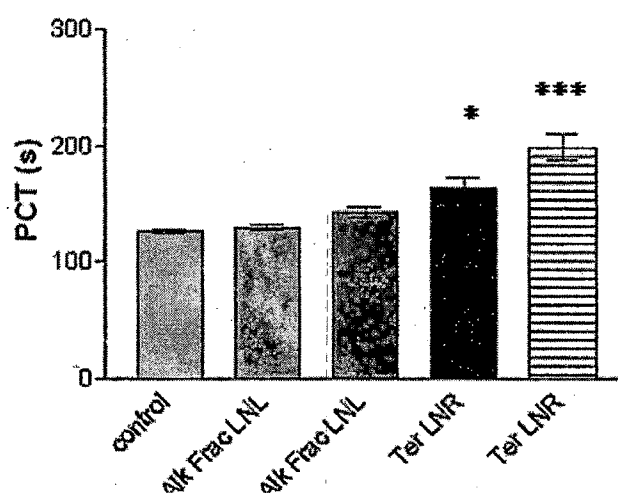


Figure 4.33: PCT (pre convulsive time) of different fractions administered to guinea pigs. *(p<0.05) and ***(p<0.001) significance level Alk Frac LNL: alkaloid fraction of LNL (50 and 100 mg/kg), Ter LNR: terpene fraction of LNR (50 and 100 mg/kg)

Results and Discussion

Terpene fraction of LNR (50 mg/kg) significantly delayed the onset of convulsions in guinea pigs caused by acute bronchospasm induced by histamine aerosols. It was more effective with pretreatment of fractions for 7 days in this model. These observations substantiate its protective effect against bronchoconstriction. Thus it can be concluded that these studies corroborate the folklore reports of the preventive effects of *L. nepetaefolia* in bronchial asthma, bronchitis and other respiratory disorders.

4.2. *Oxalis corniculata*

The detailed systematic pharmacognostical and phytochemical evaluation of plant and plant material provides means of standardization of an herb that can be used as drug or as raw material [288]. Here we are reporting preliminary data for identification of *O. corniculata* and its extract for use of this plant as drug.

4.2.1. Macroscopic Features



Figure 4.34: Whole plant of *Oxalis corniculata*

Oxalis corniculata Linn is a small procumbent herb also known as yellow Indian wood sorrel, with stems rooting and pubescent with appressed hairs, leaves palmately 3-foliolate. This plant is well known for its medicinal value as a good appetiser and as a remover of *kapha*, *vata* and piles. *O. corniculata* is also used in Ayurvedic medicine as *changeri ghrita*.

Leaves are palmately compound, trifoliolate. Petiole is green, thin, about 3-9 cm long, cylindrical, pubescent. Leaflets are green and 1-2 cm long, obcordate, glabrous, sessile or sub-sessile with

Results and Discussion

base cuneate. Taste is somewhat sour. Stem is creeping, brownish red, very thin, soft with hairs on it. Roots are dark brownish, thin, about 1-2 mm thick, branched, rough and soft. Stem and root are odourless and tasteless. Flowers are axillary, sub-umbellate and yellow in colour. Fruits are cylindrical capsules and tomentose shaped. Seeds are tiny, dark brown, numerous, broadly ovoid and transversely striate

4.2.2. Microscopic Features

4.2.2.1. Root – Transverse section (T.S.) of root shows 3-4 layers of cork, consisting thin-walled rectangular cells, brownish in appearance. Cortex is a wide zone, composed of rectangular and oval, thin-walled parenchymatous cells filled with simple starch grains, yellowish pigment. Cortex is followed by thin strips of phloem consisting of sieve tubes, companion cells and phloem parenchyma. Xylem consists of vessels, tracheids, fibres and xylem parenchyma. Few starch grains simple, round to oval measuring 3-11 μ in dia., are present scattered throughout the region.

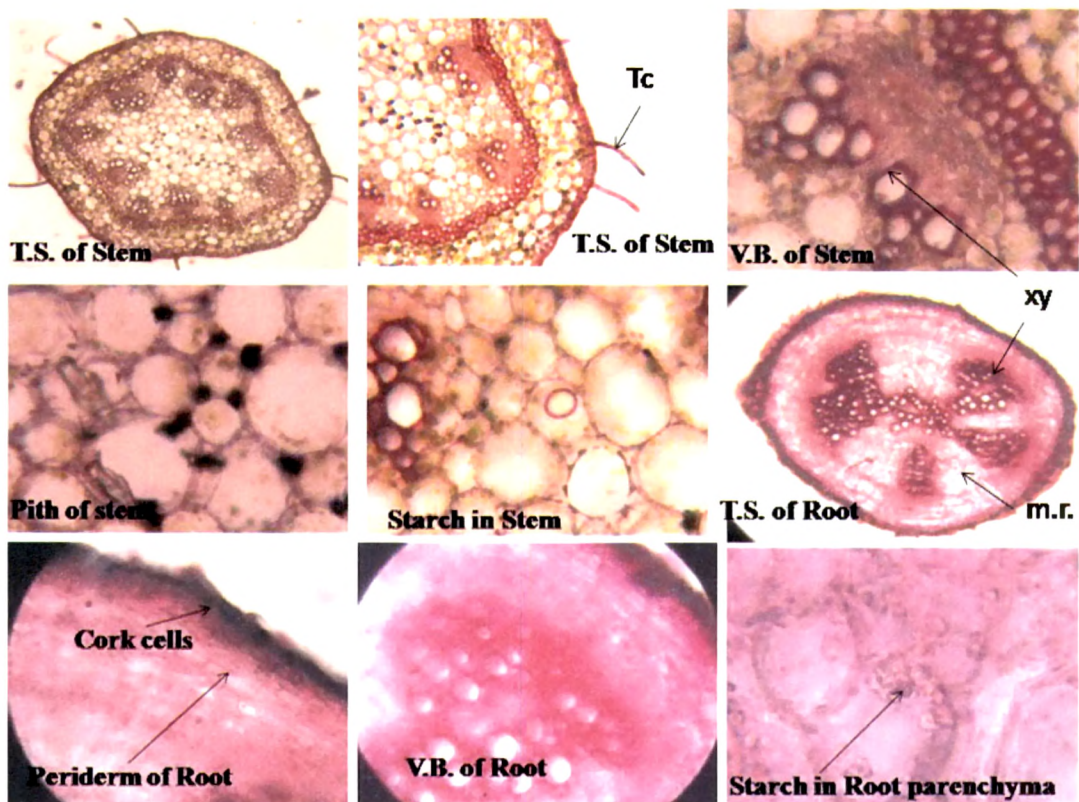


Figure 4.35: TS of stem and root of OC; Tc-trichomes; Ph-phloem; Xy-xylem; ck-cork cells; m.r.-medullary rays

Results and Discussion

4.2.2.2. Stem: Transverse section shows single layered epidermis, composed of rectangular to oval cells, some of which are elongated to become unicellular covering trichomes. Cortex consists of 4-5 layers of thin-walled, circular and polyhedral parenchymatous cells. Endodermis is single layered of thin-walled rectangular cells, pericycle composed of two or three layers of squarish and polygonal sclerenchymatous cells. Vascular bundles are 6-7 in number, arranged in a ring, composed of a few elements of phloem towards outer side and xylem towards inner side. Xylem composed of pitted vessels, tracheids, fibers and xylem parenchyma. Central region is occupied by pith composed of thin-walled, parenchymatous cells, a few simple, round to oval starch grains measuring 3-11 μ in dia, scattered throughout the region.

4.2.2.3. Leaf: Petiole shows single layered epidermis of rectangular or circular, thin-walled cells. Cortex is 3-4 layered consisting thin-walled, circular, oval or polygonal parenchymatous cells. Endodermis shows single layer of cells followed by 2-3 layers of sclerenchymatous pericycle, less developed towards upper side of petiole. Vascular bundles are 5 in number, arranged in a ring, consisting of phloem towards outer side and xylem towards inner side. Starch grains are present at the centre. Lamina shows single layered epidermis on upper and lower surfaces, composed of rectangular cells. Trichomes are unicellular covering and warty. Single layered palisade cells composed of thin-walled, columnar cells, filled with green pigment, below palisade 2-3 layers of thinwalled, spongy parenchyma consisting of circular to oval cells filled with green pigment. Stomata are anomocytic.

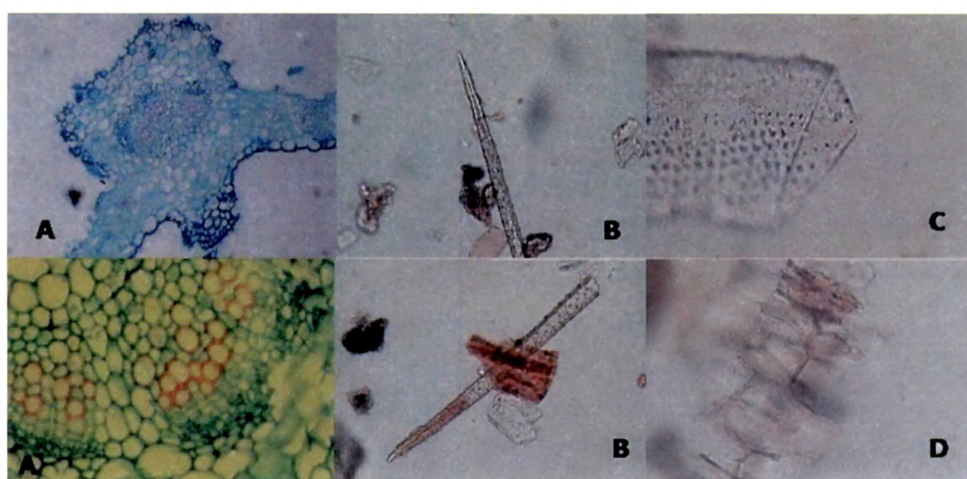


Figure 4.36: A: TS of OC leaf; B: unicellular covering warty trichome; C: vascular elements; D: pieces of mesophyll parenchyma

Results and Discussion

Powder is greenish-brown in color. Fragments of trichomes (unicellular covering and warty), lignified vascular bundles, parenchymatous, sclerenchymatous cells, fibres, epidermis are seen. Starch grains are present as simple, round to oval, measuring 3-11 μ in diameter.

The quantitative determination of some pharmacognostic parameters is useful for setting standards for raw herbal material. The vein islet, and vein termination numbers and the other parameters determined in the quantitative microscopy, are relatively constant for plants and can be used to differentiate closely related species. In quantitative microscopy, the stomatal index for upper and lower surfaces was found to be 2.8 to 4.0 to 5.6 and 5.7 to 8.3 to 10.0 respectively. Vein islet number and vein-let termination number are 3 to 5 (Average 4) and 8 to 11 (Average 9.5) respectively.

4.2.3. Proximate analysis

The physical constant evaluation of the drugs is an important parameter in detecting adulteration. The moisture content of the plant drug is not too high, thus it could discourage bacterial, fungi or yeast growth. The ash value determinations are equally important. The total ash is particularly important in the evaluation of purity of drugs, i.e. the presence or absence of foreign inorganic matter such as metallic salts and/or silica [289]. Whole plant was dried in shade and powdered herb was used for analysis of all the parameters

Moisture content was found to be $6.94\% \pm 0.4765$ indicates crude drug can be stored for a longer period of time in an air tight container. A total ash value was found to be $21.98 \pm 1.234\%$ w/w which is higher and indicates presence of higher amounts of inorganic salts of oxalates. There were no noticeable amounts of mucilage and saponins found in the plant drug. Detailed parameters are presented in following table 4.21. Phenolics and flavonoids were found in the methanol extract of plant material.

Results and Discussion

Table 4.21: Proximate analysis of whole plant of *O. corniculata*

<i>Parameters</i>	<i>Values (%w/w)*</i>
Moisture content (%w/w)	6.94±0.4765
Foreign matter (%w/w)	2.35
Total Ash Value (%w/w)	21.98±1.234
Acid Insoluble ash value (%w/w)	10.67±0.7946
Water soluble ash value (%w/w)	8.65±0.8505
Alcohol soluble extractive value (%w/w)	17.71±0.9607
Water soluble extractive value (%w/w)	24.64±1.078
Total Phenolic content (%w/w)	10.32±1.027
Total Flavanoid content (%w/w)	9.483±0.0839
Foaming Index	Less than 100
Swelling Index	Less than 1 cm
Haemolytic Index	78.4±1.652
Elements	
• Sodium	2.03 ppm
• Potassium	14.82 ppm
• Magnesium	490.28 ppm
• Manganese	68.23 ppm
• Copper	11.69 ppm
• Zinc	65.23 ppm
• Mercury	Nil
• Lead	0.21 ppm
• Cadmium	Nil
• Arsenic	Nil

*Values are expressed as average of three determinations with ±SEM

4.2.4. Phytochemical screening and TLC studies

Powdered plant material was subjected to successive extraction in a soxhlet extractor by using solvents of increasing polarity. Phytochemical studies of successive extracts (Table 4.23) shows presence of fats and fixed oils, carbohydrate and glycoside, saponins, flavanoids, proteins, amino acids and phytosterols.

Results and Discussion

Table 4.22: Successive extracts of whole plant of *O. corniculata*

Solvent	Extractive value (% w/w)	Colour & consistency
Pet. Ether (60-80 °C)	2.56	Dark green & sticky mass
Benzene	2.48	Dark green & dry powder
Chloroform	1.78	Green & dry powder
Ethyl Acetate	2.34	Green and dry powder
Methanol	16.64	Green and dry
Water	18.43	Brown and dry

Table 4.23: Phytoconstituents present in successive extracts of *O. corniculata*

Extracts → Group of compounds ↓	Petroleum ether extracts	Benzene extract	Chloroform extract	Ethyl acetate extract	Methanol extract	Water extract
Alkaloids	-	-	-	-	-	-
Glycosides	-	-	-	-	+	+
Terpenoids	+	+	+	-	-	-
Fats and fixed oils	+	+	+	-	-	-
Saponins	-	-	-	-	-	+
Flavanoids	-	-	-	+	+	+
Proteins and amino acids	-	-	-	-	+	+
Phenolics and tannins	-	-	-	+	+	+
Carbohydrate	-	-	-	+	+	+
Phytosterols	+	+	-	-	-	-

Results and Discussion

Table 4.24: TLC profile of successive extracts of whole plant of *O. corniculata*

	Solvent system	Detection	Pet. Ether	Benzene	Chloroform	Et. Ac.	Methanol	Water
Carbohydrate	Butanol: GAA: H ₂ O (4:1:5)	10% H ₂ SO ₄						
Phenolics	Tol: Et Ac: F A: Water (20:100:10:10)	5% FeCl ₃						
Flavonoid	Et Ac: GAA: FA: H ₂ O (100:11:11:26)	Alk KOH & NPPEG						
Alkaloids	Tol:EA:DEA (7:3:1)	Dragendroff's reagent						
Sterols and steroids	Pet Eth: Et Ac (4:1)	Libermann burchad's reagent	0.35, 0.43, 0.53, 0.66, 0.78, 0.94	0.42, 0.45, 0.63, 0.84, 0.95	0.34, 0.54, 0.58, 0.92	0.36, 0.56,	0.23, 0.47, 0.82	
Terpenoid	Benzene : Ether (2:3)	20 % SbCl ₃ in CHCl ₃		0.58, 0.65, 0.86	0.53, 0.71, 0.89	0.46, 0.68, 0.93		

4.2.5. HPTLC Studies of methanol extracts

TLC fingerprinting of methanol extract was done on CAMAG HPTLC system and phytoconstituents were separated in three different mobile phases of varying polarity. Different proportions of hexane, toluene, chloroform, ethyl acetate, methanol and water were tried, among these Hexane: Ethyl acetate (3:1), Ethyl acetate: chloroform: methanol (4:0.5:0.5), Toluene: ethyl acetate: formic acid: water (20:100:10:10) mobile phases were found most suitable for separation of non polar, medium polar and polar compounds. Detection was carried out by scanning plates at 254 and 366 nm and than at 540 nm post derivatised with anisaldehyde-sulphuric reagent.

Results and Discussion

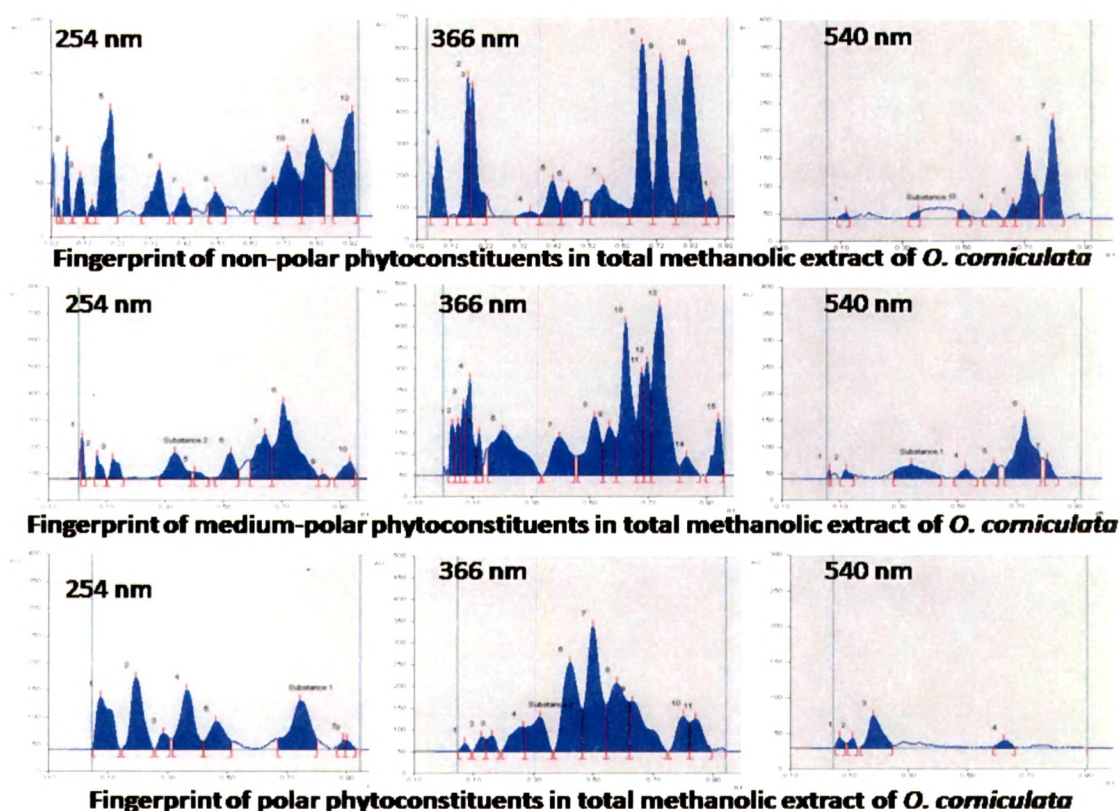


Figure 4.37: HPTLC fingerprint of methanol extract of whole plant of *O. corniculata* in different solvents

4.2.6. Estimation of secondary metabolite

Successive extraction process separated polar and non polar constituents. It was evaluated by TLC method and major secondary metabolite like phenolic and flavonoids were estimated by reported methods. Higher amounts of flavonoids (32.3% w/w of total aqueous extract) were observed in total aqueous extract.

Table 4.25: Secondary metabolites in different extracts of *O. corniculata*

Plant extract	Successive ethyl acetate extract	Successive methanol extract	Successive water extract	Total methanol extract	Total water extract
Total phenolics (% w/w)	14.24	16.24	20.12	20.61	24.65
Total Flavonoids (% w/w)	18.62	21.63	24.61	28.34	32.63

Results and Discussion

4.2.7. Fractionation and HPTLC studies of fractions

Unsaponifiable fraction of OC (yield 0.873 % w/w) was prepared to understand non polar components present in the plant. Flavonoids were found rich in OC and it is used as antioxidant, therefore, flavonoids rich fraction of OC (yield 7.43 % w/w) was prepared. Total methanol extract was fractionated as chart shown below for bioactivity guided isolation of active compound as protective in heart disease. All the fractions were monitored by TLC and finger print was obtained in three mobile phases. Non-polar, medium polar and polar compounds were separated on HPTLC and developed chromatograms were scanned and peaks of separated compounds are shown in Figures. HPTLC fingerprints of the fractions were developed using suitable solvent systems which were optimized to resolve the major phytoconstituents present in particular fraction.

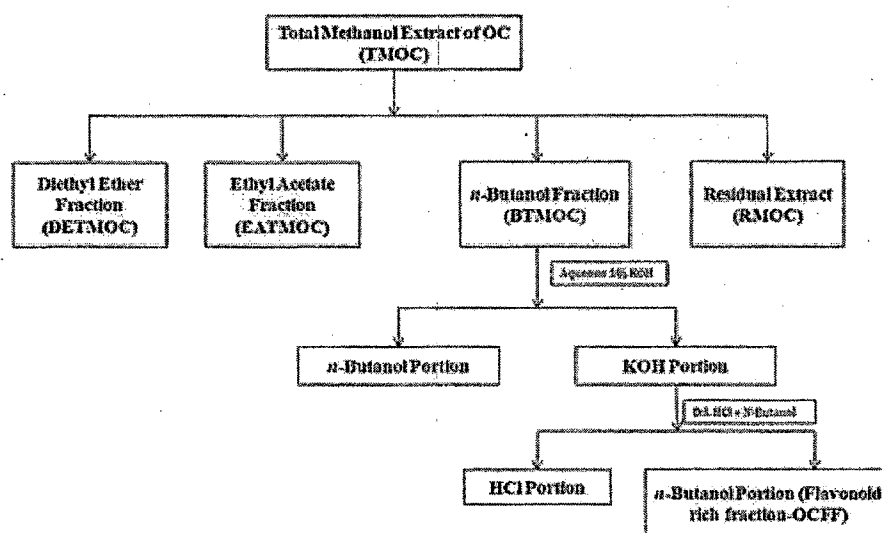
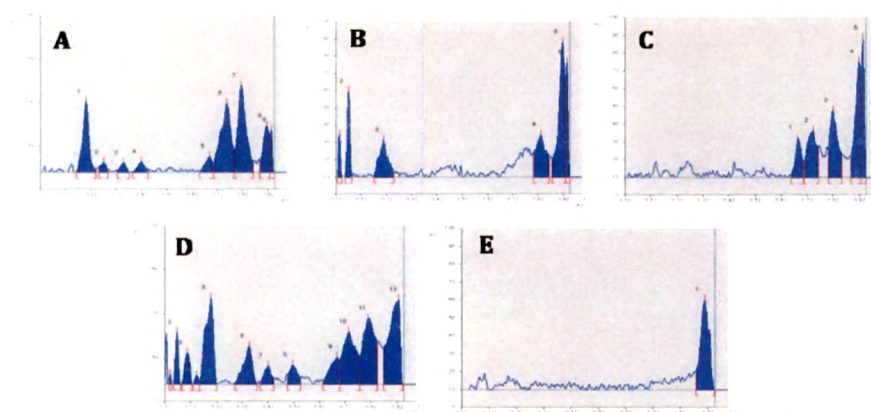


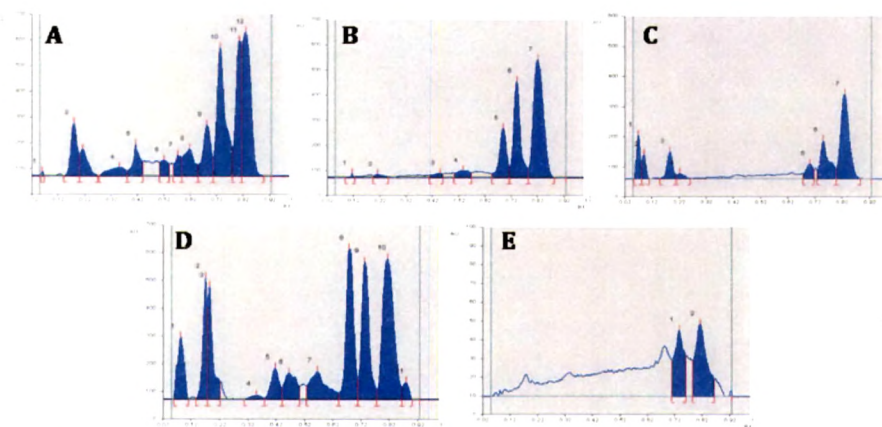
Figure 4.38: Fractionation of plant material of *O. corniculata*

Hexane: Ethyl acetate (3:1 v/v), Ethyl acetate: chloroform: methanol (4:0.5:0.5 v/v), Toluene: ethyl acetate: formic acid: water (20:100:10:10 v/v) mobile phases were found most suitable for separation of non polar, medium polar and polar compounds from extracts of *O. corniculata*. Developed plates were scanned in CAMAG scanner at absorption maxima of 254 nm and 366 nm. Plates were then sprayed with anisaldehyde sulphuric reagent, heated in an oven at 105°C for 10 min. and scanned at 540 nm for presence of various phytoconstituents

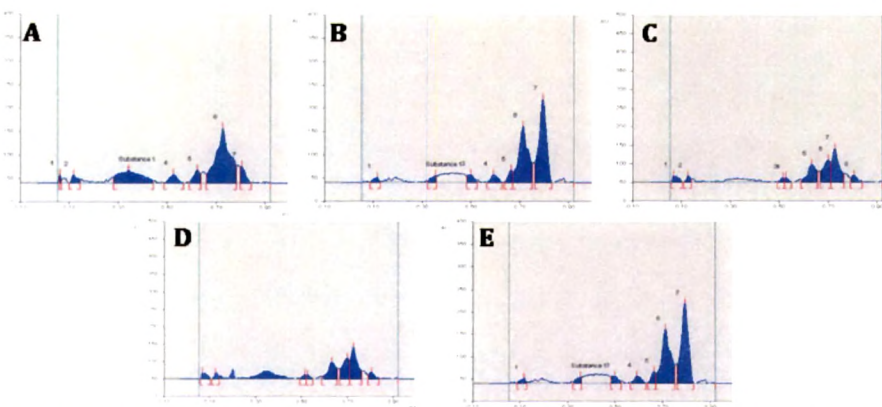
Results and Discussion



Fingerprinting of *O. corniculata* fractions for non-polar compounds at 254 nm



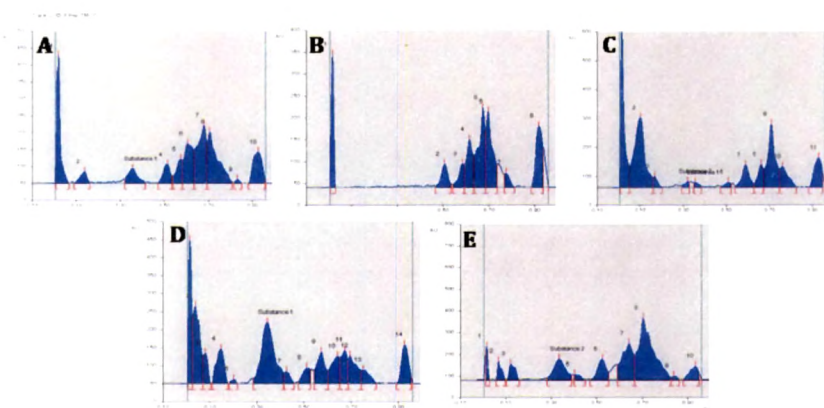
Fingerprinting of *O. corniculata* fractions for non-polar compounds at 366 nm



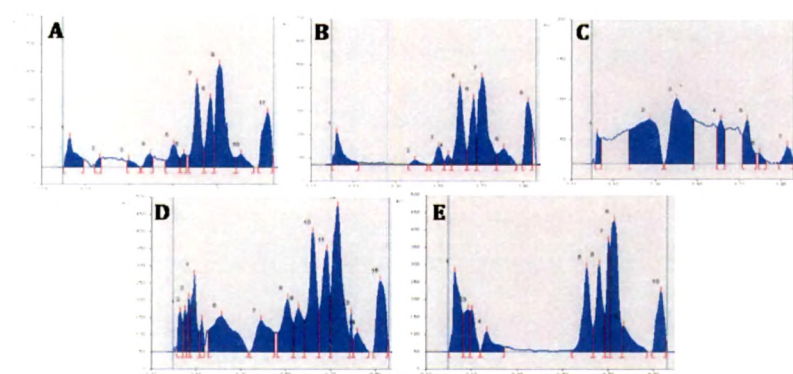
Fingerprinting of *O. corniculata* fractions for non-polar compounds at 540 nm

Figure 4.39: HPTLC fingerprinting of OC fractions **A:** Total methanol extract of OC (TMOE); **B:** Ether fraction of TMOE; **C:** Ethyl acetate fraction of TMOE; **D:** flavonoid fraction of OC (OCFF); **E:** Residual methanol of TMOE

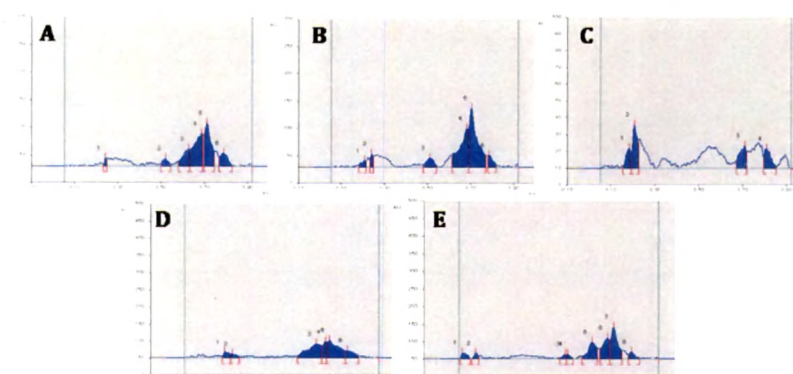
Results and Discussion



Fingerprinting of *O. corniculata* fractions for medium polar compounds at 254 nm



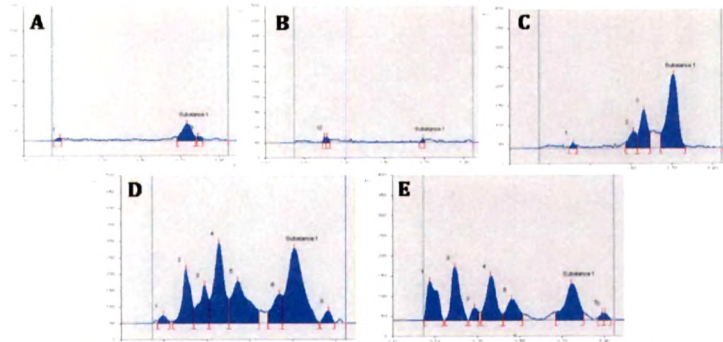
Fingerprinting of *O. corniculata* fractions for medium polar compounds at 366 nm



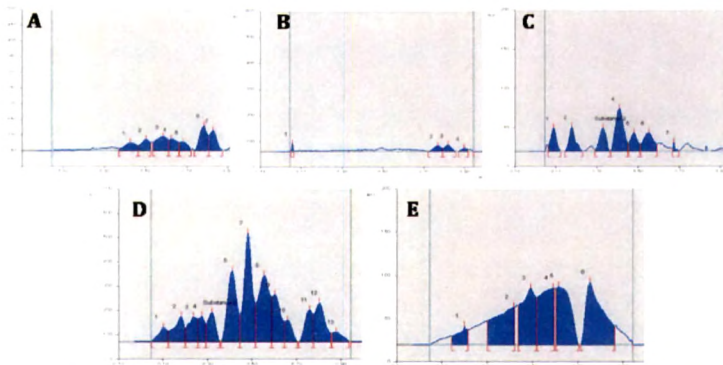
Fingerprinting of *O. corniculata* fractions for medium polar compounds at 540 nm

Figure 4.40: HPTLC fingerprinting of OC fractions **A:** Total methanol extract of OC (TMOC); **B:** Ether fraction of TMOC; **C:** Ethyl acetate fraction of TMOC; **D:** flavonoid fraction of OC (OCFF); **E:** Residual methanol of TMOC

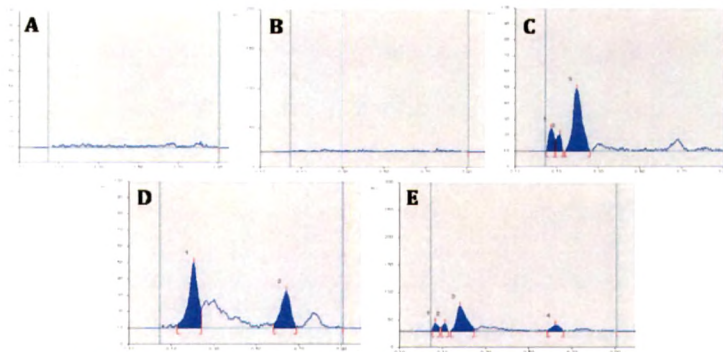
Results and Discussion



Fingerprinting of *O. corniculata* fractions for polar compounds at 254 nm



Fingerprinting of *O. corniculata* fractions for polar compounds at 366 nm



Fingerprinting of *O. corniculata* fractions for polar compounds at 540 nm

Figure 4.41: HPTLC fingerprinting of OC fractions **A:** Total methanol extract of OC (TMOC); **B:** Ether fraction of TMOC; **C:** Ethyl acetate fraction of TMOC; **D:** flavonoid fraction of OC (OCFF); **E:** Residual methanol of TMOC

Results and Discussion

4.2.8. Quantitative estimation of OC-01 in *O. corniculata* by HPTLC

Different compositions of the mobile phase were tested and the desired resolution of OC-01 with symmetrical and reproducible peaks was achieved by using mobile phase of ethyl acetate: methanol: water (4:0.5:0.5 v/v) with 20 min of chamber saturation with the mobile phase. A peak corresponding to OC-01 was seen at R_f 0.48. Flavonoid fraction of *O. corniculata*, when subjected to TLC, showed the presence of OC-01 peaks. A comparison of the spectral characteristics of the peaks for isolated OC-01 and that of the fraction revealed the identity of flavonoid present in plant. Peak purity test of OC-01 was done by comparing its UV-visible spectra in standard and sample track.

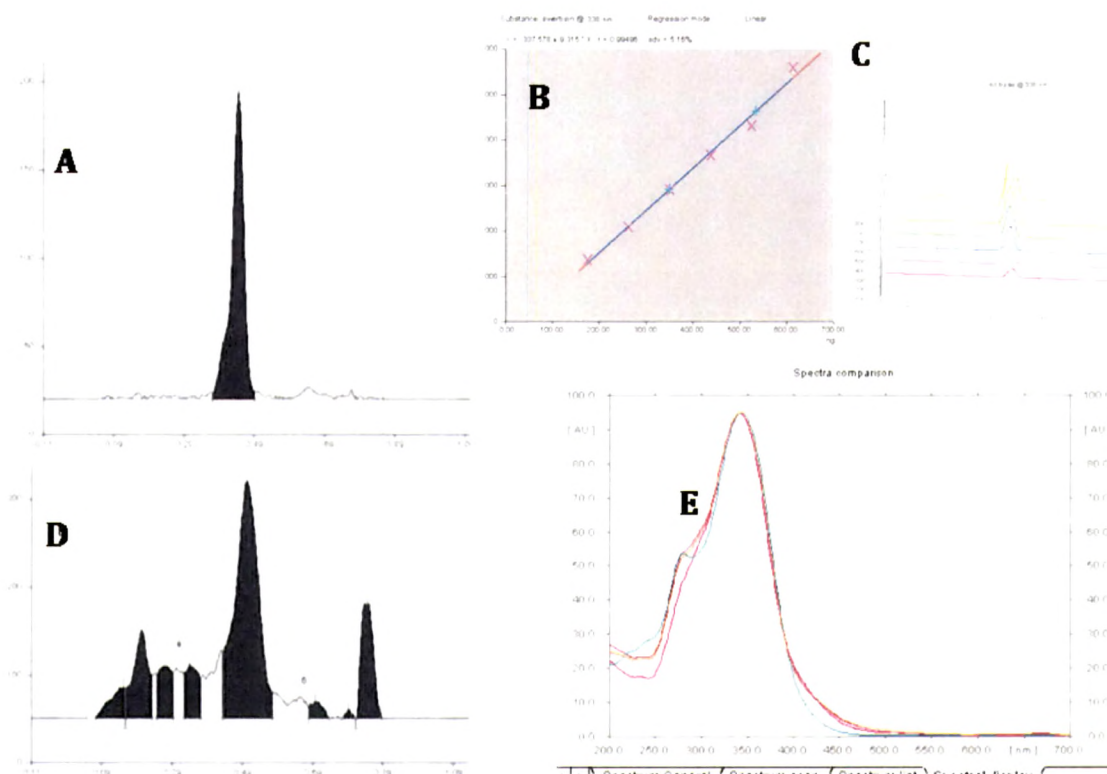


Figure 4.42: Quantification of OC-01 in flavonoid fraction of *O. corniculata* by HPTLC A) Track represents isolated OC-01 B) Calibration curve of OC-01 C) All tracks at 338 nm D) Track represents fraction of *O. corniculata* E) Overall UV spectra of OC-01 of standard and test track.

Results and Discussion

4.2.8.1. Method validation

Linearity was checked by applying standard solutions of OC-01 at six different concentration levels. The calibration curve was drawn in the concentration range of 100–600 ng/spot. Results of regression analysis on calibration curve and detection limits are presented in Table 4.26. Instrumental precision was checked by repeated scanning of the same spots (200 and 500 ng/spot) of standard OC-01 three times and the RSD values were 2.46 and 3.53 for 200 and 500 ng/spot, respectively. To determine the precision of the developed assay method 200 and 500 ng/spot of OC-01 standard was analyzed three times within the same day to determine the intra-day variability. The RSD values were 3.63 and 2.48 for 200 and 500 ng/spot, respectively. Similarly, the inter-day precision was tested on the same concentration levels on two days and the RSD values were 1.72 and 3.21, respectively.

Table 4.26: Validation parameters of quantification of OC-01 by HPTLC

Parameters	Values
Detection wavelength	338 nm
Range	100-600 ng/spot
Limit of Detection (LOD)	35 ng
Limit of Quantification (LOQ)	116.5 ng
Regression equation	$Y = 3359.43 + 42.25 * X$
Correlation coefficient (linearity)	0.9984
Recovery study	
80% level	96.25 ±0.289
100% level	98.63 ±2.129
120% level	102.69 ±0.832
Precision study (%RSD)	
Intra-day	3.63
Inter-day	1.72

Sample Analysis and Recovery Studies

The content of OC-01 in the *O. corniculata* leaves by HPTLC method was found to be 0.241% w/w. For the examination of recovery rates, 80, 100 and 120% of pure OC-01 were spiked to

Results and Discussion

preanalyzed sample and quantitative analysis was performed. Recovery study ranged from 96.25 % to 102.69%.

4.2.9. Quantitative estimation of OC-01 in *O. corniculata* by HPLC

OC-01 was estimated by HPLC in flavonoid fraction of *O. corniculata* at 338 nm wavelength with flow rate of 0.8 mL/min. The retention time (R_t) of isolated flavonoid was found to be 4.68 min. in mobile phase consisting acetonitrile: water (1:3 v/v). OC-01 was quantified in flavonoids fraction by using regression equation $y = 5.696x + 10.95$ with correlation coefficient $R^2 = 0.997$.



Figure 4.43: HPLC Chromatogram of isolated OC-01

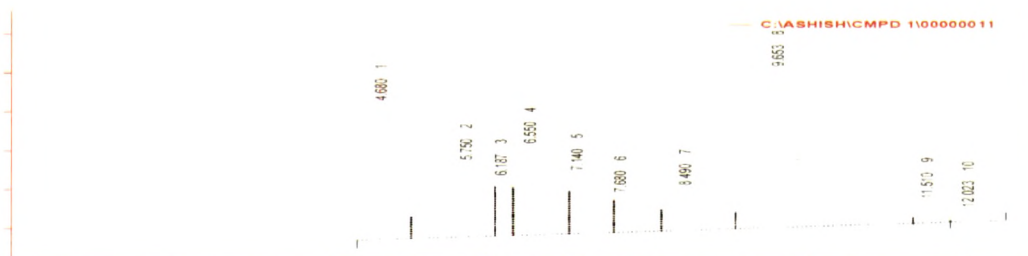


Figure 4.44: HPLC Chromatogram of flavonoids fraction of OC

4.2.9.1. Method validation

The calibration curve was drawn in the concentration range of 10-100 $\mu\text{g/mL}$. Results of regression analysis on calibration curve and detection limits are presented in Table 4.27.

Linearity was checked by applying standard solutions of OC-01 at six different concentration levels. Instrumental precision was checked by repeated injection of the sample (50 $\mu\text{g/mL}$) of

Results and Discussion

standard OC-01 five times and the mean % RSD value was 0.62 ± 0.0832 . To determine the precision of the developed assay method 50 and 100 $\mu\text{g}/\text{injection}$ of flavonoid standard was analyzed three times within the same day to determine the intra-day variability. The RSD values were 1.024 and 1.062 for 50 and 100 $\mu\text{g}/\text{mL}$, respectively. Similarly, the inter-day precision was tested on the same concentration levels on two days and the RSD values were 0.932 and 1.122, respectively.

Concentration ($\mu\text{g}/\text{mL}$)	Area (mV^2S)
10	56.27
20	125.87
30	186.25
40	236.85
50	311.31
100	573.24

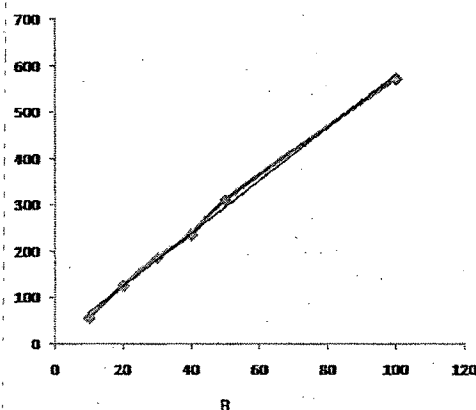


Figure 4.45: calibration curve for the estimation of OC-01 by HPLC

Table 4.27: Validation parameter for the quantification of OC-01 by HPLC

Parameters	Values
Detection wavelength	338 nm
Range	10-100 $\mu\text{g}/\text{mL}$
Limit of Detection (LOD)	3 $\mu\text{g}/\text{mL}$
Limit of Quantification (LOQ)	9.99 $\mu\text{g}/\text{mL}$
Regression equation	$y = 5.696x + 10.95$
Correlation coefficient (linearity)	0.997
Recovery study	
80% level	95.82 ± 1.032
100% level	94.52 ± 0.829
120% level	97.34 ± 0.731
Precision study (%RSD)	
Intra-day	1.024
Inter-day	0.932

Results and Discussion

The content of OC-01 in the *O. corniculata* by HPLC method was found to be 0.187% w/w. For the examination of recovery, 80, 100 and 120% of isolated alkaloid were spiked to preanalyzed sample and quantitative analysis was performed. Recovery was ranged from 94.52% to 97.34%.

4.2.10. Biological studies

4.2.10.1. In-vitro antioxidant activity

All fractions were studied for their antioxidant potential at concentration of 10, 20, 40, 80, 100 $\mu\text{g/mL}$. Three methods were selected viz. DPPH radical scavenging assay, FeCl_3 reducing power and phosphomolybdenum method. Ascorbic acid and Butylated Hydroxy Toluene (BHT) were selected as standard.

4.2.10.1.1. DPPH radical scavenging

O. corniculata constituents show antioxidant potential in DPPH radical scavenging assay. The antioxidant activity of extracts was evaluated by their ability to scavenge free radicals by using DPPH assay. The extract concentration that caused scavenging of 50% of DPPH, (IC_{50}) was detected. As shown in (Figure 4.46), IC_{50} of extracts varied from 28.89 $\mu\text{g/mL}$ to 76.13 $\mu\text{g/mL}$ giving significantly lower potencies than ascorbic acid ($\text{IC}_{50} = 10.44 \mu\text{g/mL}$).

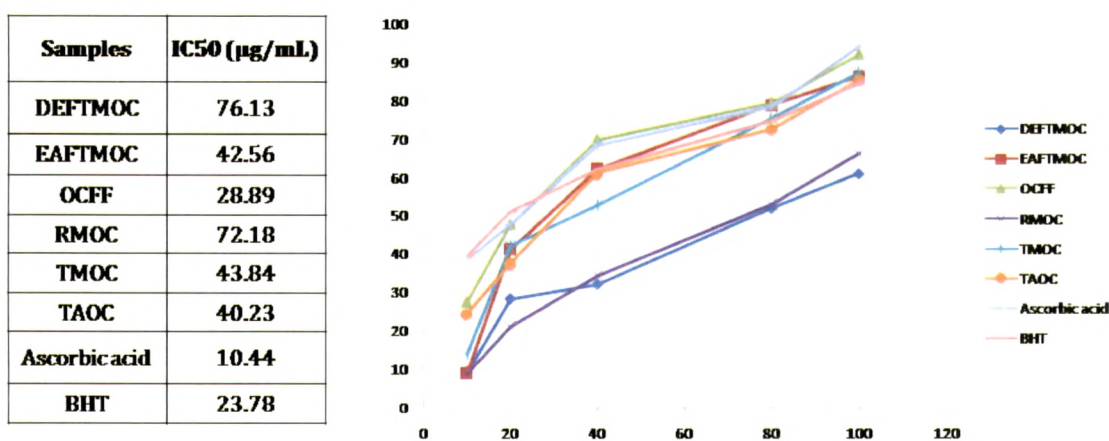


Figure 4.46: Antioxidant activity of OC fraction by DPPH with IC_{50}

Results and Discussion

4.2.10.1.2. FeCl₃ reducing power assay

The reducing power of a compound is related to its electron transferability and may serve as a significant indicator of its potential antioxidant activity. In this assay, the color of test solution changes to green and blue depending on the reducing power of test samples. The results (Figure 4.47) show following fractions; TAOC- 36.25 µg/mL, OCF- 38.73 µg/mL and TMOC- 41.74 µg/mL have IC₅₀ comparable to standard ascorbic acid- 10.44 µg/mL and BHT 23.78 µg/mL.

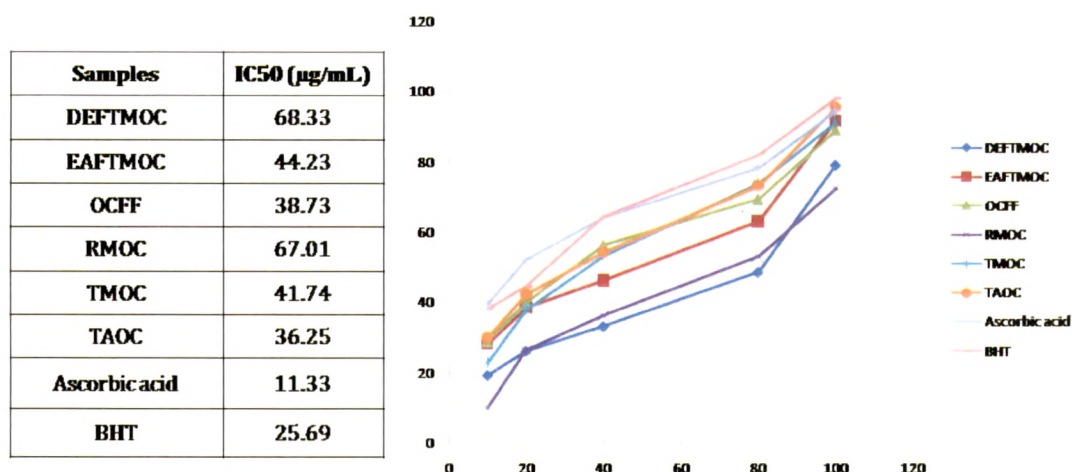


Figure 4.47: Antioxidant activity of OC fraction by FeCl₃ reducing power with IC₅₀

4.2.10.1.3. Antioxidant capacity by phosphomolybdenum method

The formation of a green-colored complex of phosphate and Mo (V) was presented by Fiske and Subbarow [238] as the basis of a spectrophotometric method to determine inorganic phosphate. This method was later revised and modified by Chen *et al.* [239].

The required reducing species should be supplied with reagent mixture to produce Mo (V) from the Mo(VI). Plant extracts/fractions contain variety of antioxidant compounds like ascorbic acid, β-carotene and flavonoids, therefore, *O. corniculata* has been evaluated for its antioxidant activity.

Results and Discussion

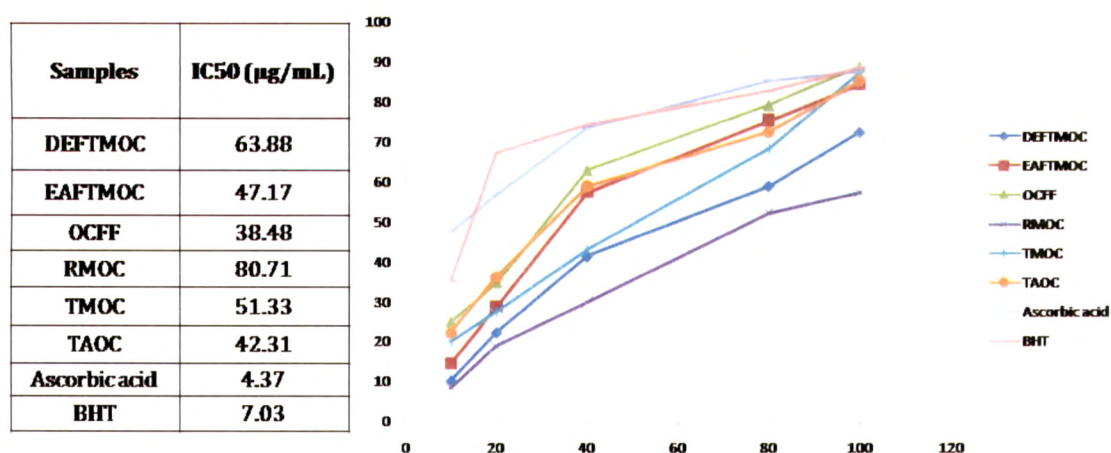


Figure 4.48: Total Antioxidant activity of OC fraction by Phosphomolybdenum method with IC₅₀ Ascorbic acid and flavonoids present in fractions of *O. corniculata* found to reduce molybdenum, IC₅₀ of fractions OCFF-38.48 µg/mL, TAOC-42.38 µg/mL, EAF TMOC-47.17 µg/mL and TMOC-51.33 µg/mL are comparable with standards.

IC₅₀ of all the fractions by three methods are presented in table. It has been observed that flavonoids rich fraction, total aqueous extract and total methanol extracts found to be most active components as antioxidant.

Table 4.28: IC₅₀ of OC fractions by three methods

Samples	IC ₅₀ (µg/mL±sdv)
DEFTMOC	69.45±6.2008
EAF TMOC	44.65±2.3334
OCFF	35.36±5.1631
RMOC	73.3±6.9183
TMOC	45.63± 5.0411
TAOC	39.596±3.0792
Ascorbic acid	8.713±3.7876
BHT	18.83±10.2665

*data presents as mean of IC₅₀ determined by three methods with ±standard deviation

Results and Discussion

4.2.11. In-vivo study

4.2.11.1. Acute toxicity studies

Acute toxicity studies were performed following OECD guidelines (2001) (OECD 423, Acute Toxic Class Method) (Roll et al., 1986) [208]. Oral dose of 2000 mg/kg and 3000 mg/kg of the test extracts and 500 mg/kg and 1000 mg/kg of fractions were given orally to different groups of female rats. The animals were observed for first 4 hours of treatment to next 14 days. There were no signs of any toxicity in animals after the administration of the test doses. All the animals showed similar food intake, body weight gain and clinical signs as that of the control group. No morbidity or mortality was observed in the treated animals. The necropsy studies did not detect any abnormality.

4.2.11.1.1. Effect of *O. corniculata* on isoproterenol-induced myocardial infarction

Isoproterenol-induced myocardial necrosis is a well established model of MI in rats [290]. The activities and capacities of antioxidant systems of heart declined following ISO challenge leading to the gradual loss of prooxidant/ antioxidant balance which accumulates into oxidative damage of cardiac myocyte. As a result of this, cytosolic enzymes such as Lactate Dehydrogenase (LDH), transaminases (ALT, AST) and Creatine Phosphokinase (CPK) were released into blood stream and serve as the diagnostic markers of myocardial tissue damage [291]. The amount of these cellular enzymes present in blood reflects the alterations in plasma membrane integrity and/or permeability. Drug from natural origin, such as naringin, silibinin and squalene on treatment evidenced by a decline in lactate dehydrogenase, glutamic oxalacetic transaminase and creatine kinase levels indicated their membrane stabilizing action [292]. Therefore, the present study evaluated the role of *O. corniculata* extracts and swertisin in combating ISO associated macromolecular damage in the myocardium of MI rats. Amongst various proposed mechanisms of ISO causing MI, generation of redundant free radicals is one of the main causative factors [293].

Yellow Indian sorrel (OC) is an edible herb and it is known to contain carotenoids, flavone glycosides, vitamin C and many antioxidants [294]. It also contains 1.8 % dry weight of palmitic acid and 3.8 % dry weight of mixture of oleic, linoleic and lenolenic acids. Nutritive value of OC is reported to be 1.36±0.3(carbohydrate), 13.2±0.7 (fatty acids), 12.5 ± 0.5 (Protein) 6.2 ±0.3 (fibre), 0.62±0.3 (tannins) 174.24±4.6 (nutritive value) [295]. Many of the above constituents may play important role in prevention from ischaemic effects of catecholamines.

Results and Discussion

4.2.11.1.2. Effect of *O. corniculata* extract/fractions on serum transaminases

Table 4.29: Serum transaminases of different group of rats

Groups	AST (IU/L)	ALT (IU/L)
Vehicle control	32.17±1.415	50.07±2.209
ISO control	55.50±1.862**	128.9±3.149**
OC01 (20 mg/kg)	42.87±1.051 [#]	105.4±4.230*
DEFTMOC (50 mg/kg)	48.07±1.001**	118.0±3.986**
DEFTMOC (100 mg/kg)	41.78±1.053	90.62±1.786* [#]
EAFMOC (50 mg/kg)	44.43±2.321**	87.54±2.311
EAFMOC (100 mg/kg)	37.43±2.34 [#]	65.21±4.212 [#]
OCFF (50 mg/kg)	43.22±1.364*	91.69±2.272
OCFF (100 mg/kg)	36.27±1.246 ^{##}	60.02±2.044 ^{##}
RMOC (50 mg/kg)	47.23±3.390*	110.0±3.213*
RMOC (100 mg/kg)	40.82±1.161	99.09±1.751
TAOC (200 mg/kg)	44.47±1.593**	100.2±3.250*
TAOC (400 mg/kg)	39.17±1.287 [#]	97.14±2.346*

All values are Mean ± SEM. One way ANOVA followed by Bonferroni test were used for analysis of biochemical data of different groups (Significance; * p<0.01, ** p<0.001 when compared to vehicle control group and # p<0.01, ## p<0.001 when compared to ISO control group)

There was a significant elevation seen in the serum transaminases (171.87% of AST and 257.43% of ALT in group 2) in isoproterenol injected animals compared to the vehicle controls (p<0.01). In the Groups 3, 7, 9 and 13 rats pretreated with compound OC01 and *O. corniculata* fractions, a significant reduction (p<0.01) in the level of transaminase enzymes compared with the isoproterenol-administered rats (Group 2) was observed (Table 4.29). Rats in Group 3 (compound OC01) and Groups 4 to13 were given *O. corniculata* fractions and isoproterenol subcutaneously at the end of the treatment period.

4.2.11.1.3. Effect of *O. corniculata* extract/fractions on serum inflammatory markers

Besides alteration in the endogenous antioxidants, changes in CPK-MB isoenzyme and LDH have been considered as one of the important diagnostic markers of myocytes damage [296]. CPK-MB isoenzyme is a marker for early detection of myocardial ischemic injury and LDH is a delayed marker of myocardial injury, begins to rise in 12–24 h following injury with peak levels

Results and Discussion

in 2–3 days. Leakage of CPK-MB and LDH from heart in present study after 48 h of isoproterenol administration precisely explains the ischemic injury of heart concurs to previous reports [297]. When myocardial cells, containing CPK-MB isoenzyme and LDH are damaged or destroyed due to deficient oxygen supply or glucose, the integrity of cell membrane gets distorted and it might become more porous and permeable or may rupture that result in the leakage of these enzymes. In this study, significant decline was observed in the activities of cardiac markers such as ALT, AST, LDH and CPK in the heart of acute isoproterenol-treated rats, which is consistent with earlier reports [298].

Table 4.30: CPK-MB and LDH levels in serum of rats

Groups	CPK-MB activity (U/L)	LDH activity (IU/L)
Vehicle control	117.2±4.114	197.8±10.84
ISO control	665.0±19.51**	523.3±19.62**
OC01 (20 mg/kg)	426.2±12.02**#	339.5±15.06**
DEFTMOC (50 mg/kg)	663.4±13.56**	455.3±17.99**
DEFTMOC (100 mg/kg)	579.0±17.32**	374.3±19.70*
EAFTMOC (50 mg/kg)	612.4±13.22**	421.5±22.34*
EAFTMOC (100 mg/kg)	483.2±16.33**	273.3±32.33##
OCFF (50 mg/kg)	364.0±18.39#	367.5±19.36**
OCFF (100 mg/kg)	269.4±31.72##	249.9±18.54##
RMOC (50 mg/kg)	575.2±32.52	412.2±16.00
RMOC (100 mg/kg)	499.5±16.68	284.7±15.11#
TAOC (200 mg/kg)	567.2±30.38*	396.9±15.95*
TAOC (400 mg/kg)	428.3±23.75##	281.1±11.02#

All values are Mean ± SEM. One way ANOVA followed by Bonferroni test were used for analysis of biochemical data of different groups (Significance; * p<0.01, ** p<0.001 when compared to vehicle control group and # p<0.01, ## p<0.001 when compared to ISO control group)

Senthil et al. observed that these cardio-specific marker enzymes are released from the heart into the blood during myocardial damage due to myofibril degeneration and myocyte necrosis. Significant increase was seen in the activities of cardiac markers (AST, ALT, LDH and CPK) in serum of isoproterenol-treated rats, which is consistent with earlier reports [299], might be due to

Results and Discussion

imbalance between the formation of oxidants and the availability of endogenous antioxidants, which determines energy metabolism of heart [296]. On the other hand pretreatment with *O. corniculata* extracts and swertisin in isoproterenol administered rats decreased the activities of these enzymes in the serum.

Table 4.30 shows the activities of CPK-MB isoenzyme and LDH levels in the serums of vehicle and drug treated rats. In ISO-control rats, the activities of these enzymes increased significantly ($p < 0.001$) when compared to vehicle-control rats i.e. 567.4% of CPK-MB isoenzyme and 264.56% of LDH levels. Groups 3, 7, 9 and 13 restored significantly the activities of these enzymes while OC-01 at dose of 20mg/kg/day significantly ($p < 0.001$) decreased the level of inflammatory markers when compared to ISO-control animals.

4.2.11.1.4. Effect of *O. corniculata* extract on antioxidant enzymes and lipid peroxidation

Catalase, GSH and SOD constitute a mutually supportive enzyme system of the first line cellular defense against oxidative injury, decomposing O_2 and H_2O_2 before their interaction to form the more harmful hydroxyl (OH^+) radical [300]. SOD plays a major role in controlling mitochondrial reactive oxygen species (ROS) generated during normal oxidative phosphorylation and protects cells against oxidative stress by catalytic removal of superoxide radicals and conversion to hydrogen peroxide [301]. After isoproterenol administration, a significant decrease in SOD indicate occurrence of oxidative stress and impaired mitochondrial energetic, required for normal cardiac function. CAT activity was also decreased which play a critical role in regulating ROS in myocardium by handling hydrogen peroxide, the product of SOD. GSH status is a highly sensitive indicator of cell functionality and viability. GSH depletion is linked to a number of disease states including cancer, neurodegenerative and cardiovascular diseases [302]. In the present study, the reduction seen in the level of GSH in heart of isoproterenol-induced myocardial infarction was either due to increased degradation or decreased synthesis of glutathione. Depletion of GSH results in enhanced lipid peroxidation and excessive lipid peroxidation can cause increased GSH consumption as observed in the present study.

Lipid peroxidation is an important pathogenic event in myocardial necrosis. Malondialdehyde (MDA) is a major lipid peroxidant end product; the increased level of MDA indicates activation of the lipid peroxidative process, resulting in irreversible damage to hearts of animals subjected to isoproterenol stress [303]. MDA, the degradation product of the oxygen-derived free radicals and lipid oxidation, reflects the damage caused by reactive oxygen species [304].

Results and Discussion

Table 4.31: Antioxidant milieu and MDA levels in rat hearts

Groups	SOD (U/min/mg)	CAT (μ mol of H ₂ O ₂ utilized/min/mg)	GSH (ng of GSH/ mg)	MDA (nmol of MDA/mg)
Vehicle control	1.424 \pm 0.024	1.670 \pm 0.164	96.53 \pm 2.390	36.80 \pm 2.865
ISO control	0.2515 \pm 0.047**	0.2107 \pm 0.006**	26.42 \pm 1.484**	82.39 \pm 2.991**
OC01 (20 mg/kg)	0.7360 \pm 0.035##	0.9943 \pm 0.061##	64.63 \pm 2.176##	51.81 \pm 1.166*#
DEFTMOC (50 mg/kg)	0.4103 \pm 0.069*	0.5473 \pm 0.036*	37.52 \pm 2.011*	68.25 \pm 1.628**
DEFTMOC (100 mg/kg)	0.6012 \pm 0.023	0.7732 \pm 0.021	48.81 \pm 2.424**	64.39 \pm 2.049*
EAFTMOC (50 mg/kg)	0.832 \pm 0.032#	0.738 \pm 0.211	42.32 \pm 2.321	67.72 \pm 3.772#
EAFTMOC (100 mg/kg)	0.718 \pm 0.042	0.922 \pm 0.084##	54.83 \pm 3.212#	52.32 \pm 2.308##
OCFF (50 mg/kg)	0.8510 \pm 0.041#	0.9772 \pm 0.036#	57.91 \pm 1.722##	48.78 \pm 0.531##
OCFF (100 mg/kg)	1.151 \pm 0.064##	1.315 \pm 0.041##	73.67 \pm 1.734##	42.73 \pm 1.162##
RMOC (50 mg/kg)	0.4657 \pm 0.017*	0.5090 \pm 0.021**	42.29 \pm 1.841**	62.94 \pm 2.169**
RMOC (100 mg/kg)	0.8090 \pm 0.015#	0.8435 \pm 0.030#	54.12 \pm 3.223	60.04 \pm 1.141*
TAOC (200 mg/kg)	0.6525 \pm 0.017	0.7692 \pm 0.028	42.79 \pm 1.555**	62.73 \pm 1.541*
TAOC (400 mg/kg)	0.9250 \pm 0.023##	0.9608 \pm 0.026##	60.48 \pm 1.924##	57.53 \pm 1.265##

All values are Mean \pm SEM. One way ANOVA followed by Bonferroni test were used for analysis of biochemical data of different groups (Significance; * p<0.01, ** p<0.001 when compared to vehicle control group and # p<0.01, ## p<0.001 when compared to ISO control group)

In present study, n-butanol fraction and OC-01 significantly decreased MDA contents near to normal levels and also prevented the isoproterenol-induced lipid peroxidation and maintained the level of CAT, SOD and reduced glutathione near normal level in heart.

Table 4.31 shows the activities of enzymes SOD, CAT and GSH and level of MDA in hearts of all rats. The antioxidant enzyme activity were decreased significantly (P<0.001) whereas a significant increased was observed in MDA level in ISO treated rats when compared to those of control rats. The activities of antioxidant enzymes and MDA level were maintained near to normal levels in animals pretreated with *O. corniculata* extracts/fractions (Group 3, 7, 8, 9 and 13) as compared to ISO treated animals (p<0.001). In all the parameters studied, *O. corniculata* extract/fractions at lower dose showed a minor effect, whereas higher dose showed a more significant effect (p<0.001).

Results and Discussion

4.2.11.1.5. Effect of *O.corniculata* extracts on TTC staining and histopathology

In histopathological examination normal architecture was observed in control animals whereas animals treated with ISO showed thrombus formation, contraction band necrosis and inflammation. Animals pretreated with *O. corniculata* extract revealed much less intensity of the above changes. Histopathological findings and TTC stain study (Figure-4.53) of the heart pretreated with OCFE and OC-01 present a well preserved normal morphology of cardiac muscle with no evidence of necrosis when compared to ISO-control heart.

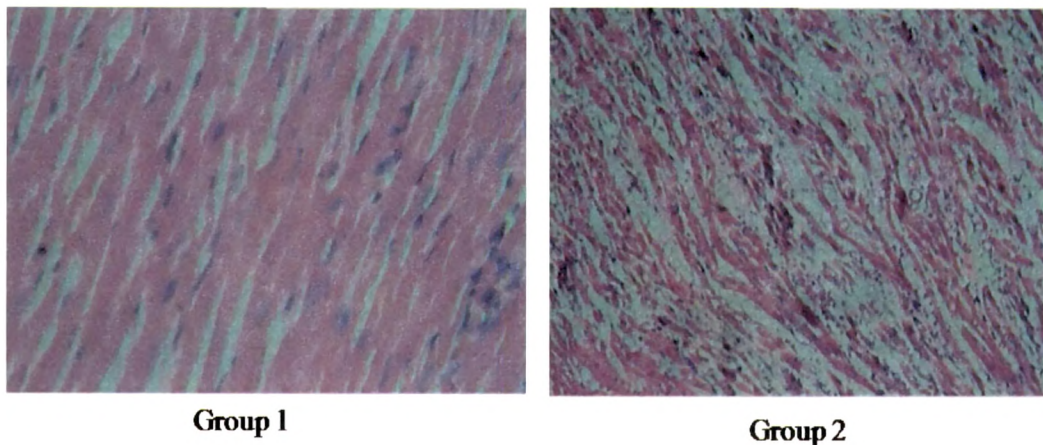


Figure 4.49: Histoarchitecture of rat hearts of various groups; Group 1: vehicle control; Group 2: ISO control

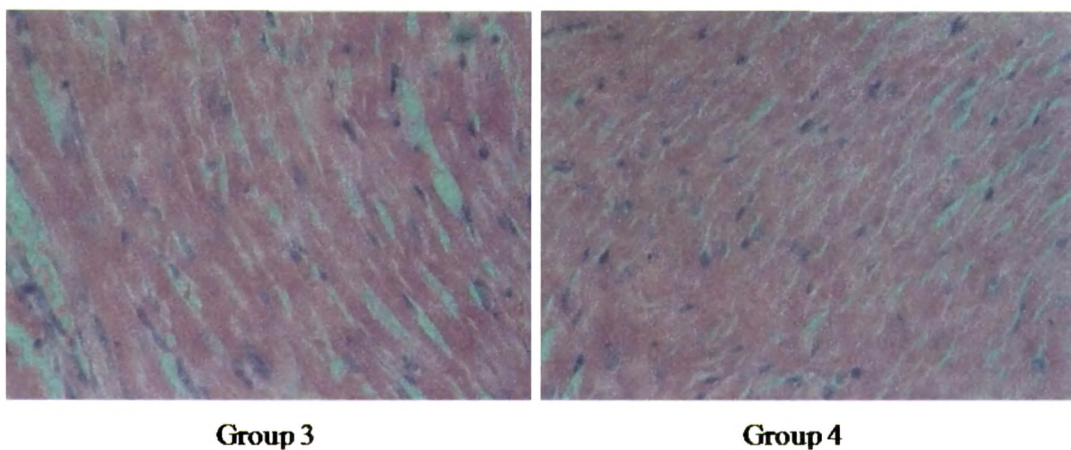


Figure 4.50: Histoarchitecture of rat hearts of various groups; Group 3: swertisin (20 mg/kg +ISO); Group 4: ETTMOE (50 mg/kg+ISO)

Results and Discussion

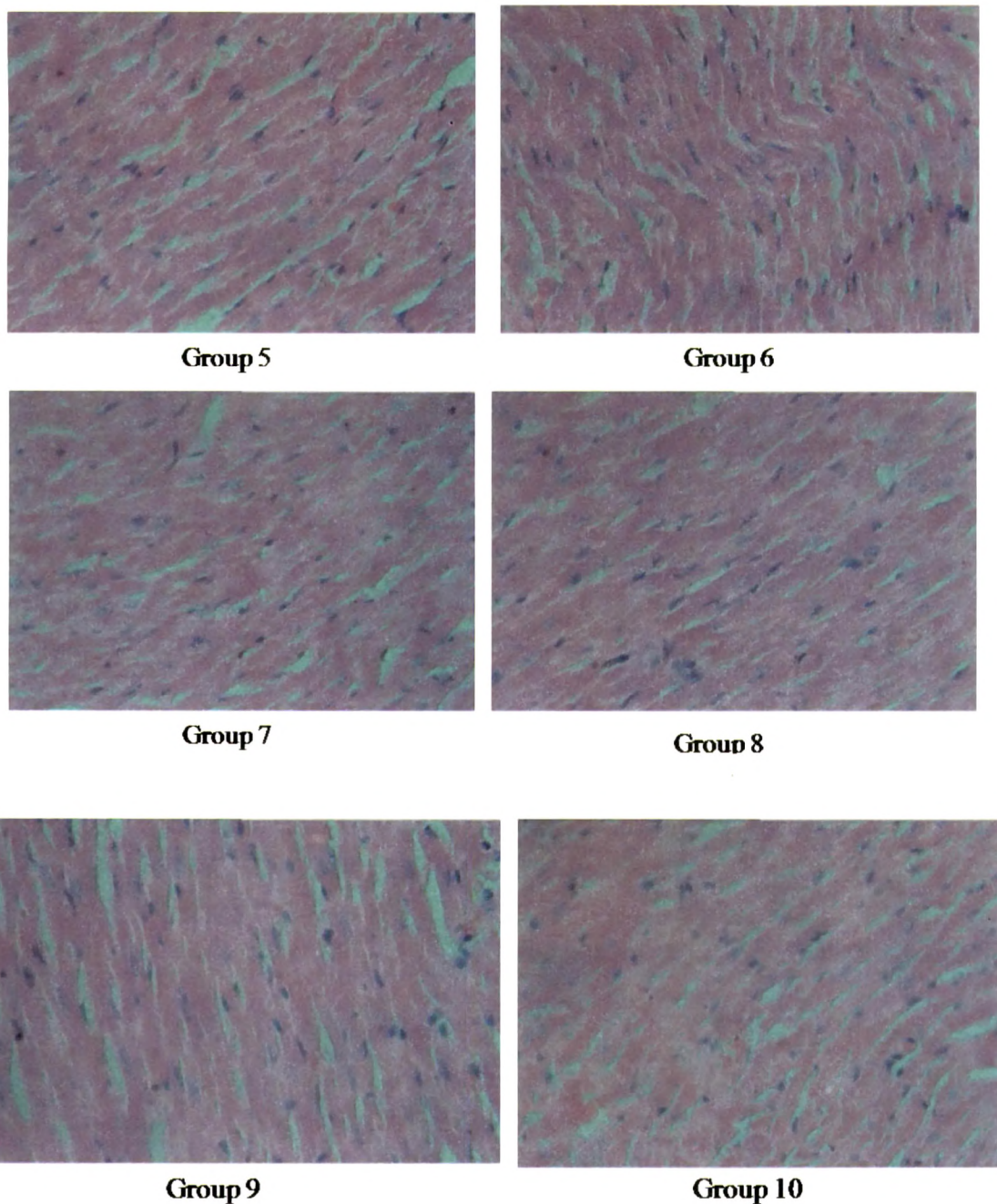


Figure 4.51: Histoarchitecture of rat hearts of various groups; Group 5: ETTMOC (100 mg/kg+ISO); Group 6: EATMOC (50 mg/kg+ISO); Group 7: EATMOC (100 mg/kg+ISO); Group 8: OCFE (50 mg/kg+ISO); Group 9: OCFE (100 mg/kg+ ISO); Group 10: RMOC (50 mg/kg+ISO)

Results and Discussion

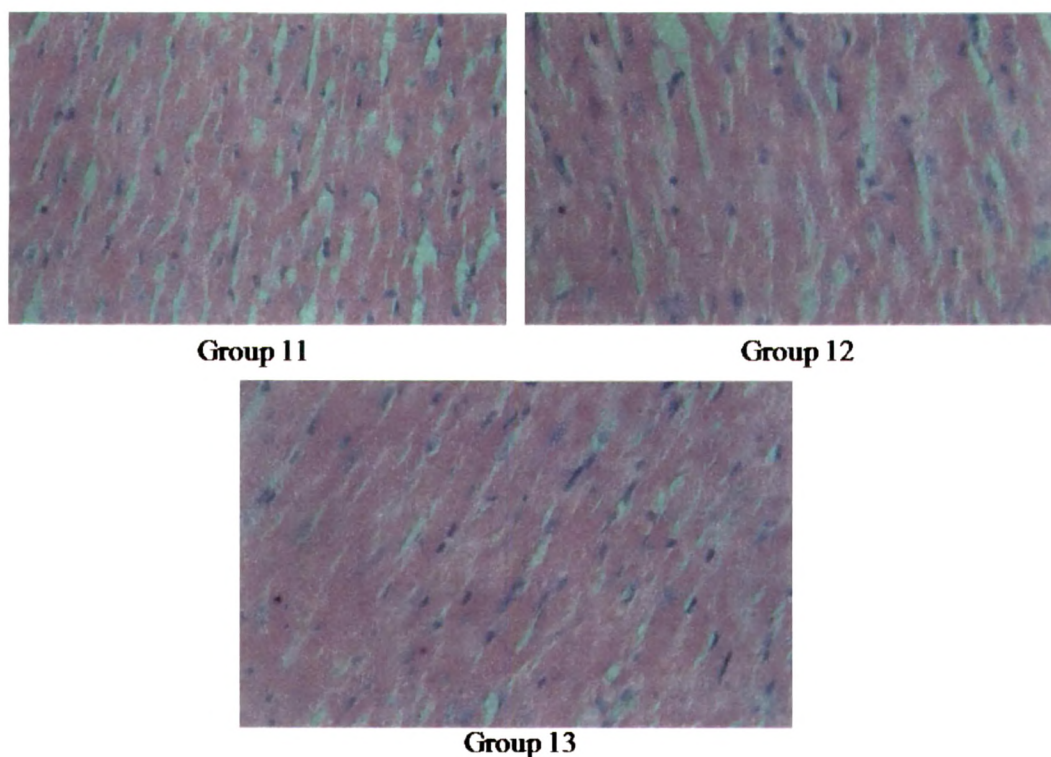


Figure 4.52: Histoarchitecture of rat hearts of various groups; Group 11: RMOC (100 mg/kg+ISO); Group 12: TAOC (200 mg/kg+ISO); Group 13: TAOC (400 mg/kg+ISO)

Hematoxylin-eosin staining was used to evaluate the extent of myocardial inflammation (Figures 4.49-4.52). Isoproterenol induced myocardial inflammatory cell infiltration, predominantly in the subendocardium. Mononuclear cell infiltrates ranged from isolated and focal in some areas to confluent in others. All groups pretreated with extracts/fractions showed some extent of myocardium protection against catecholamine induced MI. Groups treated with aqueous extract, flavonoids rich fraction of OC showed remarkable recovery in histoarchitecture.

Results and Discussion

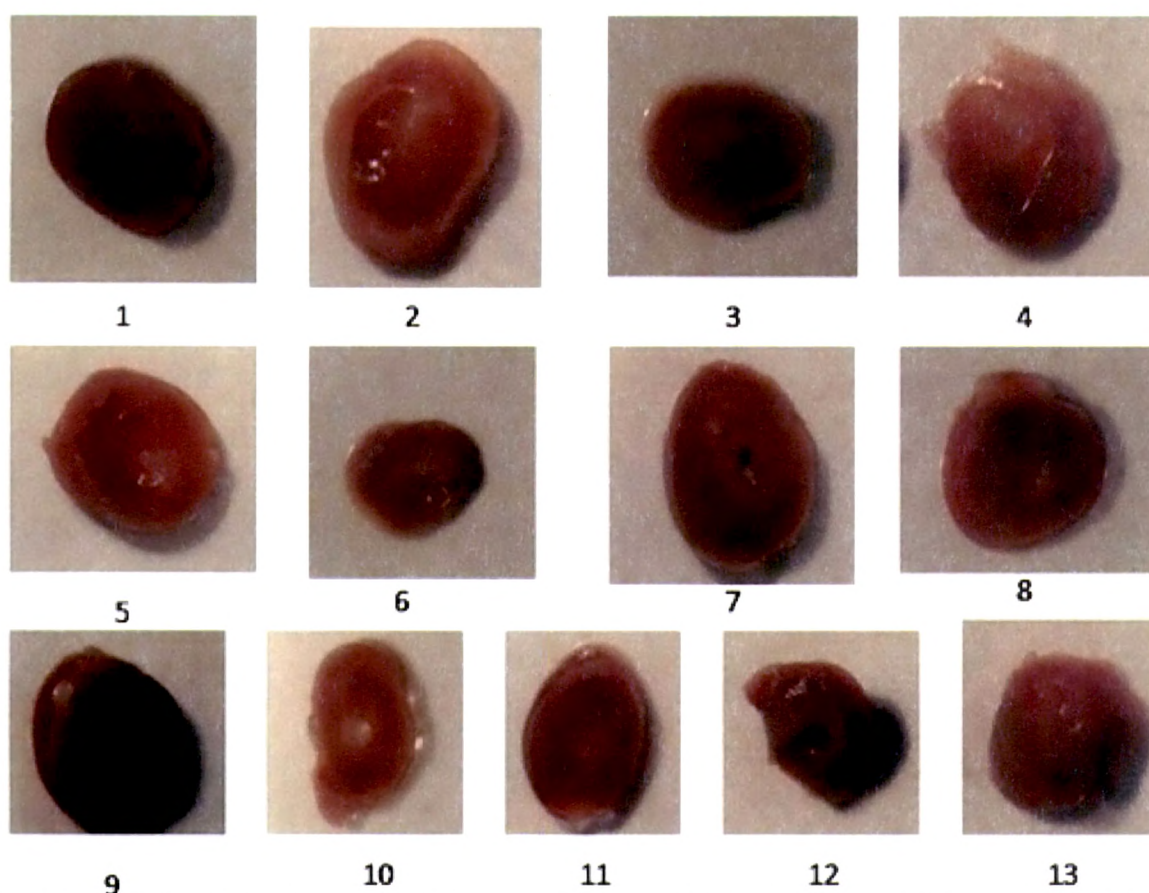


Figure 4.53: TTC stained rat hearts of various groups; Group 1: vehicle control; Group 2: ISO control; Group 3: swertisin (20 mg/kg +ISO); Group 4: ETTMOC (50 mg/kg+ISO); Group 5: ETTMOC (100 mg/kg+ISO); Group 6: EATMOC (50 mg/kg+ISO); Group 7: EATMOC (100 mg/kg+ISO); Group 8: OCFF (50 mg/kg+ISO); Group 9: OCFF (100 mg/kg+ ISO); Group 10: RMOC (50 mg/kg+ISO); Group 11: RMOC (100 mg/kg+ISO); Group 12: TAOC (200 mg/kg+ISO); Group 13: TAOC (400 mg/kg+ISO)

The heart tissues of all the groups were stained brick red (dark region) with TTC, an indicator of mitochondrial respiration. The unstained region is an indicator of total necrosis as seen in ISO treated group (Figure 4.53).

The present results showed that n-butanol fraction of *O. corniculata* have cardioprotective potential. OCFF pretreatment improved cardiac functions, the effect which can be attributed to presence of compound swertisin that has ability of maintaining redox status which is disturbed by ISO challenge, via restoration of endogenous antioxidants, controlling lipid peroxide formation and preserving activities of CPK-MB, LDH enzymes. Preservation of histoarchitectural of myocyte by OCFF pretreatment reconfirms these effects.

Results and Discussion

4.3. Characterization of compounds

Compounds that found to be active are characterized by various spectroscopic methods.

4.3.1. Compounds isolated from *Leonotis nepetaefolia*

4.3.1.1. LNLAL-01

Physical state: White crystalline powder

M.P.: 238-240°C

Percent Element Composition: C 55.5%, H 5.80%, N 14.02%, O 25.20%

Molecular formula: C₁₄H₂₁N₃O₅ (C 54.01%, H 6.80%, N 13.50%, O 25.70%-theoretical values)

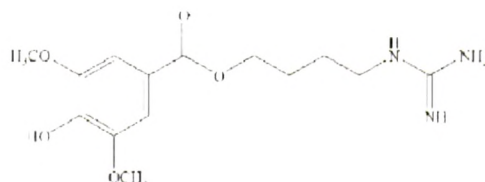


Figure 4.53: Chemical structure of leonurine

Molecular Weight: 311.33

UV spectrum: λ_{max} - 226 and 290 nm

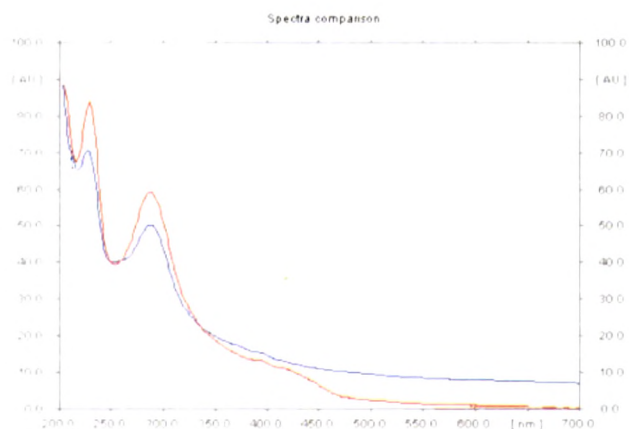


Figure 4.54: UV spectrum of LNLAL-01

Results and Discussion

Mass spectrum: m/z : molecular ion peak 312 $[M+H]^+$, base peak 155 $([M+H]^+-157)$

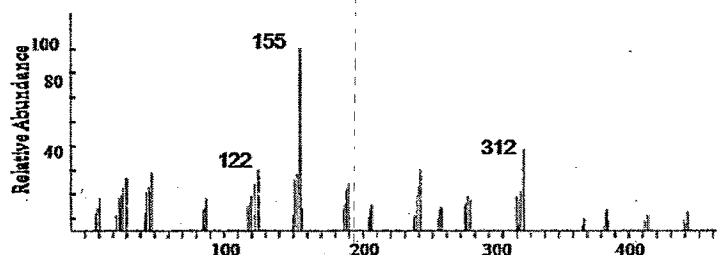


Figure 4.57: Mass spectrum of LNLAL-01

Above data were correlated from the following literature references and LNLAL-01 was confirmed as leonurine:

- Kubota, Nakajima, Isolation from leaves of *Leonurus sibiricus* L., Labiatae [305].
- Goto *et al.*, Structure of leonurine [306].
- Sugiura *et al.*, Structure and synthesis of leonurine [307].

4.3.1.2. LN-02: LN-02 was identified as β -sitosterol by co-TLC with standard obtained from Sigma chemicals.

4.3.2. Compound isolated from *Oxalis corniculata*

4.3.2.1. OC-01

Physical state: Yellow crystalline powder

M.P.- 240-242°C

Percent Element Composition: C 59.5%, H 5.05%, O 35.70%

Molecular formula: $C_{22}H_{22}O_{10}$ (C 59.19%, H 4.97%, O 35.84%-theoretical values)

Molecular Weight: 446.11

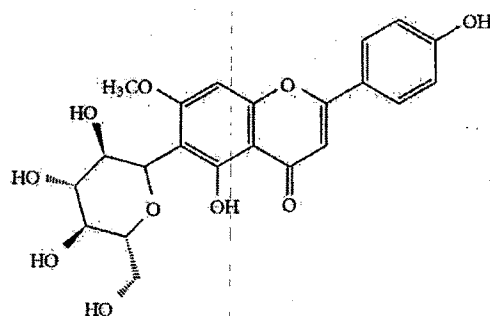


Figure 4.58: Chemical structure of swertisin

Results and Discussion

UV spectrum: : λ_{max} - 338 nm

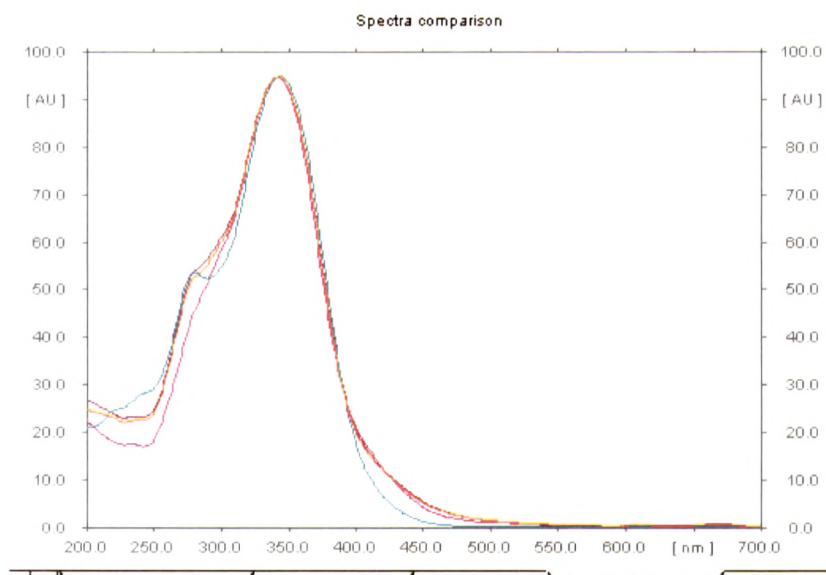


Figure 4.59: Ultra violet spectrum of isolated OC-01 overlaid with swertisin

Infrared spectrum: Major peaks obtained are 3121, 2719, 1553 and 1380 cm^{-1}

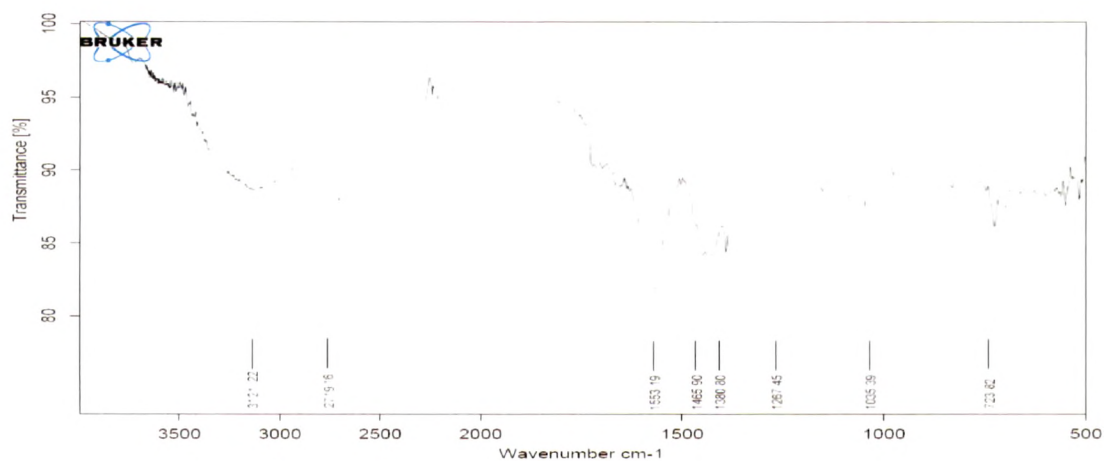


Figure 4.60: IR spectrum of OC-01

Results and Discussion

Proton NMR spectrum:

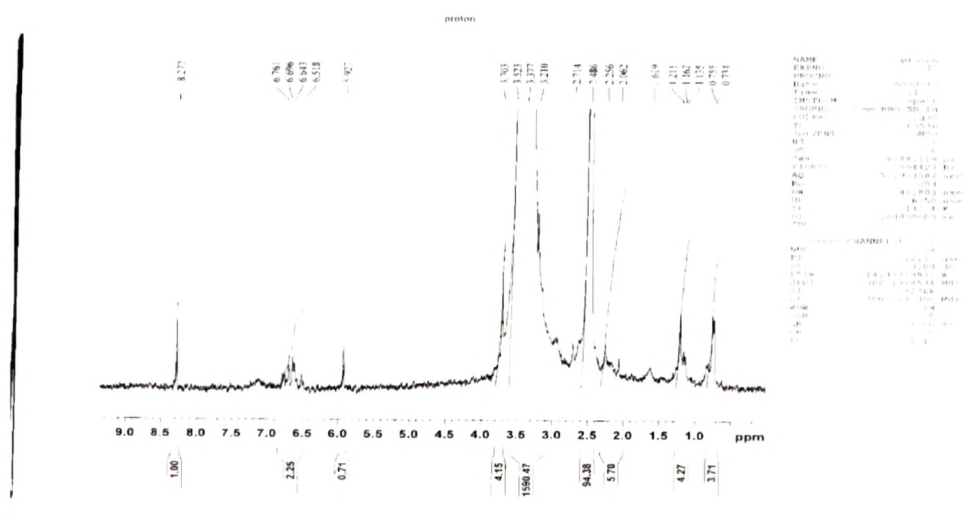


Figure 4.61: Proton NMR spectrum of OC-01

Mass spectrum: m/z : molecular ion peak 447 $[M+H]^+$, base peak 327 $([M+H]^+ - 12$

Results and Discussion

Mass fragmentation of swertisin:

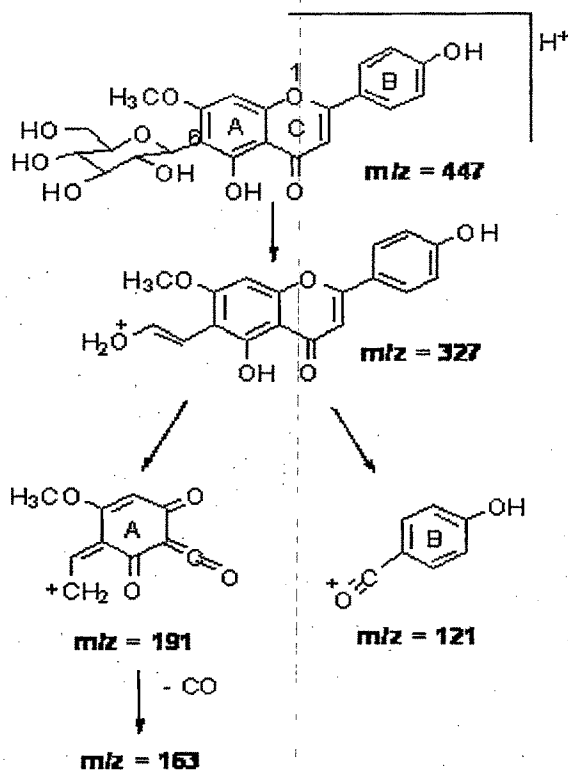


Figure 4.63: Mass fragmentation of OC-01

Swertisin is composed of two parts; a flavone and a monosaccharide unit. The existence of abundance fragment peak at m/z 327 suggests that the sugar moiety is not cleaved in its entirety, which in turn suggests a C-linked sugar. The product ion scan on m/z 327 reveals fragment ions at m/z 121, 163 and 191, the latter two of which are known to be exclusively observed for 6-C glycosyl flavones [309]. It was confirmed by earlier reports.